CHARACTERIZATION OF PULSE DETONATION ENGINE PERFORMANCE WITH VARYING FREE STREAM STAGNATION PRESSURE LEVELS

THESIS

Wesley R. Knick, Captain, USAF

AFIT/GAE/ENY/06-M34

DEPARTMENT OF THE AIR FORCE
AIR UNIVERSITY
AIR FORCE INSTITUTE OF TECHNOLOGY

Wright-Patterson Air Force Base, Ohio

AFIT/GAE/ENY/06-M34

CHARACTERIZATION OF PULSE DETONATION ENGINE PERFORMANCE WITH VARYING FREE STREAM STAGNATION PRESSURE LEVELS

THESIS

Presented to the Faculty

Department of Aeronautics and Astronautics

Graduate School of Engineering and Management

Air Force Institute of Technology

Air University

Air Education and Training Command

In Partial Fulfillment of the Requirements for the

Degree of Master of Science in Aeronautical Engineering

Wesley R. Knick, BS

Captain, USAF

March 2006

AFIT/GAE/ENY/06-M34

CHARACTERIZATION OF PULSE DETONATION ENGINE PERFORMANCE WITH VARYING FREE STREAM STAGNATION PRESSURE LEVELS

Wesley R. Knick, BS
Captain, USAF

Approved:

/signed/

Paul I. King _____ date

/signed/

Ralph A. Anthenien _____ date

/signed/

Milton E. Franke _____ date

AFIT/GAE/ENY/06-M34

Abstract

A pulse detonation engine operates on the principle that a fuel-air mixture injected into a tube will ignite and undergo a transition from a deflagration to a detonation and exit the tube at supersonic velocities. Studies in the field of combustion have shown that both ignition time and deflagration to detonation transition time can vary as a function of pressure. It can be hypothesized that if ignition and deflagration to detonation transition times can be reduced by increasing the free stream stagnation pressure level of the tube, it would then be possible to shorten the detonation tube length and increase the cycle frequency resulting in a weight savings, and an increase in overall pulse detonation engine performance. By attaching varying sizes of nozzle orifices to the exhaust exit of the pulse detonation tube of the pulse detonation engine to choke, or increase the stagnation pressure levels of the detonation tube it was possible to vary the internal pressure of the pulse detonation tube and examine the effect on the performance parameters of ignition time, and detonation wave speed, distance, and time. By varying fill fraction, spark delay and equivalence ratio in addition to nozzle orifice size, a minimum ignition and overall detonation time was found to correspond to a given orifice size to tube diameter ratio. The effects of pressure in this study produced a less beneficial effect on deflagration to detonation transition time and distance.

To my wife and daughter who bring me joy and have provided loving and wonderful support.

Acknowledgments

I would like to express my sincere appreciation to my faculty advisor, Dr. Paul I. King, for his guidance and support throughout the course of this thesis effort. His insight and experience were certainly appreciated. I would, also, like to thank my sponsor, Dr. Frederick R. Schauer, Dr. John Hoke, Mr. Royce Bradley and Mr. Curt Rice from the Air Force Materiel Command for providing the facilities, guidance and assistance to produce my research results.

I also have to thank Dr. Ralph Anthenien for also providing me with considerable guidance and help on my thesis especially in the field of combustion even when he was short on time. Lt Timothy Helfrich was a most valuable asset on those long hours every evening while I was trying to gather data after hours. His understanding of the PDE facility and initiative could not have served me better and quite often turned what would have been hours trying to figure something out or why it was broken into minutes… and yes he knows it!... But then again, he would always do about anything for a burrito at Qdoba! I also have to thank Capt Joe Hank and all my friends and colleagues who have aided in my long journey through AFIT to be able to arrive at a point in my academic career where I could be given the opportunity to produce a thesis.

Wesley R. Knick

Table of Contents

List of Figures

Page

List of Tables

Page

List of Symbols

Acronyms

ACFM	Actual Cubic Feet per Minute
AFIT	Air Force Institute of Technology
AFRL	Air Force Research Laboratory
CFD	Computational Fluid Dynamics
C-J	Chapman Jouguet (speed)
DDT	Deflagration to Detonation Transition
FF	Fill Fraction
PDE	Pulse Detonation Engine
TTL	Transistor to Transistor Logic
RTV	Room Temperature Vulcanizing
ZND	Zeldovich, vonNeumann, and Döring wave theory

Symbol

A	Area (m^2)
a, c	sonic velocity (m/s)
B	Spalding transfer number (dimensionless)
β	Seat Angle (degrees)
C_D	empirical discharge coefficient (dimensionless)
c_f	condenser capacitance (farads)
C_p	specific heat (J/kg K)
D	drop diameter (nm), tube diameter (m)
D_v	Head Diameter (mm)
d_c	critical tube diameter (mm)
ρ	density (kg/m^3)
d_q	air fuel mixture diameter (spherical volume)
E	electrical energy (J), activation energy (kJ)
E_{min}	minimum ignition energy (J)
f	friction factor (dimensionless)
F	propulsive force (N)
g_c	constant (1 kg m/N s^2)
h^0	specific enthalpy of formation (J/kg)
K	flow coefficient (CM)
$K_{nozzle\ loss}$	nozzle loss coefficient (dimensionless
L_c	cell length (mm)
L_e	effective tube length (m)
L_v	valve lift (mm)
$\dot{m}$	mass flow rate (kg/sec)

M	Mach number, velocity of approach factor
n	reaction order (a + b, ~0.5 to 2.5)
p, P	pressure (N/m^2)
q	heat per unit mass (J/kg)
Q	volumetric flow rate (m^3/sec)
q_{cond}	heat per unit mass conducted (J/kg)
R	universal gas constant (8.31451 J/gmol K)
ψ	stoichiometric ratio
T	temperature (K)
Tu	percentage turbulence intensity (100*u'*/U)
U	air velocity, wave speed (m/sec)
u, V	velocity (m/s), volume (m^3)
w	seat width (mm)
u'	RMS value of fluctuating velocity
V_i	condenser voltage (Volt)
X_{fuel}	mole percent fuel
Y	expansion factor (dimensionless)
σ	standard deviation
ϕ	equivalence ratio (dimensionless)
γ	specific heat ratio (dimensionless)
λ	thermal conductivity (J/(sec m K)), cell width (mm)
μ	viscosity (N sec/m^2)
μ'	bulk viscosity (N sec/m^2)
τ_{ign}	ignition time (sec)

Subscripts

1	upstream
2	downstream
air	referenced to air properties
atm	atmospheric
cond	conductivity
fuel	referenced to fuel properties
ign	ignition
min	minimum
mix	referenced to fuel/air mixture properties

CHARACTERIZATION OF PULSE DETONATION ENGINE PERFORMANCE WITH VARYING FREESTREAM STAGNATION PRESSURE LEVELS

I. Introduction

Detonations are of interest in the field of propulsion as a detonation is an efficient means of burning a fuel-air mixture and releasing energy content. The Air Force has had an interest in the Pulse Detonation Engine (PDE) as a propulsion device for a variety of applications ranging from both manned and unmanned aircraft and aerial vehicles, to cruise missiles. The concept of the pulse detonation engine dates back to the pioneering work of Hoffman (Hoffman, 1940). Hoffman explored detonations as early as 1940 using both gaseous acetylene and benzene as a liquid hydrocarbon fuel mixed with oxygen with intermittent detonation results but most research for propulsion applications has taken place only in the last 50 years due to the complex nature of rapidly mixing the fuel and air at high speeds, and initiating and sustaining a detonation using a controlled and cyclic method in fuel-air mixtures. PDEs offer the potential for high thrust and efficiency in a large operational envelope with the advantage of being mechanically very simple to operate, and are of relatively low weight and cost. The addition of thrust tubes in a multi-tube arrangement also offers the potential for increased thrust as well as increasing the frequency with which as single tube can be fired. Because of the rapid burning or material conversion rate, several orders of magnitude faster than in a flame, there is not

enough time for pressure equilibration and the overall process is more thermodynamically similar to a constant volume process than the constant pressure process typically found in conventional propulsion systems (Kailasanath, 1999:1)

Operation of the pulse detonation engine involves a dynamic process of filling a detonation tube with a fuel/air mixture at ambient conditions followed by ignition, deflagration, transition to a detonation wave, and the detonation wave followed by combusted gases exiting the tube. Research in the field of pulse detonation engines and combustion suggests that two important pulse detonation engine parameters of ignition and deflagration to detonation transition (DDT) time vary as pressure in the detonation tube is varied (Schauer et al, 2005:1; Schultz et al, 1999:9). If it is possible to decrease both ignition and DDT time, potential exists to increase the engine cycle frequency subsequently the overall thrust of the PDE. If the overall combined effect of decreasing ignition and deflagration to detonation transition time and distance, the axial distance down from the entrance of the tube, is decreased it might also be possible to decrease the overall length of the detonation tube with a resultant weight savings to the engine and aircraft combination. An important ability of the pulse detonation engine if it is to ever be used as a viable source of propulsion for powered aircraft is for the engine to be able to regulate pressure within the detonation tube during flight as atmosphere pressure drops as an aircraft ascends. Pressure decreases as altitude increases producing a diminishing effect on the important pulse detonation engine performance parameters of ignition time, deflagration to detonation transition time, detonation wave speed velocity and most importantly thrust. The dynamic pressure encountered at various Mach numbers will also

have a significant, though mostly an assumed positive and beneficial effect on the fill and purge pressure within a pulse detonation engine tube, but the pressure and flow rate must continue to be regulated as overfilling a straight detonation tube does not offer, at present, any appreciable performance benefits. But how does one increase the pressure inside a tube to which a fuel/air mixture is injected and then ignited? Unlike the internal combustion engine to which supercharging or turbo-charging will increase performance through mechanical pre-compression, attempting to increase the pressure inside the detonation tube will only produce a higher flow exiting the tube and result in higher fuel/air consumption without any appreciable increase in performance. A converging-diverging nozzle similar to that used in modern rocket engines provides a possible solution to increasing the free stream pressure inside a detonation tube of a pulse detonation engine. However, unlike the modern rocket engine which operates at a steady state condition, the pulse detonation engine has a pulsing and characteristically unsteady flow and must continue to be able to fulfill the three part flow cycle of fill, fire, and purge. The question then remains, is it even possible, and by how much can the flow of a pulse detonation tube be restricted and provide an appreciable performance benefit? The ability to restrict the flow upstream using a nozzle could possibly provide for a larger initial pressure and overall amplitude during the fill cycle of the pulse detonation engine to which ignition and DDT time are expected to decrease providing an increase in overall PDE performance.

Research Motivation and Approach

The objective of this research was to examine the effects, using a variation of methods, of increasing the free stream detonation tube stagnation pressure on the PDE performance parameters of ignition time and deflagration to detonation transition time and distance, and wave speed. Wave speed was examined by comparing the measured wave speed to the known Chapman Jouguet (C-J) for the fuel used (hydrogen) to determine whether detonation wave speeds had been measured. This research performed and documented herein examined the effects of dynamic filling and performance on a single pulse detonation engine tube using an assortment of nozzle sizes and engine run conditions to restrict the pulse detonation engine flow. Engine control parameters of spark delay, equivalence ratio, and fill fraction were examined in an attempt to determine optimum flow and performance conditions for the pulse detonation engine tube arrangement tested in this research. Other fuels are hypothetically considered by examining the effects of detonation tube pressure in multi-cycle operation on factors such as droplet evaporation in liquid fuels, critical initiation energy, ignition time and DDT time.

II. Pulse Detonation Theory and Background

Detonation Wave Theory

A pulse detonation engine (PDE) generates thrust using intermittent and pulse detonation waves. Similar in certain respects to a pulse-jet engine, the PDE uses the detonation waves to produce the thrust capitalizing on the high pressure and temperature, and very rapid material and energy conversion. In studying the pulse detonation engine it is necessary to understand two types of premixed gaseous reactions found in the pulse detonation engine. The two reactions which form the basis for operation of the pulse detonation engine are known as deflagration and detonation. A deflagration is defined as a combustion wave propagating at subsonic speed (Kuo, 2005: 356). A detonation is defined as a combustion wave propagating at supersonic speed (Kuo, 2005: 356). The formation of a detonation wave requires a deflagration to detonation transition at a time and distance occurring after ignition. Compared to a pulse-jet engine with purely a deflagration process to produce thrust, the burn rate or material conversion rate produced from a detonation wave in a PDE is typically thousands times faster than a deflagration flame. The fuel/air mixture is ignited in the closed end of an opposite open ended tube, a combustion wave is formed and if the tube is of sufficient length a detonation wave will develop. The burned gas products of the initial deflagration cause the specific volume to increase to approximately 5 to 15 times the unburned gases ahead of the flame front. Each preceding compression resulting from the expansion heats the unburned gaseous mixture increasing the sound velocity with each succeeding wave catching up with the initial wave. The preheating that results from the compression increases the flame speed

further accelerating the unburned gas mixture until turbulence develops in the unburned gases. The unburned gases and compression waves further accelerate to an even greater velocity until a shock forms strong enough to ignite the gas mixture ahead of the wave front. A detonation wave is formed as the reaction zone behind the shock sends forth a continuous compression wave to reinforce the shock front and prevent decay (Glassman, 1996:233). The coalescing of the compression waves that occurs produces the supersonic wave sustained by the chemical reaction or detonation. Compared to a detonation, a deflagration is a subsonic wave sustained by a chemical reaction and differs mostly by the flame speed and pressure drop across the flame. Figure 1 shows a diagram of a one-dimensional combustion wave characteristic of a deflagration or detonation wave in a pulse detonation wave tube (Kuo, 2005:356). The figure depicts a right to left moving wave in the tube with u_1 being the reactant velocity with respect to the flame front and u_2 the product velocity with respect to the flame front. Table 1 shows the qualitative differences between detonations and deflagrations of gases. A comparison of values for deflagration versus detonation shows much larger values of M_1, p_2/p_1, and ρ_2/ρ_1 for detonation than deflagration.

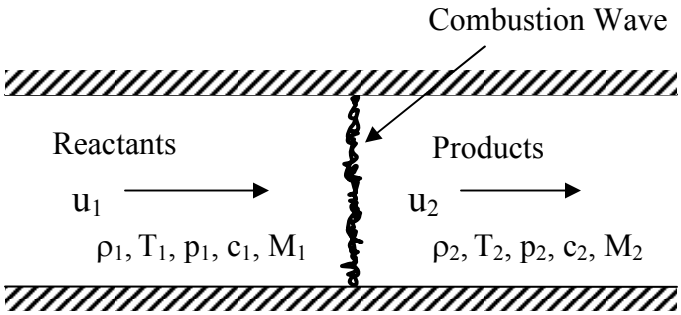

Figure 1. Schematic diagram of one-dimensional combustion wave

Table 1. Differences of Detonations & Deflagrations of Gases (Kuo, 2005:357)

Ratio	Typical Magnitude of Ratio	
	Detonation	Deflagration
u_1/c_1 (M_1)	5 - 10	0.0001 - 0.03
u_2/c_2 (M_2)	1	0.003
u_2/u_1	0.4 - 0.7 (deceleration)	4 - 6 (acceleration)
p_2/p_1	13 - 55 (compression)	≈ 0.98 (slight expansion)
T_2/T_1	8 - 21 (heat addition)	4 - 16 (heat addition)
ρ_2/ρ_1	1.7 - 2.6	0.06 - 0.25

Using the one-dimensional model to consider the relationships between the unburned and burnt properties of the premixed gaseous mixtures for a constant area tube of the pulse detonation engine it is possible to find the solution of any steady state deflagration or detonation wave on the Hugoniot curve. Assuming the combustion wave propagates at a steady-state speed with no heat loss to the surrounding wall it is possible to derive the conservation equations for steady one-dimensional flow, with negligible body forces, no external heat addition or loss, and negligible Dufour and species inter-diffusion effects (Kuo, 2005:357):

Continuity:
$$\frac{d(\rho u)}{dx} = 0 \qquad \text{where } \rho u = \text{constant} \tag{1}$$

Momentum:
$$\rho u \frac{du}{dx} = -\frac{dp}{dx} + \frac{d}{dx}\left[\left(\frac{4}{3}\mu + \mu'\right)\frac{du}{dx}\right] \tag{2}$$

Energy:
$$\rho u\left[\frac{d}{dx}\left(h + \frac{u^2}{2}\right)\right] = -\frac{d}{dx}q_{cond} + \frac{d}{dx}\left[u\left(\frac{4}{3}\mu + \mu'\right)\frac{du}{dx}\right] \tag{3}$$
$$\text{where } \quad q_{cond} = -\lambda\frac{dT}{dx} \quad \text{and} \quad h = C_p T + h^0$$

The bulk viscosity μ' is small and often neglected: $\mu' \ll \mu$

Integrating the continuity, momentum and energy equations from above gives (Kuo, 2005:358):

$$\rho u = \text{constant} \equiv \dot{m}$$

$$\rho u \frac{du}{dx} + u \frac{d}{dx}(\rho u) = -\frac{dp}{dx} + \frac{d}{dx}\left(\frac{4}{3}\mu \frac{du}{dx}\right) = 0 \tag{4}$$

From continuity: $$\frac{d}{dx}(\rho u) = 0 \tag{5}$$

The momentum equation then becomes:

$$\frac{d}{dx}\left[\rho u^2 + p - \frac{4}{3}\mu \frac{du}{dx}\right] = 0 \tag{6}$$

Integration with respect to x gives:

$$\rho u^2 + p - \frac{4}{3}\mu \frac{du}{dx} = \text{constant} \tag{7}$$

Integration of the energy equation with respect to x gives:

$$\rho u\left(C_p T + h^0 + \frac{1}{2}u^2\right) - \lambda \frac{dT}{dx} - u\left(\frac{4}{3}\mu \frac{du}{dx}\right) = \text{constant} \tag{8}$$

Both du/dx and dT/dx are equal to zero in the fully burned and unburned regions providing the conservation equations providing the relationships of the flow properties in the two regions (Kuo, 2005:358):

$$\rho_1 u_1 = \rho_2 u_2 = \dot{m} \tag{9}$$

$$p_1 + \rho_1 u_1^2 = p_2 + \rho_2 u_2^2 \tag{10}$$

$$C_p T_1 + \frac{1}{2}u_1^2 + q = C_p T_2 + \frac{1}{2}u_2^2 \quad \text{or} \quad h_1 + \frac{1}{2}u_1^2 + q = h_2 + \frac{1}{2}u_2^2 \tag{11}$$

$$\text{and} \quad p_2 = \rho_2 R T_2 \tag{12}$$

$$q \equiv h_1^0 - h_2^0 \quad \text{where} \quad h^0 = \sum_{i=1}^{N} Y_i \ \Delta h_{f,i}^0 \tag{13}$$

The four equations above relate the five unknowns: $u_1, u_2, \rho_2, T_2, p_2$. Combining equations (9) and (10) above it is possible to derive the *Rayleigh-line relation:*

$$\rho_1^2 u_1^2 = \frac{p_2 - p_1}{1/\rho_1 - 1/\rho_2} = \dot{m}^2 \tag{14}$$

Figure 2 below is an example plot of lines of constant mass flux known as Rayleigh lines. Increasing the mass flux causes the slope to increase through the initial values (P_1, $1/\rho_1$). At an infinite mass flux the Rayleigh line would be vertical. At zero mass flux the Rayleigh line has a zero or horizontal slope. Given the limits of the Rayleigh line slopes, no possible solutions can exist in regions A or B in Figure 2 which represent an imaginary mass flux and ultimately determine what final states are possible for a detonation wave (Turns, 2000:603).

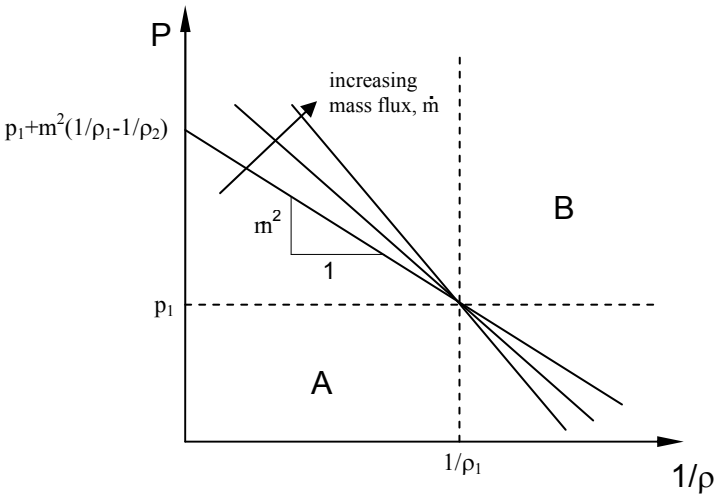

Figure 2. Rayleigh lines of constant mass flux

`Using the *Rayleigh-line relation,* the Mach number relation $M_1 \equiv u_1 / c_1$, the relationship for specific heats, and the above equations, a single equation called the Rankine-Hugoniot equation relating only two unknowns p_2 and ρ_2 can ultimately be derived (Kuo, 2005:360):

$$\frac{\gamma}{\gamma-1}\left(\frac{p_2}{\rho_2}-\frac{p_1}{\rho_1}\right)-\frac{1}{2}\left(p_2-p_1\right)\left(\frac{1}{\rho_1}+\frac{1}{\rho_2}\right)=q \tag{15}$$

The Hugoniot relation can also be expressed in terms of total (thermal plus chemical) enthalpy h (Kuo, 2005:361):

$$h_2-h_1=\frac{1}{2}\left(p_2-p_1\right)\left(\frac{1}{\rho_1}+\frac{1}{\rho_2}\right) \tag{16}$$

A plot of the Hugoniot curve is shown below illustrating the solutions segments corresponding to different conditions of combustion. The two points tangent to the curve extending from the origin are called the Chapman-Jouguet (C-J) points. Point L represents the lower C-J point and point U represents the upper C-J point on the diagram. The Hugoniot curve represents all the possible solutions of the Hugoniot equation for the burned mixture however, as illustrated in the figure by region V, not all solutions are possible. In region V $p_2 > p_1$ and $1/\rho_2 > 1/\rho_1$, a physically impossible region given that the Rayleigh-line expression implies that $\dot{m}$ is imaginary (Kuo, 2005:361). In studying the characteristic nature of the Hugoniot curve at the C-J points it can be determined that $M_2 = 1$ (Kuo, 2005:362). In the detonation regions of the Hugoniot curve (regions I and II) the density and pressure of the products exceed that of the reactants $1/\rho_2 < 1/\rho_1$, $p_2 > p_1$ and $u_1 > u_2$. Pulse detonation engines are designed to operate in regions I and II

of the Hugoniot curve at the upper C-J point where products follow the detonation wave with a velocity slower than the reactants. Under most experimental conditions, detonations are Chapman-Jouguet waves and occur at the upper C-J point representing the usual solution on the detonation branch of the Hugoniot curve [0:363]. The upper C-J point corresponds to the minimum detonation wave speed with a large pressure ratio and a state of minimum entropy (Kuo, 2005:367).

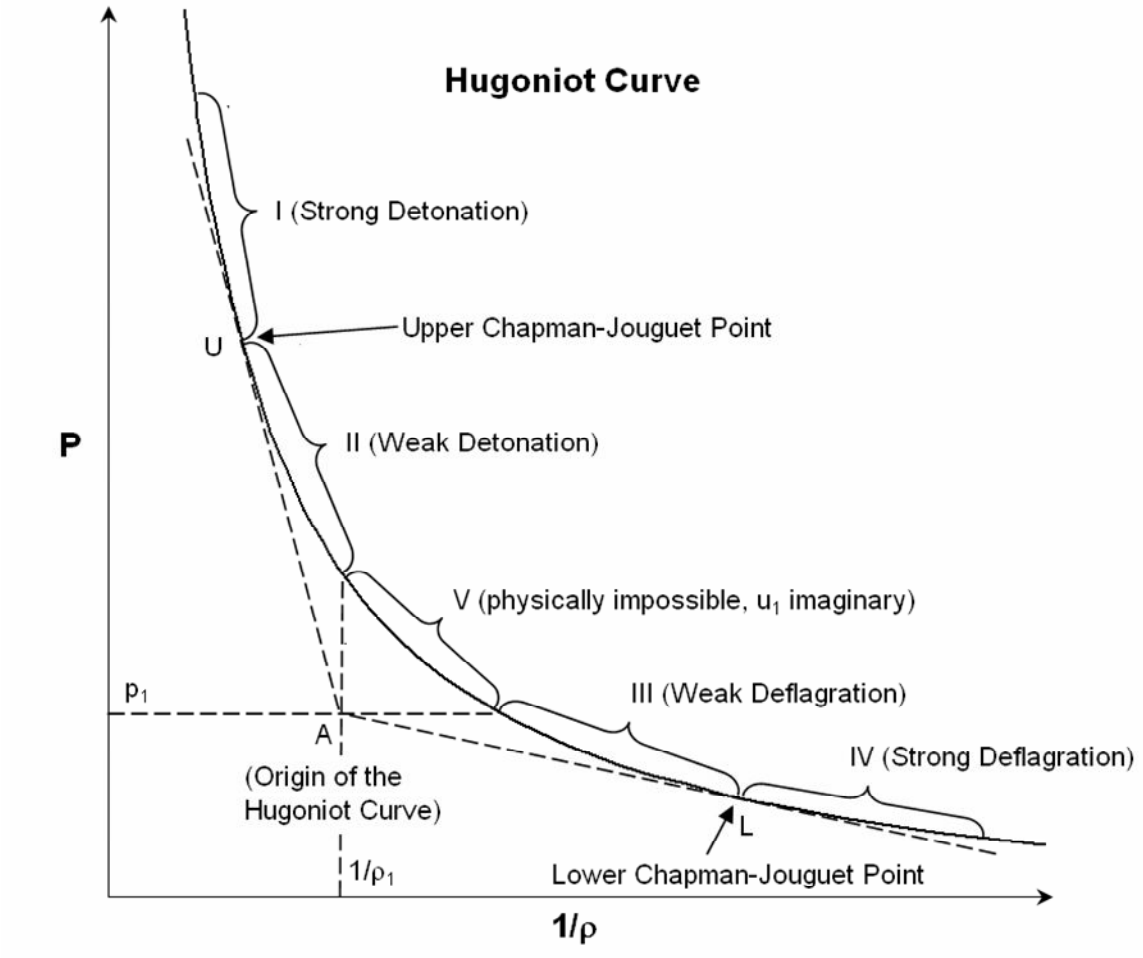

Figure 3. Hugoniot curve of p versus 1/ρ

In comparison to the upper C-J point the lower C-J point has a maximum wave speed for all deflagrations and corresponds to a maximum entropy state (Kuo, 2005:367). Near the lower C-J point the unburned gas pressures and densities is slightly greater than the burned gases and the burned gases move away from the combustion wave front (Kuo, 2005:364). The burned gases flow away from the deflagration wave, a significant difference of the deflagration wave in comparison to the detonation wave.

Zel'dovich, von Neumann and Döring (ZND) Theory of Detonations

As a further development on the theory of the C-J theory, Zel'dovich, von Neumann, and Döring assumed the flow in a detonation wave is one-dimensional and steady relative to detonation front (Kuo, 2005:380). The detonation wave is a shock wave driven by, and part of the trailing combustion wave. The shock wave heats the reactants to a sufficient temperature to allow the reaction rate of the ensuing deflagration to propagate as fast as the shock wave (Kuo, 2005:380). The shock-wave region thickness is on the order of a few mean free paths of the gas molecules and with very limited reactions. A relatively very small number of collisions occur between molecules within the shock wave and most of the heat release is from a thick region of gas behind the shock wave.

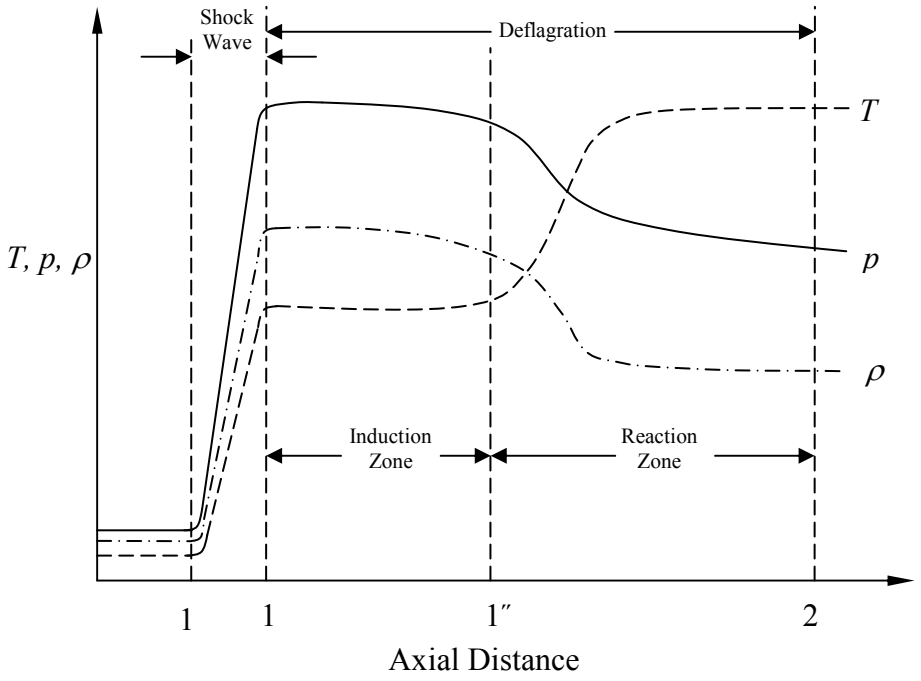

Figure 4. ZND Wave Structure and physical properties (Kuo, 2005:382)

An understanding of the mechanisms by which combustion occurs in a detonation wave is important to properly assess how to predict performance for a variation of fuels and initial conditions. The variation in physical properties of the one-dimensional ZND detonation wave is shown in Figure 4 with the magnitude of the pressure, temperature, and density behind the shock depending on the fraction of reacted gaseous mixture. With a slow reaction rate that follows the Arrhenius law immediately behind the shock where the temperature is not high, a relatively flat density profile can be observed immediately behind the shock front known as the induction zone. Following the induction period, the reaction rate increases dramatically with a sharp change in gas properties that reach equilibrium when the reaction is completed. The shock front and fully reacted location distance is approximately 1 cm (Kuo, 2005:382).

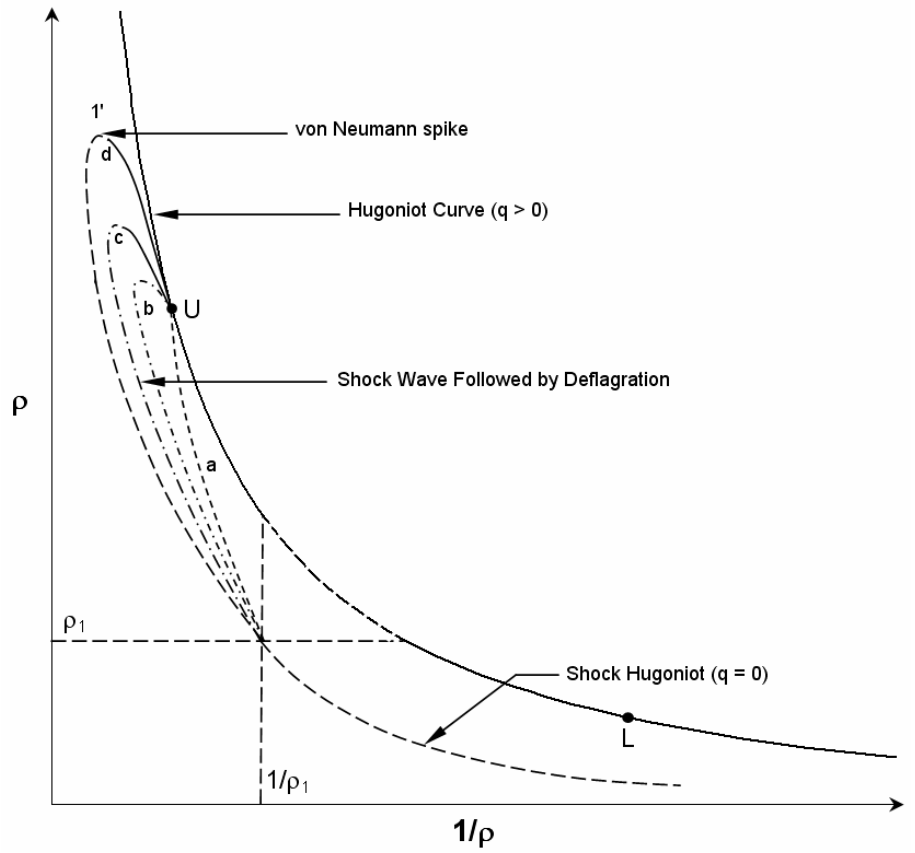

Figure 5. ZND detonation structure on (ρ, 1/ρ) diagram (Kuo, 2005:383)

Figure 5 above represents the reacting mixture on the Hugoniot plot and shows multiple paths by which the reacting mixture may pass through the detonation wave to state of complete reaction. Each of the conservation equations can be satisfied by any one of the paths a, b, c, or d. Path a is highly unlikely to have sufficient energy release to sustain the wave as the path would require a reaction to occur at all points on the path. Path b would represent mixtures with fast chemical kinetics (Kuo, 2005:383). Path c would represent slow chemical kinetics. Path d represents the zero chemical-energy release in the shock wave with the initial portion coinciding with the shock Hugoniot curve. The peak pressure behind the shock wave corresponds to the von Neumann spike in Figure 5.

Pulse Detonation Engine Cycle and Operation

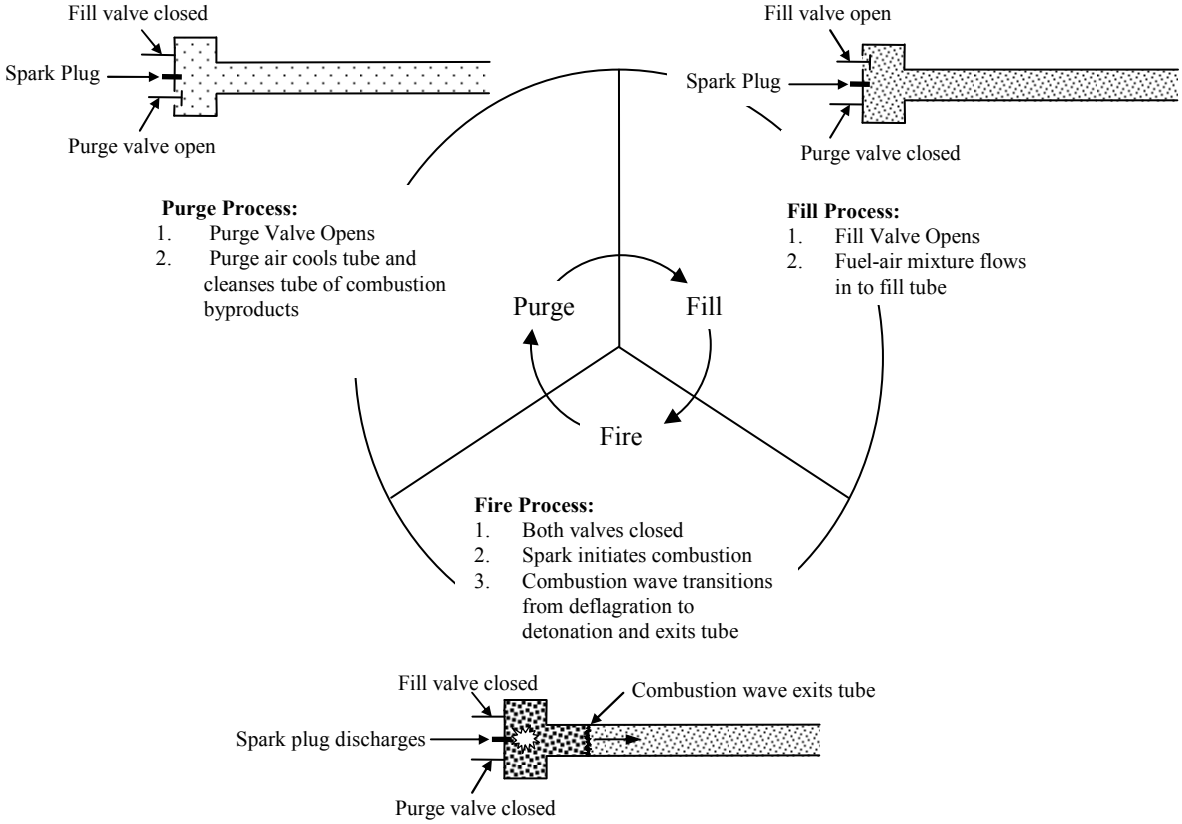

Figure 6. Pulse Detonation Engine 3 part cycle (120° equal time each part)

A pulse detonation engine operates on a three part cycle composed of a fill, fire and purge process shown above in Figure 6. The fill portion of the cycle begins the process by filling the pulse detonation tube with a combustible fuel air mixture through a valve ported through the closed end of the tube. The fill valve then closes to begin the fire portion of the three part cycle. The fire portion of the cycle begins with ignition of the fuel air mixture. Both the purge and fill valves are closed. The ignition begins the combustion wave process beginning with a deflagration wave followed by a transition to

a detonation wave exiting the tube at high (C-J) velocities. The third and final portion of the three part cycle consists of the purge valve opening to purge the tube of the products of combustion. The purge portion of the cycle also contributes to cooling of the detonation tube, an important part of the cycle to control thermal stress, hot spots and prevent mechanical failure that can result in exceeding material melting points. A hot spot or material point of high temperature can produce an alternate source of ignition similar to pre-ignition in an automobile engine disrupting normal operation of the fire portion of the engine cycle and can develop at a sharp corner or edge where the material is less insulated from the surrounding gas temperatures.

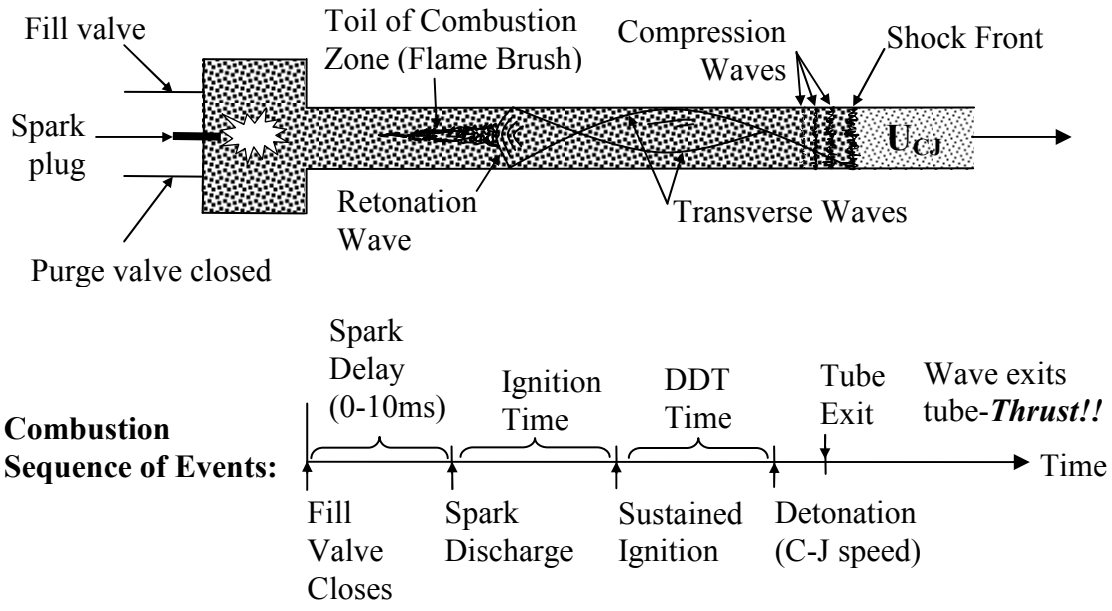

Figure 7. Detonation wave diagram & timeline sequence of events

The fire process of the three part cycle contains all events which produce thrust from the pulse detonation engine to make it a propulsive device. The fill and purge portions of the cycle are to prepare the detonation tube for ignition and combustion. Figure 7 depicts a combustion sequence of events as they occur during the fire process of

the three part cycle. The fire portion of the cycle begins when the fill valve closes. A spark or ignition stimulus is then discharged in the entrance or closed portion of the detonation tube. The ignition source can be a spark discharge, in the case of a spark plug, and delayed typically up to 10 milliseconds for a predetermined amount of time to optimize performance depending on the flow and fill conditions or also the type of fuel used. After spark discharge the reaction begins to propagate in all possible directions from the spark source through heat rise and radical production. The induction time is the critical time of radical production necessary to generate sustained reactions that lead to ignition. The ignition time, or the total of induction time and chemical time is defined as the time from initial spark to sustained combustion. If a spark is used for ignition, a minimum energy $E_{\min}$, must be deposited by the spark to achieve ignition and is given by (Kuo, 1986:758):

$$E_{\min} = C_{p,air}\rho_{air}\Delta T_{stoich}\frac{\pi}{6}d_q^3 \tag{17}$$

where for flowing mixtures:

$$d_q = \frac{0.30\ \rho_{fuel}\left(\mathrm{Tu}/100\right)U^{0.4}D^{1.4}}{\phi\ \rho_{air}^{0.6}\mu_{air}^{0.4}\ln\left(1+\mathrm{B}\right)} \tag{18}$$

and:

D = drop diameter
ϕ = equivalence ratio
B = Spalding transfer number
Tu = percentage turbulence intensity = $100u'/U$
u' = RMS value of fluctuating velocity
U = air velocity

The energy generated by a capacitance spark is given by (Glassman, 1996:342):

$$E = \frac{1}{2} c_{\mathrm{f}} \left(V_2^2 - V_1^2 \right) \tag{19}$$

where:

E = electrical energy (J)
c_{f} = condenser capacitance (farads)
V_i = condenser voltage before spark (1) and after spark (2)

In the use of a spark as an ignition stimulus the energy generated by the capacitance discharge must be greater than the minimum required ignition energy. Equation (18) above defines the minimum ignition energy as a function of drop diameter, D an important parameter when considering the ignition of liquid hydrocarbon fuels as a portion of the ignition energy must be used to vaporize the droplets resulting higher ignition times. Fuels such as hydrogen and acetylene are much easier to detonate as both exist in a gaseous state at near standard temperature and pressure. Environmental conditions and reactant properties such as heat capacity, heat of combustion, initial reaction rate (Kanury, 1975:94), heat flux and pressure (Kuo, 1986:750) can all affect ignition delay both adversely and positively depending on conditions.

After ignition a significant chain of events occur known as the deflagration to detonation transition. The principle by which the ignited fuel air mixture is able to detonate provides for the ability of the detonation tube to be considered a propulsive device. For a detonation to occur in a tube a few select criteria must be met for the detonation phenomena to occur. If a combustible fuel air mixture is placed in a tube open at both ends and ignited a combustion wave is formed which obtains only a steady

velocity (Glassman, 1996:222). If one end of the tube is closed a combustion wave occurs, and if the tube is long enough a detonation wave can develop. The combusted gas products of the initial deflagration increase in specific volume to approximately 5 to 15 times that of the unburned mixture ahead of the combustion wave (Glassman, 1996:222). Each preceding combustion wave from the resulting expansion preheats the unburned fuel air mixture increasing the sonic velocity according to the mathematical relationship, $a = \sqrt{\gamma RT}$. The preheating that results forces the succeeding wave to catch up to the preceding wave and coalesce until a shock is formed that further increases velocity and acceleration, and generates turbulence to aid in the combustion process (Glassman, 1996:223). After a shock is formed the shock itself sends forth continuous compression waves into the gaseous fuel air mixture ahead of the front strong enough to stimulate ignition and keep the shock from decaying. The resulting sequence of events is what forms the detonation (Glassman, 1996:223). Two other important phenomena have also been observed from the detonation wave that forms. A retonation wave can also be observed to emanate from the location of shock formation and proceed in the opposite direction into the burned gas mixture. Transverse vibrations from the resulting detonation can also be observed and contribute to the cellular structure of the detonation wave.

In 1926 Campbell and Woodhead, after observing spin in limit mixtures in circular tubes, showed that detonation waves travel in a manner which is locally three dimensional and non-steady. Desnisov and Troshin later adapted an experimental technique of using soot-coated plates near a spark discharge to record and observe the

transverse detonation waves left behind on the soot-coated plate to examine a three dimensional detonation wave structure. The three dimensional wave structure is able to leave an imprint on the soot-coated plate caused by the intersection of sound wave propagating past as shown below in Figure 8 (Glassman, 1996:263). The soot trace or fish-scale like pattern left behind on the smoke-foil is able to reveal presence of the triple point, an intersection of the Mach-stem, incident, and reflected shocks.

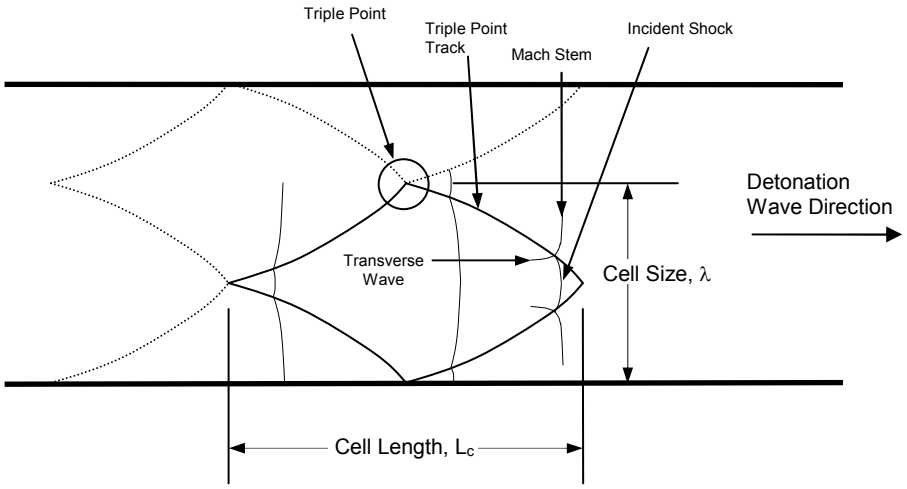

Figure 8. Schematic diagram of detonation cell structure

The cell width, λ of a detonation is defined as the width of a cell formed by the slipstream associated with the interaction of the transverse and longitudinal waves of the detonation (Kuo, 2005:405). The cellular structure is mapped when the detonation wave passes the soot covered point to reveal a pattern schematically depicted as shown in Figure 8. Over the range of possible detonable concentrations of a given fuel-oxidizer mixture, the wave structure is called a multi-head wave front (Kuo, 2005:403). For a given smooth circular tube the multi-head, self-sustained detonation becomes a single-head spinning detonation propagating at about the C-J velocity for a given mixture

composition. The single-head spinning detonation is characterized by an increase in transverse wave strength or 3 dimensional wave structure with the mixture gasses rotated about the tube axis. The single-head detonations associated with detonability limits for a given fuel-oxidizer mixture, coupled to fuel concentration can also be shown to relate to tube diameter. For each fuel concentration, there is a specific tube diameter call the critical tube diameter, d_c for which the multi-head detonation becomes a single-head detonation. It can generally be shown for the case of hydrogen as a fuel that $d_c = 13\lambda$ (Kuo, 2005:408).

Using the ZND model for the detonation structure it is possible to compute an induction time and also a corresponding induction zone length. Induction time, a characteristic of the chemical reactions in a detonation wave, is strongly coupled to the details of the transient gas dynamic processes being ultimately related to the chemical length scale, λ (or L_c), and is proportional to the induction time of the fuel oxidizer mixture (Glassman, 1996:257). It can also generally be shown that the cell length and cell width can be represented by $\lambda \simeq 0.6 L_c$ and that chemical reactions are generally completed within one cell length or cycle (Glassman, 1996:257).

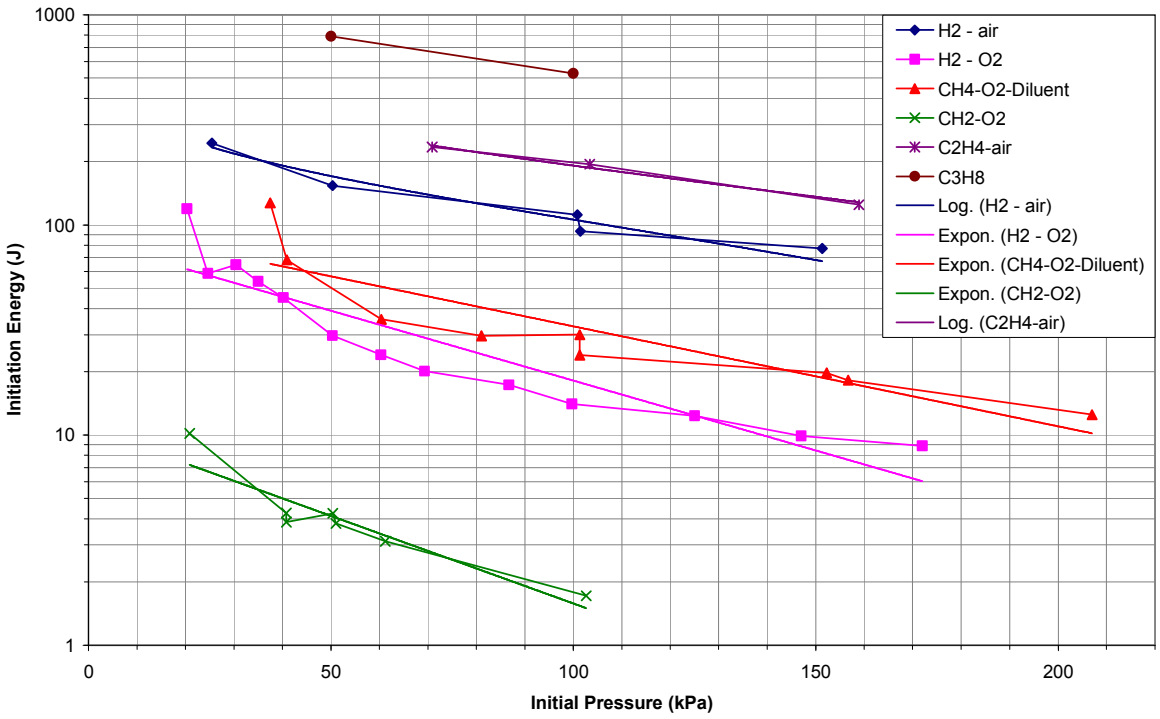

Figure 9. Initiation energy versus initial pressure, $\phi = 1$, T = 293K

The energy required to achieve a detonation can be shown to be directly related to the cell size of a detonation wave structure. The energy required to initiate a hydrocarbon fuel detonation can be on the order of 1 MJ whereas the detonation energy for hydrogen and air is generally around 5000 J (Tucker et al, 2004:18). A relationship of initiation energy to cell size can be experimentally determined to be given by (Schauer et al, 2005:2):

$$E_{initiation} = 3.375\lambda^3 \tag{20}$$

Using air or oxygen as the oxidizer the above relationship shows that the initiation energy drops by the cube of the cell size. Fuels using pure oxygen as an oxidizer require less initiation energy than fuels in a diluted oxygen environment such as air. It is possible using the above relationship to show that minimum initiation energy to achieve a

detonation directly correlates with deflagration to detonation transition (DDT) time for a fuel air mixture. Furthermore, if it is possible to relate cell size to initial pressure it possible to relate initiation energy to initial pressure for a given temperature and equivalence ratio. Figure 9 relates the initiation energy for initial pressure for a range of fuels in the pressure range of interest for a pulse detonation engine (Kaneshige and Sheperd, 1997). Trendlines through the plotted data help to denote that a clear trend can be observed for the above fuels that the energy to achieve a detonation decreases as the initial pressure is increased.

After a detonation is achieved in the confined space of the detonation tube the detonation wave exits the tube at high velocity and supersonic speeds. If the detonation is of sufficient strength it is possible for the detonation wave to achieve Chapman Jouguet (C-J) speed. For a vapor fuel such as hydrogen C-J speed is reached at approximately 1900 m/sec to 2000 m/sec. Typical fuel-air hydrocarbon mixture Chapman Jouguet speeds can range from 1400 m/sec to 2000 m/sec. The high exit velocity of the detonation wave gives rise to a mass flow behind the wave that produces the thrust to make the pulse detonation engine a propulsive device. This high velocity mass induced flow provides the propulsive thrust similar to a rocket engine using the familiar thrust equation (Humble et al, 1995:110):

$$F = \dot{m} V_{exit} + A_{exit} \left(P_{exit} - P_{atm} \right) \tag{21}$$

While the thrust tube of a pulse detonation engine may not be of a large diameter compared to that of a rocket, jet or ramjet engine it produces exit velocities considerably

higher than its comparable propulsive devices relying on a deflagration process to produce thrust.

Flammability and Limits of Ignition

The effects of varying the equivalence ratio with a variation in pressure are also examined in this study. The equivalence ratio is defined as the mass ratio of actual fuel to air, to fuel and air at stoichiometric conditions (Kuo, 2005:9):

$$\phi = \frac{\left(\frac{m_{fuel}}{m_{air}}\right)_{actual}}{\left(\frac{m_{fuel}}{m_{air}}\right)_{stoichiometric}} \tag{22}$$

where:

$0 < \phi < 1$	fuel-lean
$\phi = 1$	stoichiometric condition
$1 < \phi < \infty$	fuel-rich

At the stoichiometric condition the fuel and air mixture is completely consumed with no residual carbon dioxide, CO_2 or water, H_2O remaining after combustion. When the equivalence ratio is less than 1 the mixture is fuel lean. When the equivalence ratio is greater than 1 the mixture is fuel rich and excess fuel remains after combustion. When considering ignition time with regard to equivalence ratio, ignition time is minimal near $\phi = 1$ and increases at values of ϕ for values greater (fuel rich) or less (fuel lean) than 1. It is also important to note that the equivalence ratio is similar to the stoichiometry, Ψ of a mixture but is not identical. The stoichiometry of a mixture is defined as the ratio of mole percent of fuel in the combustible mixture to the ratio of mole percent of the fuel at stoichiometric conditions ($\Psi = X_{fuel} / X_{fuel,stoichiometric}$).

Pulse Detonation Engine Exit Nozzles

Variations on pulse detonation engine designs have been and continue to be explored but most designs are based on a central design theme. The most common configuration of the pulse detonation engine and that used in this research consists of a straight tube of sufficient length and diameter to produce the detonation wave to provide propulsive thrust. In order for the tube to produce a detonation of the fuel air mixture the tube must be of sufficient length for the initial combustion wave to form from the initial ignition and then transition from a deflagration wave to a detonation wave before exiting the tube. Various techniques have been tested and employed to reduce the ignition and deflagration to detonation process. The Schelkin spiral has been proven a highly effective device to reduce the overall deflagration to detonation process (Schultz et al, 1999:9). Mostly a spiral wound piece of heavy gage wire, the Schelkin spiral aids in increasing turbulence and enhances flame mixing. Variations on the Schelkin spiral have also been extensively tested. A Pin spiral is a series of struts extending across the diameter of the tube in a sequentially helical arrangement. Another arrangement commonly referred to as the chin spiral consists of one or more straight sections of similar diameter wire axially welded to the outer diameter of the helical spiral core to also aid in the deflagration to detonation process. The devices added to the interior of the pulse detonation tube all share a common purpose of decreasing the deflagration to detonation process. Devices which aid in the promotion of turbulence and flame mixing have all been shown to aid in decreasing the deflagration to detonation distance (Schultz et al, 1999:3). The drawback of use of such devices is that while they reduce the overall deflagration to detonation

process they can also contribute to losses in the mass induced flow behind the detonation wave as it exits the tube much the same way surface roughness can have effect on flow of a fluid medium in a pipe. The addition of the Schelkin spiral also contributes to a decreased cross sectional flow area down the length of the detonation tube. The corresponding reduced flow area results in less thrust.

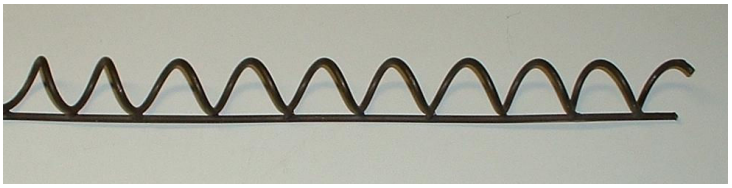

Figure 10. Schelkin Spiral

The research proposed in this report examines the possibility of reducing the deflagration to detonation distance by altering the dimensions and flow characteristics of the detonation tube so as to vary the free stream stagnation pressure inside the tube. Both ignition (or induction time) and deflagration to detonation (DDT) times have both been shown to exhibit a variation with initial pressure suggesting that potential increases in performance could be obtained through pressure changes (Schultz and Shepherd, 1997:204).

Table 2. Hydrogen-Air, varying initial pressure (T_1 = 295K, ϕ = 1, diluent = 55.6%)

P_1 (bar)	V_{CJ} (m/s)	P_{CJ} (bar)	T_{CJ} (K)	a_{CJ} (m/s)	γ_{CJ}	M_{CJ}
0.2	1935	3.1	2826	1067.1	1.160	4.767
0.4	1951	6.2	2880	1078.0	1.170	4.807
0.6	1960	9.4	2910	1084.4	1.170	4.830
0.8	1967	12.6	2931	1088.9	1.170	4.845
1.0	1971	15.8	2948	1092.2	1.170	4.857
1.2	1975	19.0	2961	1094.9	1.180	4.867
1.4	1978	22.2	2971	1097.2	1.180	4.874
1.6	1981	25.4	2981	1099.1	1.180	4.881
1.8	1984	28.7	2989	1100.8	1.180	4.887
2.0	1986	31.9	2996	1102.3	1.180	4.892

Table 2 shows how the effects of initial pressure can affect C-J properties and speeds (Schultz and Shepherd, 2000:204). From chemical kinetics ignition time can be related to the inverse of the reaction rate according to (Lefebvre et at, 1986:6):

$$\text{Ignition Time: } \tau_{ign} \propto \frac{1}{RR} \quad \text{where } RR = AT^{0.5} e^{-E/RT} \left[\text{Fuel}\right]^a \left[\text{Oxygen}\right]^b p^n \tag{23}$$

$$\text{or: } \tau_{ign} \propto \frac{1}{A} e^{E/RT} \left[\text{Fuel}\right]^{-a} \left[\text{Oxygen}\right]^{-b} p^{-n} T^{-0.5} \tag{24}$$

where:

A = *P*re-exponential Constant
E = Activiaton Energy
R = Universal Gas Constant
p = pressure
T = Temperature
$a + b$ = Reaction Order
n = experimentally determined constant (~ 0.5 to 2.5)

Using the above relationship it can be shown that ignition time can vary depending upon the pressure (atmospheres), temperature, and the fuel and oxygen concentrations based on volume.

Use of mechanical pre-compression is used quite extensively in a variety of modern engine designs either by turbo-charging or supercharging a normally aspirated internal combustion engine, or by use of a compressor rotor on a jet aircraft or turbine powered engine. The design of the pulse detonation engine is such that the combustion processes are initiated at close to atmospheric conditions and attempts to increase the initial pressure at ignition simply result in overfilling the detonation tube with little increase in pressure. In recent years several experimental and computational research studies have investigated the effects of nozzle attachments on PDE performance.

Kailasanath has presented a detailed review and summary of findings from much of this research (Kailasanath, 2001). One approach to increasing the initial pressure of the PDE is to augment the detonation tube with a restrictive device such that when the tube is filled on the fill portion of the cycle, the fuel/air mixture flowing into the detonation tube is restrained in an optimal manner so as to generate an increased pressure differential over the ambient surroundings of the operating environment. A hypothetical nozzle attachment providing some form of convergence, or decrease in diameter less than that of the detonation tube could provide a viable means to increase pressure. If the nozzle were a converging-diverging attachment to the detonation tube of a form similar to the design of the modern rocket engine nozzle the potential exists to both increase the pressure of the detonation tube at ignition and also augment the thrust at the nozzle exit via an optimally designed diverging nozzle.

The unsteady pulsing or intermittent thrust production of the pulse detonation engine, while effective at producing a very high rate of energy release from the detonation wave to produce thrust, presents several challenges with regard to analysis and PDE nozzle design. Most analytical studies have been based on computational fluid dynamics with differing nozzle configurations used for analysis (Yungster, 2003:1). Factors such as injection pressure, chamber pressure and ambient pressure all have the potential for significant influence on the experimental and analytical observations of detonation initiation. Cambier and Tegner examined the effects of various diverging nozzles on PDE efficiency for single and multiple cycles (Yungster, 2003:1). Using a detonation tube with a nozzle filled with a stoichiometric hydrogen-air mixture Cambier and Tegner

were able to computationally demonstrate the performance benefits associated with a single thrust pulse. Eidelman and Yiang numerically studied various converging and diverging nozzles using stoichiometric C_2H_2 and air mixtures on a single detonation pulse with results showing that both converging and diverging nozzles can increase PDE performance at the expense of achieving higher cyclic PDE engine efficiency for converging and straight nozzles (Yungster, 2003:1). Diverging nozzles were shown to exhibit a higher impulse while still achieving higher cycling frequency. For single-pulse operation bell shaped nozzles were shown to produce the highest performance. Several of the studies reviewed by Kailasanath observed conflicting and contradictory conclusions (Yungster, 2003:1). In general all of the studies that considered convergent nozzles showed shock reflections that propagated upstream and interfered with the fill process, a problem that requires further examination for a solution. Divergent nozzles were found to give higher impulse although in most cases occurring later in time possibly affecting cycle frequency for a multi-cycle system with a single thrust tube. With regard to divergent nozzles a bell shaped nozzle similar to the diverging nozzle of a rocket engine showed the highest increases in performance.

In another separate study Barbour examined single pulse detonation tube performance at initial pressures equal and greater than ambient pressure conditions of 1 atmosphere with a converging-diverging nozzle. Local heat flux was determined to be a significant factor in overall energy release at blow down, highly so when a converging-diverging nozzle was considered. Lower increases in specific impulse were noted at low initial pressures near ambient pressure conditions. The effects of the nozzle showed

greater overall beneficial performance in specific impulse at higher initial pressures of 2 atmospheres (Barbour and Hanson, 2005:1). .

Several computational studies indicated the rate of relaxation of the internal detonation tube pressure to ambient conditions was a limiting factor on performance. Higher specific impulse could be achieved through a slower rate of relaxation through the use of straight nozzles. Studies with the diverging nozzle suggest that diverging nozzles have the potential for better performance because of the larger effective exit area for thrust to act at the expense of a slower relaxation rate. The larger area of the nozzle also contributes to adverse performance effects from an increase in cross section drag and additional weight.

When adding a nozzle of any type to a straight pulse detonation tube the blow down process of purging and refilling the tube becomes a significant portion of the overall cycle. The process of filling the tube on the fill cycle has a longer duration in that the residual combustion products and/or ambient air from the purge cycle must be forced out of the tube for the fuel/air mixture to fill the tube in preparation for the fire cycle. The purge cycle poses a challenge in that the purge cycle helps to cool the detonation tube and purge the products of combustion in preparation for the fill cycle. Multiple thrust tubes provide for potential alternate solutions to longer cycle times in that each tube cycle could operate on different cycle phases. Each tube could produce a higher overall impulse on the fire portion of the PDE cycle when considering nozzles of differing converging and diverging area ratios.

Nozzle Orifice Fluid Flow Dynamics

Most of the studies presented have examined the effects of nozzles of various converging and diverging area ratios and have also examined the effects of increased initial detonation tube pressure on detonation tube performance. Performance parameters in most studies examined the effects of specific impulse and thrust on detonation tube performance. The focus of the experimental study conducted in this research was to examine the effects varying pressure on the performance parameters of ignition and deflagration to detonation transition (DDT) time while using a nozzle appended to the end of a pulse detonation tube in various initial conditions of multi-cycle tests. While several studies noted above have examined the effects of converging-diverging nozzles, the nozzles or flow restriction devices used this study consisted of a flow restriction orifice attached to the tube exit. Performance parameters of thrust or specific impulse were not considered in this study. Orifice diameters of incrementally varying sizes were attached at the tube exit and both flow characteristics and performance parameters of ignition and DDT times were examined. If the possibility exists to decrease both ignition and DDT time with the PDE cycle it might also be possible to increase the multi-cycle frequency and produce a corresponding increase in thrust from an increase in frequency of the thrust pulses.

Flow through an orifice attached to the end of single detonation tube creates a flow restriction similar to an orifice plate used to regulate pressure and mass flow rate. A schematic representation of orifice-type plate attached to the exit of the pulse detonation tube is shown in Figure 11. As the flow exits through the pulse detonation tube, the flow

contracts through the nozzle orifice to a diameter less than that of the orifice throat diameter. The characteristic *vena contracta* at the nozzle exit increases the flow velocity exiting the nozzle as shown by velocity at section 2 and also increases the pressure at station 1 by limiting the mass flow rate. While an exit nozzle of this geometry is not an optimal configuration to examine performance parameters of thrust or specific impulse it does provide an effective means of controlling the stagnation pressure within the detonation tube.

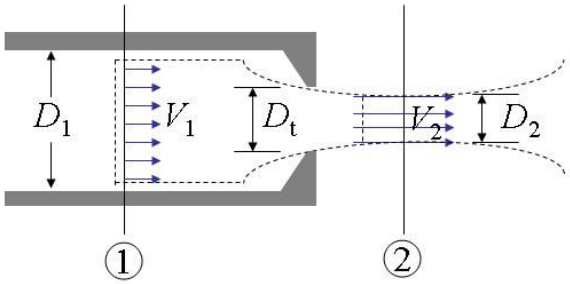

Figure 11. PDE nozzle exit orifice restriction

Given that the nozzle exit is acting as a flow-obstruction device it is possible to relate mass continuity and the Bernoulli equation to obtain a pressure drop, Δp across the nozzle exit for a given mass flow rate and nozzle orifice area at a given instant in time. If the pressure drop, Δp is related by the difference between the internal tube pressure at station 1 and the ambient or external back pressure acting at station 2 it is possible to characterize how the pressure inside the detonation tube is able to vary with nozzle orifice size and mass flow rate in the tube. Considering one-dimensional flow the continuity relation can be described by (Holman, 2001:291):

$$\dot{m} = \rho_1 A_1 u_1 = \rho_2 A_2 u_2 \tag{25}$$

Assuming $\rho_1 = \rho_2 = \rho$ for adiabatic and frictionless and incompressible flow the Bernoulli equation can be written as (Holman, 2001:291):

$$\frac{p_1}{\rho} + \frac{u_1^2}{2g_c} = \frac{p_2}{\rho} + \frac{u_2^2}{2g_c} \qquad \text{where } g_c = 1 \text{ kg m/N s}^2 \text{ in SI units} \tag{26}$$

It is then possible to solve the Bernoulli equation and mass flow relation to obtain a relationship for the ideal pressure drop (Holman, 2001:291):

$$\Delta p = p_1 - p_2 = \frac{u_2^2 \rho}{2g_c}\left[1 - \left(\frac{A_2}{A_1}\right)^2\right] \tag{27}$$

Solving for the velocity at station 2, u_2 and factoring in the area at station 2, A_2 it is possible to determine the volumetric flow rate, Q in terms of the flow areas and pressure drop, Δp (Holman, 2001:291):

$$Q = A_2 u_2 = \frac{A_2}{\sqrt{1 - \left(A_2/A_1\right)^2}} \sqrt{\frac{2g_c}{\rho}\left(p_1 - p_2\right)} \tag{28}$$

While the above relationship for volumetric flow rate represents ideal conditions it is more important to know how ideal flow is related to actual flow. An empirical discharge coefficient is used to relate the two parameters and is given by (Holman, 2001:292):

$$C = \frac{Q_{actual}}{Q_{ideal}} \tag{29}$$

The discharge coefficient varies as a function of Reynolds number and diameter ratio D_t / D_1. When ideal gas flow is considered, the ideal gas law given by $p = \rho RT$ can be applied to the steady flow energy equation for reversible adiabatic flow for an ideal gas (Holman, 2001:292):

$$c_p T_1 + \frac{u_1^2}{2g_c} = c_p T_2 + \frac{u_2^2}{2g_c} \tag{30}$$

Combining the equation for continuity the steady flow energy equation above and the ideal gas law and recognizing $\dot{m} = \rho Q$ a relation for mass flow can be derived (Holman, 2001:292):

$$\dot{m}^2 = 2g_c A_2^2 \frac{\gamma}{\gamma - 1} \frac{p_1^2}{RT_1} \left[\left(\frac{p_2}{p_1} \right)^{2/\gamma} - \left(\frac{p_2}{p_1} \right)^{\gamma + 1/\gamma} \right] \tag{31}$$

If the velocity of approach at station 1 is assumed small the above relationship can be simplified to (Holman, 2001:292):

$$\dot{m} = \sqrt{\frac{2g_c}{RT_1}} A_2 \left[p_2 \Delta p - \left(\frac{1.5}{\gamma} - 1 \right) (\Delta p)^2 + \ldots \right]^{1/2} \tag{32}$$

where $\Delta p = p_1 - p_2$ and the ratio of specific heats is given by $\gamma = c_p / c_v$.

When $\Delta p < p_1/10$ further simplification of the above equation gives (Holman, 2001:292):

$$\dot{m} = A_2 \sqrt{\frac{2g_c}{RT_1} (p_1 - p_2)} \tag{33}$$

When $\Delta p \ll p_1$, the above relation may be used to approximate the flow of a compressible fluid in the same manner as an incompressible fluid.

When considering the flow of a compressible fluid such as a fuel/air mixture an additional parameter must be considered. For a nozzle orifice attached to the exit of the detonation tube as used in this research an empirical relation is given by considering an *expansion factor*, *Y* as (Holman, 2001:293):

$$Y = 1 - \left[0.41 + 0.35 \left(\frac{A_2}{A_1} \right)^2 \right] \frac{p_1 - p_2}{\gamma p_1} \tag{34}$$

From the above relations a semi-empirical relation can derived for a nozzle orifice in compressible flow (Holman, 2001:294):

$$\dot{m}_{actual} = YKA_2 \sqrt{2 g_c \rho_1 \left(p_1 - p_2 \right)} \tag{35}$$

where: $$M = \frac{1}{\sqrt{1 - \left(A_2 / A_1 \right)^2}} = \text{velocity of approach factor} \tag{36}$$

and: $$K = CM = \text{flow coefficient}$$

Solving for the pressure drop across the nozzle exit in terms of the upstream mass flow rate:

$$\Delta p = p_1 - p_2 = \frac{1}{2 g_c \rho_1} \left(\frac{\dot{m}_{actual}}{YKA_2} \right)^2 \tag{37}$$

The diameter and corresponding area at station 2 is unknown and more pronounced from the vena contracta of the flow exiting the flow nozzle and limits the ability to accurately pressure drop for a given mass flow rate or mass flow rate for a given pressure drop. The diameter at station 2 is generally equated to the throat diameter, D_t and all flow effects are considered in the estimate of the flow coefficient, K.

In considering compressible flow and high flow rates the pressure differential becomes too large and sonic flow conditions dominate at the minimum flow area and the flow becomes choked. The flow rate then becomes a function of the given inlet conditions at a maximum value. The pressure ratio for a given Mach number is represented by the isentropic relation (Holman 2001:305):

$$\frac{p_1}{p_2} = \left(1 + \frac{\gamma - 1}{2} M^2\right)^{\gamma/(\gamma-1)} \tag{38}$$

where M represents the Mach number at the throat and p_1 is the total or stagnation pressure upstream of the shock. At a choked flow condition the Mach number at the nozzle orifice exit plane is sonic and equal to 1 (Holman 2001:305):

$$\left(\frac{p_2}{p_1}\right)_{\text{critical}} = \left(\frac{2}{\gamma + 1}\right)^{\gamma/(\gamma-1)} = 0.5283 \text{ for air with } \gamma = 1.4 \tag{39}$$

Combining the above equation with equation (31) gives the mass flow rate for a choked nozzle condition (Holman 2001:305):

$$\dot{m} = C_D A_2 p_1 \sqrt{\frac{2g_c}{RT_1}} \left[\frac{\gamma}{\gamma + 1}\left(\frac{2}{\gamma + 1}\right)^{2/(\gamma-1)}\right]^{1/2} \tag{40}$$

The above equation shows that mass flow rate is dependent upon the upstream stagnation conditions only calculated from the upstream temperature and pressure. Equation (40) above becomes an important factor when considering the pulse detonation engine cycle. When the nozzle exit becomes choked a change in mass flow rate is dependent upon the upstream stagnation temperature and pressure conditions. This becomes an important limiting factor when successfully filling and purging the detonation tube. On the fill portion of the cycle the fuel/air mixture flows into the tube increasing the pressure and forcing the existing ambient air from the tube. If the pressure increases high enough the nozzle exit becomes choked and the tube completes only a partial fill before the fill valve closes and the fire cycle begins with ignition of the fuel/air mixture. Using equation (37) for flow through an orifice it is possible to estimate the pressure drop, Δp at the nozzle

for a given mass flow rate. A family of curves similar to that shown below in Figure 12 can be produced to estimate flow conditions for a given density, expansion factor, flow coefficient and nozzle orifice size, D_2/D_1 (the ratio of nozzle orifice to tube diameter, and also making the assumption $D_t \approx D_2$). Given the cyclic nature of the pulse detonation engine and variable mass flow rate Figure 12 serves to illustrate the variation in pressure of a nozzle appended to the end of at detonation tube with a varying mass flow rate.

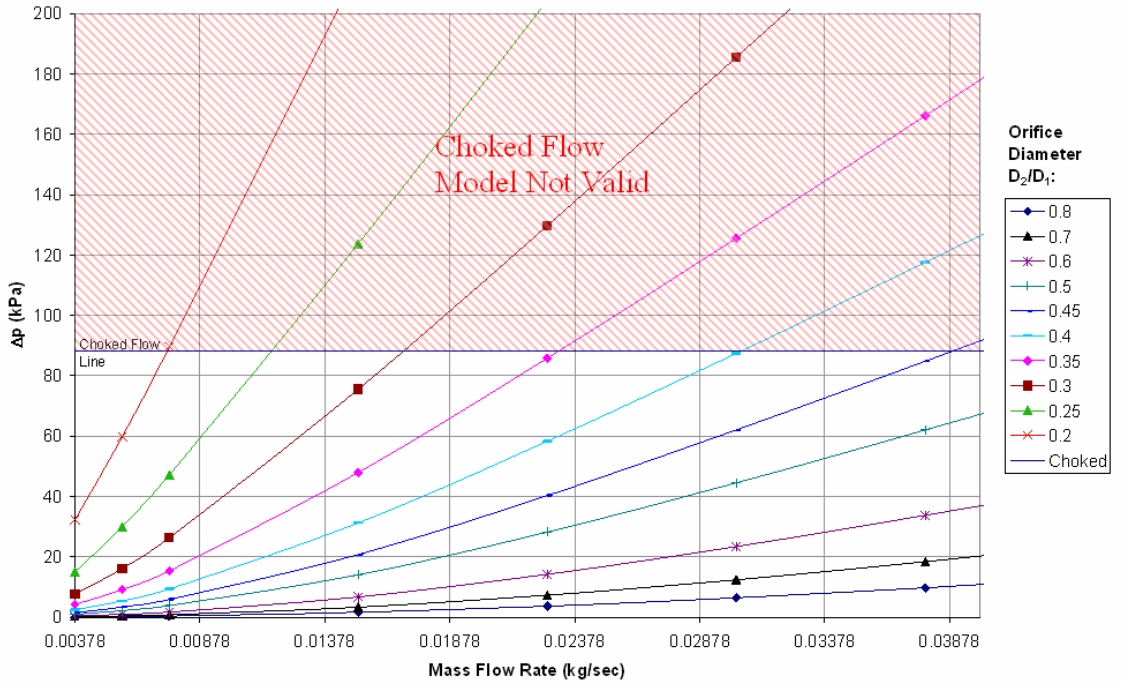

Figure 12. Pressure drop (Δp) versus mass flow rate for varying nozzle orifice diameters

Cylinder Head Poppet Valve Flow Dynamics

Upstream of the nozzle exit at the head of the detonation tube the fill and purge valves are continuously opening and closing to fill the tube with the fuel/air mixture and purge the combustion products from the tube in multi-cycle operation. Similar to the nozzle exit the fill and purge valves upstream of the can be characterized by compressible

flow equations. The Quad 4 cylinder head is a standard cylinder head with a dual overhead camshaft. As when installed in an automobile engine each camshaft independently opens and closes a set of 8 purge and 8 fill valves. The camshaft lobes are each geometrically designed for given lift and duration. The lift of a camshaft lobe refers to the overall distance the valve will be moved off the seat at maximum lift. The duration of a camshaft lobe describes how long the valve will be off the seat for a given cycle frequency the camshaft is rotated.

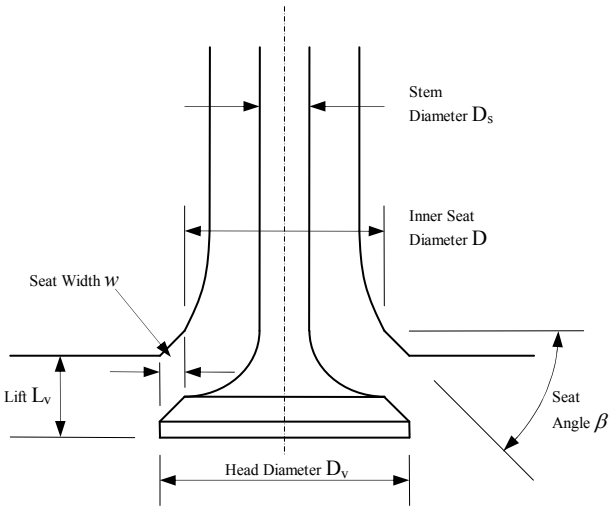

Figure 13. Cylinder head poppet valve geometry

Valve geometry is a significant part of flow through an automotive cylinder head. The valve geometry is defined above by Figure 13. The instantaneous flow area around the valve depends on several other factors in addition to lift and include the geometric details of the valve head, seat, and stem. A larger valve flow area provides for a higher flow rate and is a limit if the valve chokes the flow upstream of the cylinder head chamber.

There are essentially three separate stages of the flow area as the valve lift increases (Heywood, 1988:222). At low valve lift the minimum flow area defined corresponds to a frustrum of a right circular cone between the conical face of the valve and the seat, which is perpendicular to the seat. At this stage (Heywood, 1988:222):

$$\frac{w}{\sin\beta\cos\beta} > L_v > 0 \tag{41}$$

The minimum area at this stage of lift is given by (Heywood, 1988:222):

$$A_m = \pi L_v \cos\beta\left(D_v - 2w + \frac{L_v}{2}\sin 2\beta \right) \tag{42}$$

The second stage of lift has a minimum area given by the slant surface of a frustrum of a right circular cone with the slant surface no longer perpendicular to the valve seat. The base angle of the cone increases from $\left(90-\beta\right)^\circ$ to that of a cylinder at 90° (Heywood, 1988:222):

$$\left[\left(\frac{D_p^2 - D_s^2}{4D_m}\right) - w^2\right]^{1/2} + w\tan\beta \geq L_v > \frac{w}{\sin\beta\cos\beta} \tag{43}$$

The area for the second stage of lift is then given by (Heywood, 1988:222):

$$A_m = \pi D_m\left[\left(L_v - w\tan\beta\right)^2 + w^2\right]^{1/2} \tag{44}$$

where D_p is the port diameter, D_s is the valve stem diameter, and D_m is the mean seat diameter $\left(D_v - w\right)$.

The final stage of lift occurs when the minimum flow area is no longer defined between the valve head and valve seat. At this stage the flow rate is limited to the

difference between the port flow area and the cross sectional area of the valve stem (Heywood, 1988:224):

$$L_v > \left[\left(\frac{D_p^2 - D_s^2}{4D_m}\right) - w^2\right]^{1/2} + w\tan\beta \tag{45}$$

The flow area is then described by (Heywood, 1988:224):

$$A_m = \frac{\pi}{4}\left(D_p^2 - D_s^2\right) \tag{46}$$

In the same manner for describing flow through the nozzle orifice at the tube exit the flow through cylinder head valves can described using the same compressible flow equations through a flow restriction. Derived from the same one dimensional isentropic analysis with real gas flow effects and an experimentally determined discharge coefficient included, the air flow rate can be related to the upstream stagnation pressure p_0 and stagnation temperature T_0, static pressure downstream of the flow restriction, p_T and a reference area A_R characteristic of the valve design. The mass flow rate through the valve can then be characterized with the following equation (Heywood, 1988:226):

$$\dot{m} = \frac{C_D A_R p_0}{\left(RT_0\right)^{1/2}}\left(\frac{p_T}{p_0}\right)^{1/\gamma}\left\{\frac{2\gamma}{\gamma-1}\left[1-\left(\frac{p_T}{p_0}\right)^{(\gamma-1)/\gamma}\right]\right\}^{1/2} \tag{47}$$

For choked flow, $p_T / p_0 \le \left[2/(\gamma+1)\right]^{\gamma/\gamma-1}$ the equation then becomes (Heywood, 1988:226):

$$\dot{m} = \frac{C_D A_R p_0}{\left(RT_0\right)^{1/2}}\gamma^{1/2}\left(\frac{2}{\gamma+1}\right)^{(\gamma+1)/2(\gamma+1)} \tag{48}$$

For flow through the intake valve p_0 is the upstream intake manifold pressure upstream of the fill valve and p_T is the downstream detonation tube pressure. The experimentally determined discharge coefficient, C_D and the reference area, A_R make up the effective flow area. The reference area used can be from any three of the above equations (42), (44) or (46) for the three stages of valve lift depending on the portion of the cycle considered. The geometric flow area is characterized by a complex function of valve and valve seat dimensions, and valve lift. A convenient and often used reference area in the interest of simplicity is the valve curtain area which is simply the valve head area times the distance the valve is off the seat as it varies linearly with valve lift (Heywood, 1988:226):

$$A_C = \pi D_v L_v \tag{49}$$

If a pressure drop down the length of the detonation tube is known per given orifice restriction it is possible to relate p_T from equation (47) and p_1 from equation (35) and relate the manifold pressure to the mass flow rate through the nozzle orifice at a given instant of time during the PDE cycle.

Tube Fill and Fill Fraction

Operation of the PDE involves filling the detonation tube with a fuel/air mixture followed by ignition, detonation and thrust from the mass induced flow exiting the detonation tube. The fill fraction of pulse detonation engine used in this research is defined as the ratio of the volume of the tube filled with fuel and air mixture on the fill

portion of the cycle to the volume of air that fills the tube on the purge at atmospheric conditions to the actual volume of the tube:

$$Fill\ Fraction = FF = \frac{\text{Volumetric amount of gas flowed into tube at 1 atm}}{\text{Actual tube volume}} \quad (50)$$

The fill fraction is an important parameter for PDE operation. It defines how the engine control system correctly meters the proper proportion of fuel/air mixture on the fill cycle in preparation for ignition on the fire cycle. If the fill fraction is equal to 1 then the system meters the correct amount of fuel/air mixture at the predetermined equivalence ratio to ideally fill the detonation tube completely with no excess before ignition. If the fill fraction is increased to 2 the system meters an appropriate amount of fuel air mixture to fill the tube by twice the volume. In the case of a detonation tube with no restriction or nozzle attached to the end of the tube for a fill fraction of 2 the tube is filled once on the fill cycle and then filled again by the second volume of fuel/air mixture at atmospheric conditions. Essentially the excess fuel/air mixture from the first volume of fill is pumped out of the tube in preparation for the second volumetric flow of fuel/air mixture at atmospheric conditions. The flow passes through the tube largely unrestricted with the exception of frictional wall effects on pressure which can generally be represented by the equation for total head loss from frictional effects in fully developed and constant area tubes (Fox et al, 2003:336):

$$\frac{P_{head} - P_{\infty}}{\rho_{air}} = \frac{V_{exit}^2}{2}\left(1 + f\left(\frac{L_e}{D}\right) + K_{nozzle\ loss}\right) \quad (51)$$

where:

f = friction factor

L_e = effective tube length

D = tube diameter

$K_{nozzle\ loss}$ = nozzle loss coefficient

V_{exit} = exit velocity

The above equation also shows that an increased pressure differential is possible for a given length of tube when considering flow in an open detonation tube. If the tube is of sufficient length it is possible to increase the pressure at the closed tube head without a flow restriction at the nozzle exit.

When adding a restrictive device to the exit of the pulse detonation tube an amount of fuel/air mixture is restrained in the tube and the pressure is increased per unit time. Conceptually, if the tube were completely closed at the exit end of the tube and flow were introduced into the tube at a fill fraction of 2 with 1 atmosphere of gas (air) already filling the tube the tube would be filled at 2/3 of fuel/air mixture at the proper equivalence ratio. In the same scenario if the closed tube were filled with a fill fraction of 3 at 1 atmosphere of gas already present in the tube the tube would be ¾ full of fuel/air mixture as shown by the ideal gas law, $P = \rho RT$ that pressure is proportional to density and inversely proportional to volume.

When a flow restriction device such as a nozzle is added to the exit of the detonation tube some amount of initial flow in the tube is restrained in the tube for a given nozzle orifice size and the pressure is increased when flow is introduced to the pulse detonation tube. On the fill cycle the tube is initially filled with the ambient air and the fuel air mixture is then introduced into the detonation tube at a given fill fraction. The fuel/air mixture begins to flow into the detonation tube raising the pressure. For a

given nozzle size, the flow at the exit of the tube through the nozzle orifice begins to flow from the exit of the tube. The exact amount of flow from the detonation tube, or tube blow down, is a function of nozzle orifice size, upstream and downstream (ambient) pressure, and nozzle loss and expansion/contraction effects. The time for the tube to blow down to ambient pressure is a function of the initial pressure and the nozzle exit orifice size. If the flow is choked the mass flow exiting the tube is still a function of nozzle orifice size and nozzle loss effects but only the upstream pressure determines how much flow exits the tube during the fill cycle.

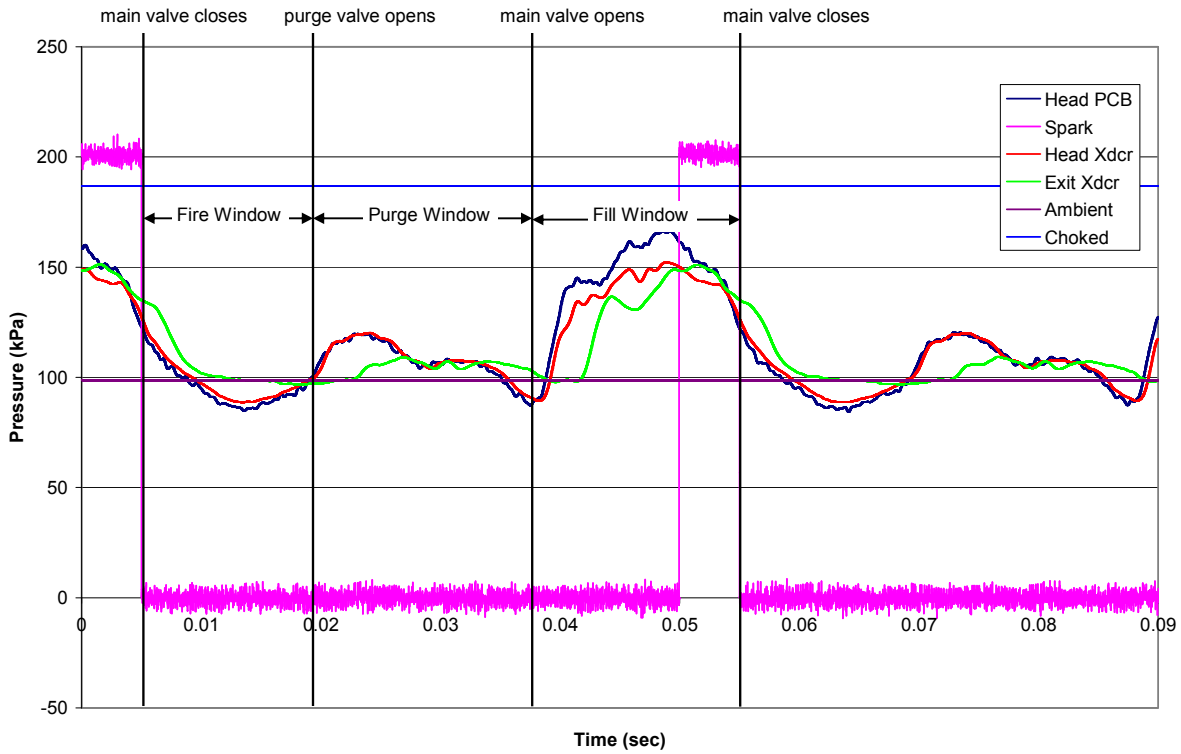

Figure 14. PDE cycle pressure trace versus time ($D_2/D_1 = 0.75$, spark delay = 0, FF = 2.5)

Attachment of a flow restrictive device the nozzle exit results in a different pressure and transient flow condition from the non-restricted open tube case. Because the flow is restricted through a nozzle at the tube exit, both the fill and purge cycles result in

increasingly larger amplitude of pressure pulse to maintain the same system mass flow rate for a predetermined fill fraction. Both the intake manifold pressure and the tube transient maximum pressure peaks on the fill and purge portions of the cycle will increase to maintain the same flow condition as can be seen in Figure 14 where the intersection of the head PCB dynamic pressure transducer trace and the vertical line detonating where the main valve closes. In the figure the closing of the main fill valve also represents where the spark discharge occurs for a zero millisecond delay. The internal tube pressure can be increased with by decreasing the nozzle size or by increasing the fill fraction for a given nozzle size until the detonation tube flow becomes choked at the nozzle exit and any change in mass flow rate becomes a function of the upstream tube pressure inside the tube.

The spark discharge is represented where the second vertical line occurs as shown in Figure 14 above. The preceding vertical line represents the charge applied to the ignition coil to force the spark to discharge through the spark plug gap in the cylinder head. When a spark delay greater than zero milliseconds is preset the spark trace (also referred as the z-pulse) moves to the right in relation to the pressure trace, crossing at a different pressure where the second vertical discharge line intersects the pressure trace.

III. Facilities and Instrumentation

Facility and Engine Control System

The Pulse Detonation Research Facility, Building 71A, D Bay, part of the Air Force Research Laboratory, Propulsion Directorate (AFRL/PR) is a converted, explosion proof aircraft turbojet engine test facility with high capacity inlet and exhaust stacks located at Wright-Patterson Air Force Base, Ohio. The converted jet engine test facility has since been converted and modified for pulse detonation engine research. The facility has a test bay with a static thrust test stand capable of measuring thrust up to 60,000 lbf (267 kN). For pulse detonation engine testing a smaller 1000 lbf (4.45 kN) damped thrust stand was installed above the larger engine test stand to accommodate the lower and more sensitive thrust levels produced by the pulse detonation engine. A fuel room is located adjacent to the to the test cell and control room for liquid fuel supply to the test apparatus.

A control room and fuel room sit adjacent to the test bay behind a 2 ft (0.61 m) thick reinforced concrete barrier wall, to protect personnel during testing, and contains all engine monitoring and control equipment. A facility specific control panel (Figure 15) and LabView control software installed and run on two separate personal computers provide the input interface for all engine input control parameters. Real time high speed data was recorded through 16 available, 5MHz each data acquisition channels using a LabView, *Online Wave Speed* program developed in house at AFRL/PRTC for pulse detonation engine research and development. The *Online Wave Speed* program has capability for a variety of sensor inputs to include spark pulses, pressure transducers, ion probes, and thermocouple data.

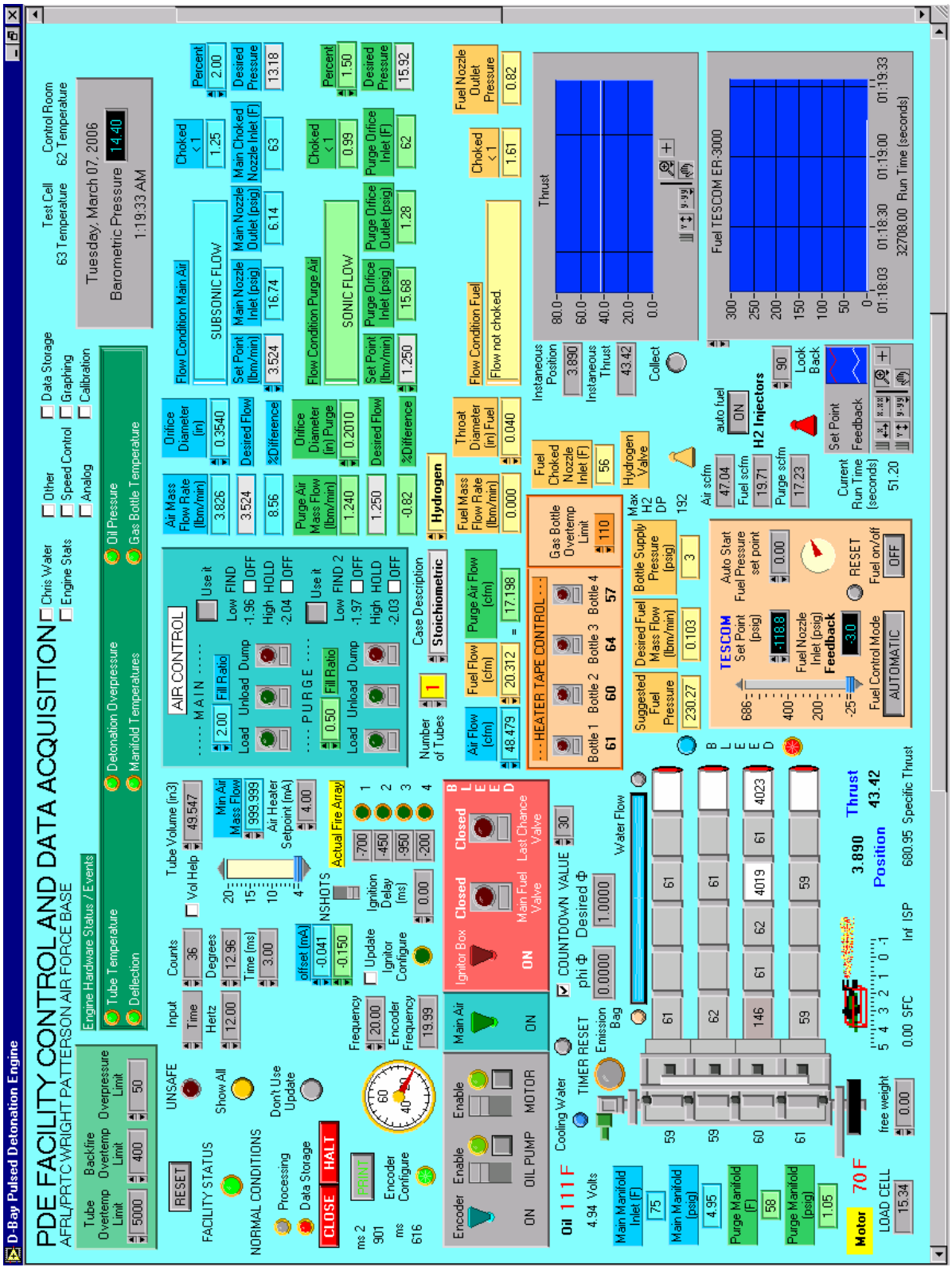

Figure 15. Engine Control Panel

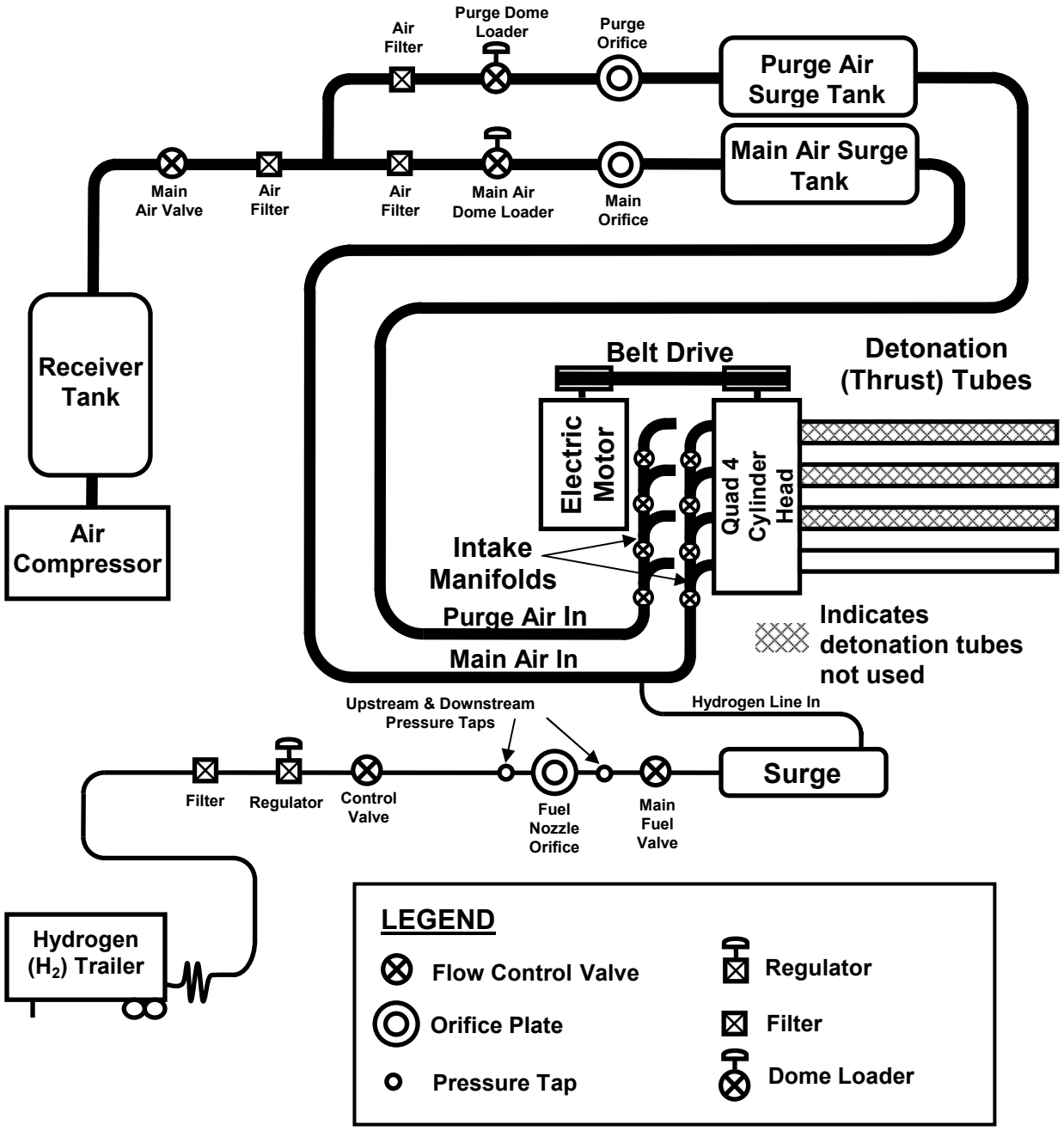

Figure 16. PDE hydrogen and air supply system schematic

PDE Engine Test Rig and Supply System

The engine test stand for pulse detonation engine testing consists of a General Motors Quad 4 cylinder head positioned with the valve ports in a horizontal direction. An electric motor providing 0.5 to 50 Hz through a belt driven pulley arrangement rotates the dual overhead camshaft (DOHC) arrangement to open the valve for both fill and purge. Two valves for fill (automotive intake valve) and two valves for purge (automotive exhaust valve) per cylinder are used for fuel and air supply to the detonation tubes throughout the three part cycle of fill, fire and purge. Each tube is mounted horizontally to the cylinder head to where the automotive engine block and pistons would normally operate in front of the cylinder head.

Air Supply

Compressed air for both the fill and purge portions of each cycle is supplied by one of two selectable Ingersoll-Rand PAC AIR 3000 air compressors capable of supplying 6 lb/sec (2.72) kg/sec at 100 psia (0.69MPa) as shown in Figure 16. After passing through the 6.4 m^3 receiver tank where the compressed air is stored the air flow passes through the main air valve, an air filter and then branches into both the main (fill) and purge flow supply lines. Each flow independently passes through another air filter, through a dome loader, an orifice plate and a surge tank before passing through the cylinder intake manifold to flow into the cylinder head. The orifice plates are used in conjunction with the dome loaders to actively regulate the air supply mass flow rate and pressure upstream of the cylinder intake manifolds by the engine control panel in the control room. For testing two selected orifice plates are used at 0.201 in (5.1054 mm)

diameter and 0.354 in (9 mm) diameter. The 0.201 in diameter orifice plate is used for fill fractions of 2 but is replaced for increased fill fractions at the upstream supply pressure supplied by the air compressor output. For optimal flow control the orifice plate must remain choked for all flow conditions. The air flow supply system has the ability to operate the orifice plates at the un-choked subsonic flow condition but with a less accurate and less responsive ability to control the flow when considering changing flow conditions. The engine control panel on the facility computer calculates and calibrates the flow rate set by the user input. The purge and main orifice plates can be changed to accommodate large changes in required mass flow rate. At each cylinder intake manifold are separate flow control valves to independently control the fuel/air supply to each cylinder. The intake manifold flow control valves can be independently opened or closed to test any number of 1 to 4 detonation tubes desired. The cylinder valves are opened and closed by the automobile camshafts rotated by the belt drive connected to the electric motor.

Fuel Supply

Hydrogen is used as the fuel for all researching and testing in this report as it is relatively easy to detonate, considerable data already exists for comparison, and can be described by a simple chemical reaction when compared to most available hydrocarbon fuels. Liquid hydrocarbon fuels and most military grade turbine fuels require a complex system for atomization or mixing of the fuel or the use of a flash vaporization system for use in a pulse detonation engine. The hydrogen is stored externally on a hydrogen trailer of approximate volume 15.7m^3 with 38 separate hydrogen bottles each supplying 16.6

MPa of initial pressure. The hydrogen supply bottles are stored externally to the facility on a truck trailer and supply pressure for testing until draining to a minimum for the particular test before being exchanged for a new bottle. When the series of valves are opened, including the main fuel valve, hydrogen is allowed to mix with the main air at a branch junction just upstream of the main (fill) cylinder intake manifold. Identical to the airflow orifice plate the gaseous fuel supply system also operates on a similar principle of choked nozzle orifices to regulate flow. A nozzle orifice of 0.027 in (0.6858 mm) diameter regulates flow for a fill fraction of 2 with a 0.040 in (1.016 mm) diameter nozzle regulating fill fractions of greater than 2 for this research. Injection of the hydrogen fuel far upstream of the intake manifold helps to minimize the fuel/air mixture fluctuations that can result from the pulsating air mass flow rate of the intake valves opening and closing.

Air and Fuel Flow Control Calculations

Figure 16 depicts the PDE feed system the fill and purge valves supplied by a single air supply from a central air compressor. The hydrogen fuel is pressure fed from a trailer source external to the test facility. Both fuel and air lines feed directly into separate purge and fill manifolds upstream of the fill and purge valves in the Quad 4 cylinder head. The camshaft to open the fill and purge valves is rotated by a belt driven electric motor. The control computer continuously calculates the proper amount of fuel and air flow conditions as set by the computer by determining the total tube volume of fuel and air mixture consumed each cycle at atmospheric conditions from the measured

manifold temperature. The fuel and air flow requirements for each cycle are determined by simultaneously solving the following equations (Tucker, 2004:42):

$$\dot{V}_{total} = V_{tube} \times Frequency$$ Required volumetric flow rate (m^3/sec) (52)

$$\dot{V}_{total} = \dot{V}_{air} + \dot{V}_{fuel}$$ Volumetric flow determined by air and fuel flow (53)

$$\dot{m}_{air} = \dot{V}_{air} \frac{P_{atm}}{R_{air} T_{mix}}$$ Perfect gas relationship for air (kg/sec) (54)

$$\dot{m}_{fuel} = \dot{V}_{fuel} \frac{P_{atm}}{R_{fuel} T_{mix}}$$ Perfect gas relationship for gaseous fuel (kg/sec) (55)

$$R_{fuel} = \frac{R}{MW_{fuel}}$$ Specific gas constant for vaporized fuel (kJ/kg/K) (56)

$$T_{mix} = \frac{\dot{m}_{fuel} T_{fuel} + \dot{m}_{air} T_{air}}{\dot{m}_{fuel} + \dot{m}_{air}}$$ Mass averaged mixture temperature (K) (approx) (57)

$$\frac{\dot{m}_{fuel}}{\dot{m}_{air}} = 0.029129042$$ Stoichiometric ratio for hydrogen and air (58)

Spark Ignition System for PDE Operation

The spark used to ignite the fuel air mixture in the PDE detonation tube is provided by a 12 volt DC automotive digital ignition system through the automotive spark plug mounted in the Quad 4 cylinder head and delivered 105 to 115 milli-Joules per spark using a capacitive discharge. A 5 msec pulse is delivered every 50 msec at a cycle frequency of 20 Hertz.

Detonation Tube Setup

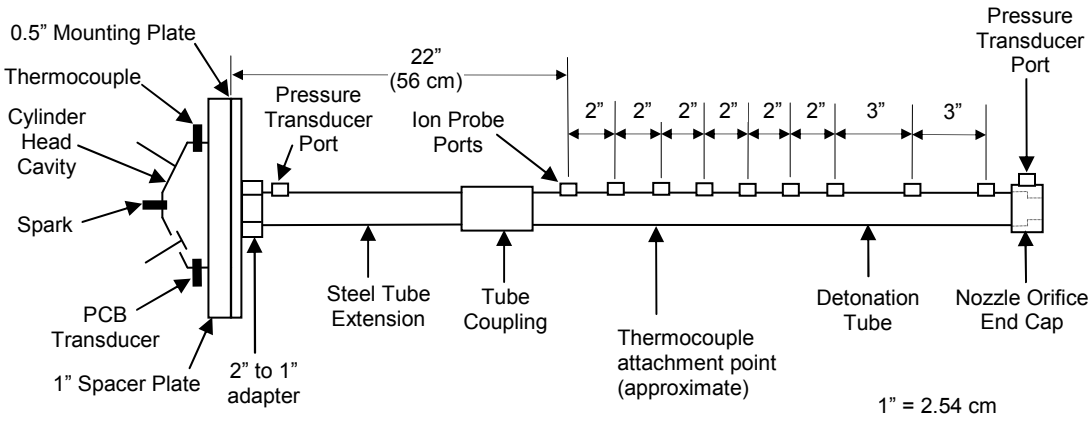

Figure 17. Experimental detonation tube setup

All testing performed in this report uses a standard 1 inch (2.54 cm) inner diameter steel tubing for the detonation tube. The 1 inch (2.54 cm) steel detonation tube mounted to the Quad 4 cylinder using a 0.5 inch (1.27 cm) thick adapter plate and 2 inch (5.08 cm) to 1 inch adapter fitting as shown in Figure 17. A 1 inch (2.54 cm) spacer plate mounted to the cylinder provided spacing between the attached detonation tubes and valve operation. The spacer and adapter plate volumes are added to the detonation tube volume for the proper fuel/air flow rate according to the preset equivalence ratio and fill fraction. Testing was initially performed using a Schelkin spiral. After initial data analysis it was experimentally observed that hot spots in the tube were possibly providing alternate sources of ignition from the forced ignition of the spark discharge. In the interest of removing the hot spots, the Schelkin spiral was removed, the tube lengthened using an extension to provide adequate distance to achieve detonation wave speeds, and final testing performed using an 18 inch (45.7 cm) long extension inserted between the adapter plate and detonation tube. The detonation tube is an identical 24 inch (61 cm)

long piece of steel tubing as the extension with the addition of ion ports welded axially down the outside of the tube to measure wave speeds.

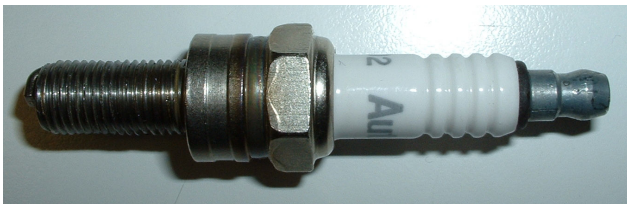

Figure 18. Autolite spark plug (part# 4302) used as ion probe

Ion Probes and Data Acquisition Cards

A conventional automobile engine spark plug is used as an ion probe sensor to measure combustion wave speeds as shown in Figure 18. The passage of the combustion wave is determined when the voltage of approximately 4.5 volts decreases sharply across the center electrode. The combustion of the fuel air mixture produces ions from the combustion process which short the spark plug electrode and allow current to flow which is read recorded using *Online Wave Speed* through a National Instruments Corporation NI PCI-6110 input board with three connected BNC-2110 input/output connector blocks. The PCI-6110 data pseudo-differential acquisition card is capable of 12 bit analog to digital input with a maximum of 5 mega-samples per second per channel with a voltage input range of ± 0.2 to ± 42 volts . The BNC-2110 and PCI-6110 data acquisition equipment also accepted inputs for the dynamic pressure transducer, ignition voltage trace and pressure measurements using the Sensotec precision gage/absolute pressure transducers.

The ion probe ports are spaced as shown in Figure 17 to measure wave speed passage using the ion probe voltage drop method. The time between the ion probes is recorded and the distance known to provide a wave speed velocity between two successive ion probe ports. Spacing of 2 inches (5.1 cm) and 3 inches (7.6 cm) apart between the remaining 3 ports to most accurately capture the wave speed velocity and detonation distance and time. Spacing too close among adjacent ion probe ports requires time measurement beyond the resolution of the measuring and data processing equipment. Spacing too large among adjacent ion probe ports provides greater difficulty in accurately measuring changes in wave speed velocity as the velocity measured is an average taken between two adjacent points given the time and distance traveled.

Ignition Time

Ignition data is determined via a dynamic pressure transducer inserted into the Quad 4 automotive cylinder head as shown in Figure 17. The dynamic pressure transducer is a PCB Piezotronics pressure transducer, model number 102M232 capable of pressure measurements calibrated to 5000 psi (34.474 MPa) at 1037 psi/volt (7.15 MPa/volt). Dynamic pressure is measured in the PCB dynamic pressure transducer through a piezoelectric quartz crystal producing an output voltage when pressure is applied. The PCB is actively cooled by coolant from the cylinder head and protected by an ablative RTV shield.

Figure 19. Example nozzle orifice end caps used to restrict flow with and without pressure tap (0.8 inch, (2.032 cm) and 0.85 inch, (2.159 cm) shown)

Nozzle Orifice Flow Restriction

For flow restriction at the detonation tube exit standard steel plumbing end caps were drilled open and machined to a range of specific diameters. Selected end caps are fitted with a threaded pressure port tap for attaching a pressure transducer as shown in Figure 19. The nozzle orifice end caps are threaded allow for easy screw-on attachment and removal to the end of the pulse detonation tube.

Figure 20. Sensotec 100 psia (0.69MPa) Model TJE/0713-10JA pressure transducer

Cold Flow (No Ignition) Tube Head and Exit Pressure Measurements

The cold flow pressure measurements to obtain the pressure measurements at the tube head and exit with no ignition were obtained using two 100 psia (0.69 MPa) Sensotec Precision Gage/Absolute Pressure Transducers, Model TJE. The Sensotec TJE pressure transducer is a strain gage based sensor that references the primary pressure sensing diaphragm to the atmosphere. Accepting a 10 volt input for operation the pressure transducer provides a 3mV/V output. The transducer output signal is amplified using a Preston 8300 XWB Series Floating Differential Amplifier and read using the *Online WaveSpeed* data acquisition software package. The data output is processed using a Savitzky-Golay filter to produce the pressure trace data for examining the no ignition cold flow through the detonation tube.

IV. Test Planning, Methods and Procedures

Development of the Baseline Test Setup

The test methods to produce the data contained in this report were developed from a trial and error process of performing testing, examining the data for conclusive data trends, and then subsequently adjusting test conditions and equipment to further examine the results. The final detonation tube setup to produce the optimal conditions for measuring combustion wave speeds consisted of an 18 inch (45.72 cm) extension coupled to a 24 inch (60.96 cm) detonation tube with ion probe ports to produce a detonation tube of total length 43 inches (109.22 cm) and 1 inch (2.54 cm) in diameter as shown in Figure 17. The 1 inch diameter, 43 inch long tube provides adequate length to produce and measure the detonation wave speeds to produce detonation wave data required of the research presented in this report.

Initially the arbitrary 2 foot long approximately 1 inch diameter tube contained a Schelkin spiral (Figure 10) and was attached to the 1 to 2 inch adapter plate and mounted to the Quad 4 cylinder head. Testing was performed, data taken using the data acquisition software package, *Online WaveSpeed* and examined, and performance trends were noted. Initial measured data showed erratic data trends for both ignition and DDT times with the Schelkin spiral installed. An additional 9 ion probe ports were added to the initial 4 ion probe ports in an attempt measure both DDT times and distances with greater resolution. It was experimentally observed that as the orifice diameter was decreased to further choke the fuel/air flow through the tube, the engine became increasingly more susceptible to a backfire condition whereby the fuel/air mixture was ignited while the fill valve was open.

Localized areas of heating, or hot spots were ultimately determined to be the source of the backfire problem both at broken welds on the Schelkin spiral and sharp edges at the ion probe port on the inner diameter of the detonation tube.

A backfire condition presents a problem of both gathering acceptable data as well as the inability to continuously run the engine and gather data. Localized hot spots, or alternate sources of ignition within the detonation tube will ignite the fuel/air mixture while the detonation tube is being filled on the fill cycle as well as providing an ignition source at a location other than the head of the detonation tube. If the fuel/air mixture is ignited at the midpoint of the tube for example, a combustion wave will begin to travel in both directions of the tube, neither of which will cause a detonation and provide for a less than optimal thrust and performance condition. The purge portion of the PDE cycle provides for cooling of the detonation tube and cleansing of the combustion by-products in preparation for the fill cycle. As the end of the detonation tube is choked by decreasing the nozzle orifice size, the flow becomes increasingly restricted and cooling of the detonation tube can become a concern. The performance of the pulse detonation engine with the Schelkin spiral is well documented and experimental testing has demonstrated the ability of the Schelkin spiral to reduce both ignition and DDT (Schauer et al, 2005:1). After observation that the backfire condition became more problematic as the nozzle diameter used the initial stages of testing decreased, the decision was made to simply remove the Schelkin spiral and perform further experimentation with an open unobstructed tube. The inner walls of the detonation tube at the ion probe ports were also deburred and chamfered to the maximum extent possible, to remove any remaining

sources of localized heating beyond the broken welds of the spiral and to prevent additional sources of pre-ignition. Removal of the Schelkin spiral revealed broken welds between the attachment of the straight connecting chin portion of the spiral and the spiral itself. The sharp edges at the broken weld joints due to thermal and mechanical stresses on the Schelkin spiral provided alternate ignition sources or hot spots and became increasingly more difficult to cool as the nozzle orifice sizes decreased.

A detonation can be achieved with an open unobstructed tube of sufficient length for a given tube diameter. As part of the trial and error process of testing the detonation tube was lengthened using tube extensions of initially 6 inch (15.24 cm), then 12 inch (30.48 cm) extensions using a standard pipe coupling and experimentally tested until detonation wave (C-J) speeds could be measured using the ion probes prior to the detonation wave exiting the detonation tube. The 12 inch (30.48 cm) tube extension only provided for a length adequate to read measure detonation wave speeds between the last two remaining ion probe ports. Theory presented earlier in this report predicted that both the ignition and DDT time will decrease as the pressure is increased, and the detonation location and time will occur earlier and take place in a shorter distance. As the nozzle orifice sizes are decreased under the initial unrestricted tube diameter to increase the pressure, it can be expected that the detonation location will move closer to the head of the tube.

The extension ultimately chosen for primary testing in this report was 18 inches (45.72 cm) in length providing for the optimal detonation tube length to measure the detonation time and location in the length of the detonation tube. Removal of the

Schelkin spiral required a longer tube length to achieve a detonation, a measure seemingly counterproductive to an overall objective of the research effort of ultimately decreasing the detonation tube length, however its removal allowed for a more optimal and independent observation of the effects of detonation tube pressure on PDE performance. The longer tube length and open internal tube diameter provided the opportunity to make an easier comparison between the open detonation tube and the nozzle restricted detonation tube. Figure 17 represents the detonation tube arrangement used to produce the data contained in the experimental results section. Test data for testing with the 12 inch (30.5 cm) extension is also contained in the appendix and shows a relative comparison of the effects of tube length on detonation tube performance to the longer 18 inch (45.72 cm) tube extension tests.

Hot Ignition Test Procedure

The test procedure for this research to run the pulse detonation engine used a hard start method to gather data. The pulse detonation engine is started and the fuel/air mixture flowed into the detonation tube until the appropriate equivalence ratio for the fuel/air mixture is achieved. When the desired equivalence ratio for the given test is achieved the spark source is turned on and ignition, DDT and wave speed data are measured using *Online WaveSpeed*. Following a period of cooling the procedure is again repeated for a new test condition corresponding to a different nozzle size, equivalence ratio, fill fraction or spark delay depending on the engine test. The temperature of the pulse detonation tube is measured using a thermocouple attachment located approximately at the midpoint of the detonation tube as shown in Figure 17. Allowing

the detonation tube temperature to cool to room temperature conditions before performing subsequent tests removed the temperature wall effects from the detonation tube and aids in the prevention of hot spots in the detonation tube.

Hydrogen is easy to ignite and detonate, and in comparison to a liquid fuel such as JP-8 or other liquid fuels, fuel droplet evaporation is not a concern with gaseous hydrogen. When using liquid fuels the fuel droplets are evaporated by a heat and mass transfer process with a portion of the spark ignition energy used for droplet evaporation, increasing the overall minimum ignition energy slowing the ignition time. Radiant heating from the detonation tube wall has the potential to aid in the process of droplet evaporation when a fuel other than a gaseous fuel such as hydrogen. In the interest of controlling localized heating or hot spots in the detonation tube structure, the detonation tube must be kept as cool as possible while measuring wave speed data by waiting for the proper fuel and air flow conditions before hard starting the PDE.

Table 3. Ignition Test Matrix

Hole Dia	Baseline	Ign Delay (0-10ms)	Equivalence Ratio	Fill Fraction
D_2/D_1	Test	0, 5, 10 ms delay	ϕ = 0.8, 1.0, 1.2	2, 2.5, 3, 3.5
0.5	X	X	X	X
0.55	X			
0.6	X	X	X	X
0.65	X			
0.7	X	X	X	X
0.75	X			
0.8	X	X	X	X
0.85	X			
0.9	X	X	X	X
1	X	X	X	X

Baseline Test Conditions: FF = 2
Ign Dly = 0 ms
ϕ = 1
Frequency = 20

X = Condition Tested

Table 3 above presents the test matrix for experimental testing using the 18 inch (45.72 cm) tube extension. Testing using the 43 inch (109.22 cm) tube length (with 18 inch extension) was conducted on the baseline test conditions of a fill fraction equal to 2, an ignition delay of 0 ms, and equivalence ratio (ϕ) equal to 1 with nozzle sizes of varying orifice sizes 0.5 to 0.9 inches (1.27 cm to 2.286 cm). A baseline test of the straight tube without a nozzle attachment was also tested to make performance comparisons. The test conditions were then varied independently on each parameter of spark delay, equivalence ratio, and fill fraction for a corresponding nozzle size. Ignition delay was independently varied at 0, 5 and 10 ms at a fill fraction of 2, and equivalence ratio (ϕ) of 1. Next the equivalence ratio was varied and testing performed at 0.8, 1.0 and 1.2 with a fill fraction of 2 and ignition delay equal to zero. Fill fraction was then increased from a fill fraction of 2 to 3.5 in increments of 0.5.

Cold Flow Measurement Test Procedure

Pressure data was gathered independently using a separate series of tests to examine the same flow conditions for the various fill fractions, ignition delay and nozzle sizes. Selected nozzle orifice end caps were fitted with a pressure port to measure pressure just upstream of the nozzle orifice exit and at the head of the detonation tube as shown in Figure 17. Using selected nozzle end caps fitted with 100 psia (0.69MPa) Sensotec pressure transducers pressure measurements were recorded without the spark discharge to initiate combustion, nor was hydrogen flowing through the detonation tube at the simulated identical test conditions to that of the hot, ignition tests. The selected

nozzle end caps fitted with pressure transducer ports and independently tested are summarized below in Table 4:

Table 4. Cold Flow Test Matrix

Hole Dia	Spark Delay	Fill Fraction
(D_2/D_1)	0, 5, 10 ms	FF = 2, 2.5, 3, 3.5
0.85	X	X
0.75	X	X
0.675	X	X
0.6	X	X
0.5	X	X
0.4	X	X

X = Condition Tested

The nozzle orifice sizes and test conditions span a reasonable range of pressure and test conditions to which test points for nozzle orifice sizes not pressure tested during cold testing could be interpolated to after the pressure data was recorded. The cold flow pressure measurements were run at identical test conditions to the actual ignition tests and provided data on the pressure at ignition, pressure variations lengthwise in the tube at all fill and flow conditions and pressure at the nozzle exit. Engine manifold and flow conditions are presented in Appendix A and serve to show that while both fill fraction and nozzle size were varied the mass flow rate remained relatively constant and the manifold pressure increased to maintain the same flow rate. For gathering cold flow pressure data, the hydrogen was not flowing during testing. It was observed that the upstream manifold pressure for the cold flow pressure measurements were approximately 3 to 6 psi (20.7 to 41.4 kPa) lower without the flow of hydrogen fuel. Comparisons are illustrated in Appendix A. The method by with corrections to the baseline test conditions are performed is presented in the next chapter.

The pressure at spark discharge was recorded at each test condition of varying fill fraction, ignition delay, nozzle size and equivalence ratio for each the cylinder head pressure, detonation tube head pressure and pressure immediately upstream of the nozzle orifice exit. Though the hydrogen was not flowing during the cold flow testing resulting in a lower overall mass flow rate and lower manifold pressure, the pressure measurements taken provided for a firm understanding of the effects of the flow dynamics on the nozzle restricted detonation tube by visual comparison of the individual pressure traces from a variation in engine control parameters of fill fraction, equivalence ratio and spark delay. The output of the complete set of pressure measurements is presented in Appendix E.

V. Data Reduction and Error Analysis

This chapter addresses the data processing method and techniques used to obtain quantifiable results. The chapter also examines to the extent possible the fidelity of the data measured. Sources of error or uncertainty exist in the system used for testing with regard to data measurement and include ion probe location, pressure transducer measurements, data sampling rates, fluctuations in mass flow rates, temperature and pressure, and spark discharge.

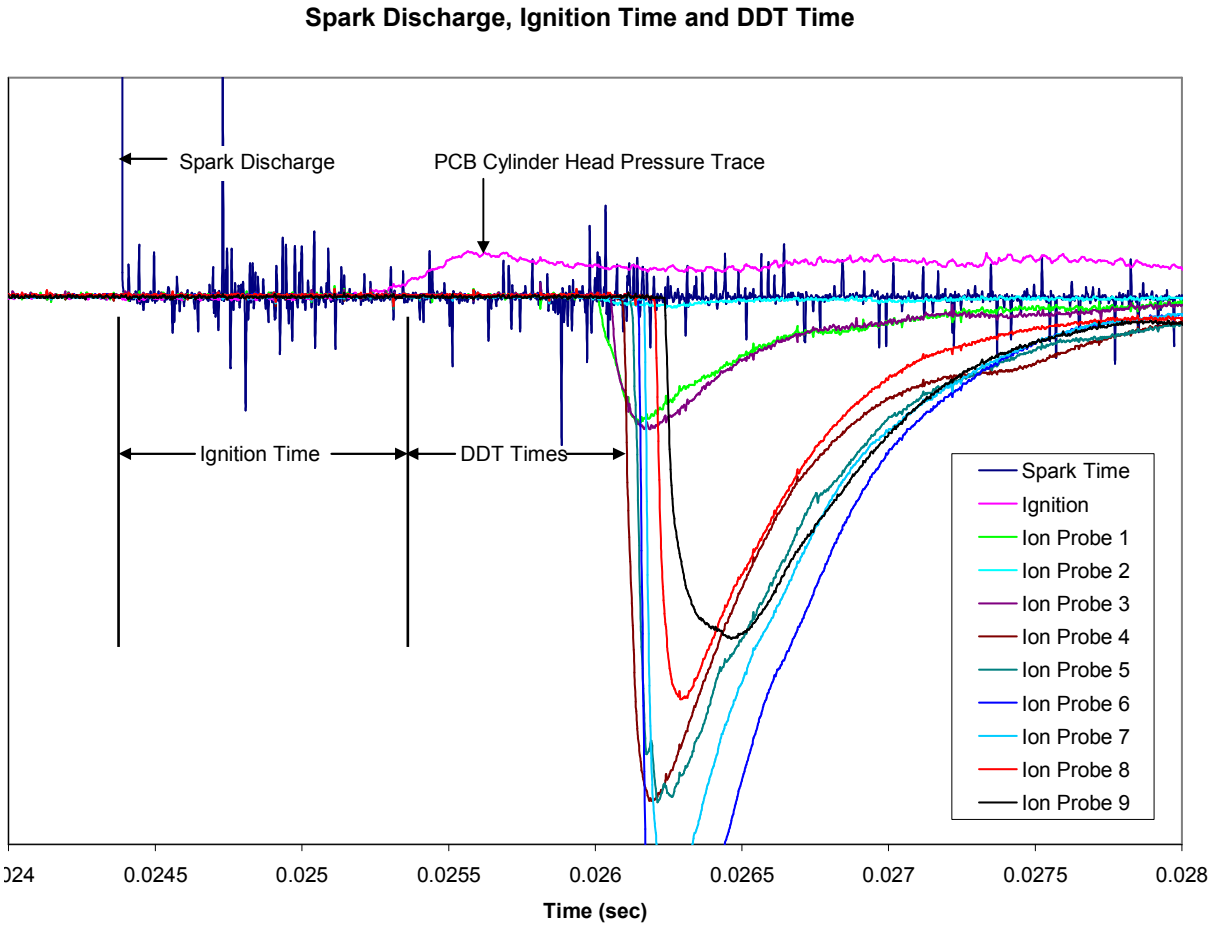

Figure 21. Ignition and DDT time referenced from spark discharge

Data Acquisition and Sampling

The data gathered using *Online Wave Speed* was sampled over 0.8 seconds each run using 11 channels at 1 Mhz per channel and encoded directly from the analog to digital converter as 2 byte integers. The data reduction was accomplished using a software application entitled *PT Finder*. A curve saved in the data file from the output converts the values back to floating point. From the square wave spark plug signal trace, *PT Finder* separates each engine cycle into a separate binary data file for processing. *PT Finder* processes each file in two scans to determine ignition time and wave speed. From the extracted detonation and ignition times, wave speed and DDT times are determined as represented by Figure 21.

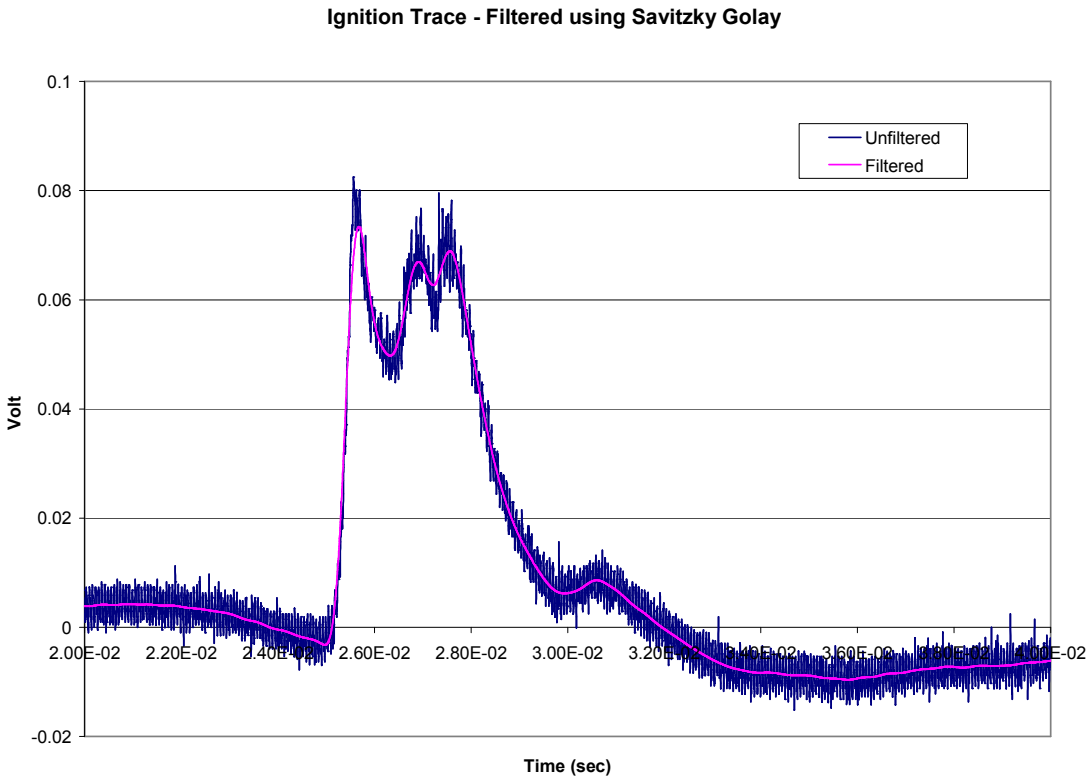

Figure 22. Ignition trace processed with Savitzky-Golay filter

Determination of Ignition Time

To determine ignition time the ignition data is passed through a fourth-order, 401 point Savitzky-Golay digital finite-impulse response filter. The filter smoothes the data to remove high frequency noise and data scatter in the apparent slope as shown in Figure 22. A linear regression is then performed on the data set, subject to user input and examines the slope in the data set until the indicated threshold has been exceeded. The slope for determining ignition time for data production in this research is set to a pressure rise rate of 5 volts/sec (5000 psi/sec). A group of 600 data points, or 600 microsecond set of data is independently examined for the user specified threshold and if the threshold is not exceeded the next data set is read until the ignition time is determined. A sensitivity analysis of the selection of a range of data points to determine ignition time reveals a minimum standard deviation at 300 points either side (600 total) and was considered optimal for data reduction as shown below in Figure 23.

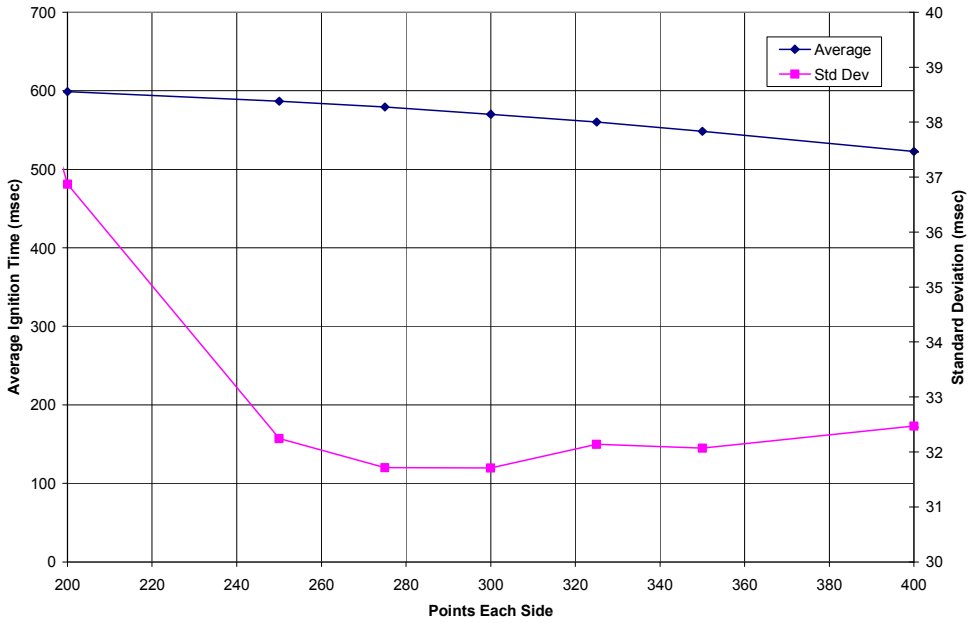

Figure 23. Sensitivity Analysis ($D_2/D_1 = 0.9$, $\phi = 2$, spark delay = 0)

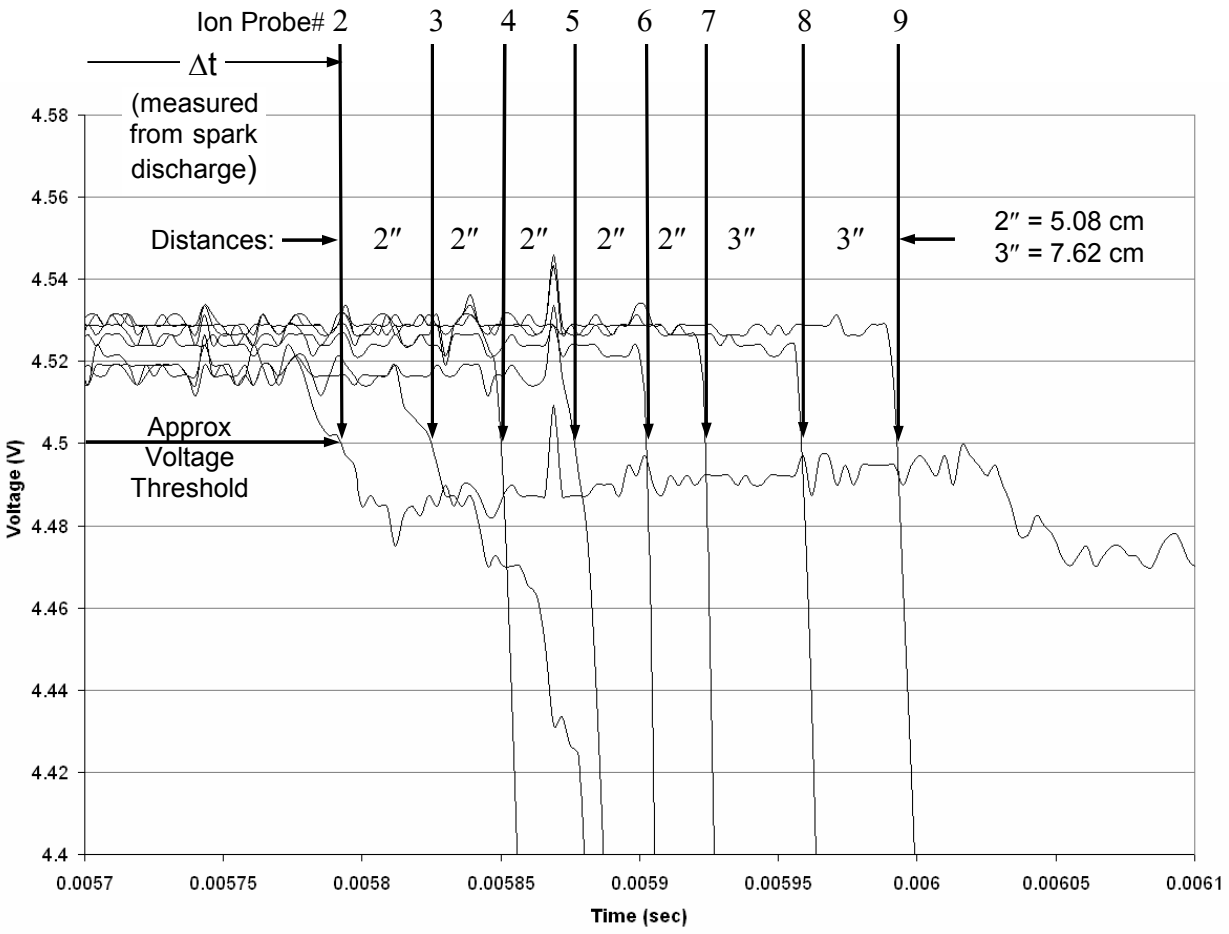

Figure 24. Sample ion probe voltage drop for measuring combustion wave passage (voltage trace for ion probe 1 not shown)

Determination of Wave Speed

Wave speed is determined by examining a preset voltage threshold. The point of measurement for the wave speed is selected using a software algorithm with an initial 1000 points in the current engine cycle averaged for each channel to provide a baseline for the data set. Wave speed is determined from the first point in an initial group of 500 data points to breach a voltage threshold amount preset by the user. The time from initial

spark drop to ion probe voltage drop determines the wave speed from the specified distance determined by the test equipment as shown in Figure 24.

Detonation time is determined by comparing the average combustion wave speed between two ion probe voltage drops to a reference C-J velocity of approximately 1970 m/sec for use of hydrogen as a fuel and forecasted using a linear regression to predict an earlier distance and time where the detonation occurred. DDT time is determined by subtracting the ignition time from the recorded detonation time.

Detonation and DDT Time

Figure 24 is an example of a typical ion probe voltage trace used to the determine combustion wave speeds. The voltage drops are determined using a voltage threshold method. When the combustion wave passes the ion probe the presence of ions opens the circuit through the spark plug gap allowing current to flow. A strong detonation wave yields a more sharply defined voltage drop as can be noted in ion probe readings 4 through 9. The quality of the voltage drop becomes important in determining the time of combustion or detonation wave passage. A deflagration wave that has yet to transition into a detonation wave will have a less sharply defined voltage drop as can be seen from ion probe readings 2 and 3 in Figure 24 above. A deflagration wave, in comparison to a detonation wave, is a much less well defined combustion wave in that ignition has occurred yet turbulent mixing is taking place over a thicker region with less ions being produced in the process of combustion. The deflagration wave passes the ion probe over a larger period of time versus the sharply defined shock driven combustion of a detonation wave. The quality of the voltage drop becomes important when examining

combustion wave speed times in that a deflagration wave will produce a correspondingly and less sharply defined voltage drop that breaches the voltage threshold at a time other than when beginning of passage of the combustion wave passes the ion probe. It can therefore be observed that the voltage threshold method of determining combustion wave speed passage is more suited to examination of detonation wave versus deflagration wave time of passage. A voltage drop from a deflagration wave can begin at a specified time before it is actually measured using the voltage threshold method and has to be considered qualitatively when examining wave speed data using *Online WaveSpeed.*

Wave Speed Measurement Uncertainty

Data was acquired at the rate of 1E6 points per second, or 1 data point was recorded every microsecond with an error of approximately $\pm 0.5 \mu$sec of error. The ion probes were located with accuracy of approximately 0.0625 in (1.58 mm) or ± 0.03125 in (± 0.79 mm). At the speed to determine detonation, C-J speed (1970 m/sec) with a minimum distance of 2 in (5.08 cm) between ion probes the time was nominally 25.8 μsec resulting in a wave speed error of approximately ± 30.64 m/sec.

Data Standard Deviation and Confidence

All ignition, detonation and DDT times were averaged from all measured events, and a standard deviation, σ determined from:

$$\sigma = \sqrt{\frac{\sum_{i=1}^{n} \left(x_i - \overline{x}_i \right)^2}{n-1}} \tag{59}$$

where n is the number of samples and $\overline{x}$ is the average of all sample data measured.

Plotted data was shown with a 95% confidence interval given by:

$$\bar{x} \pm 1.96\left(\frac{\sigma}{\sqrt{n}}\right) \tag{60}$$

Cold Flow Data Reduction for Pressure

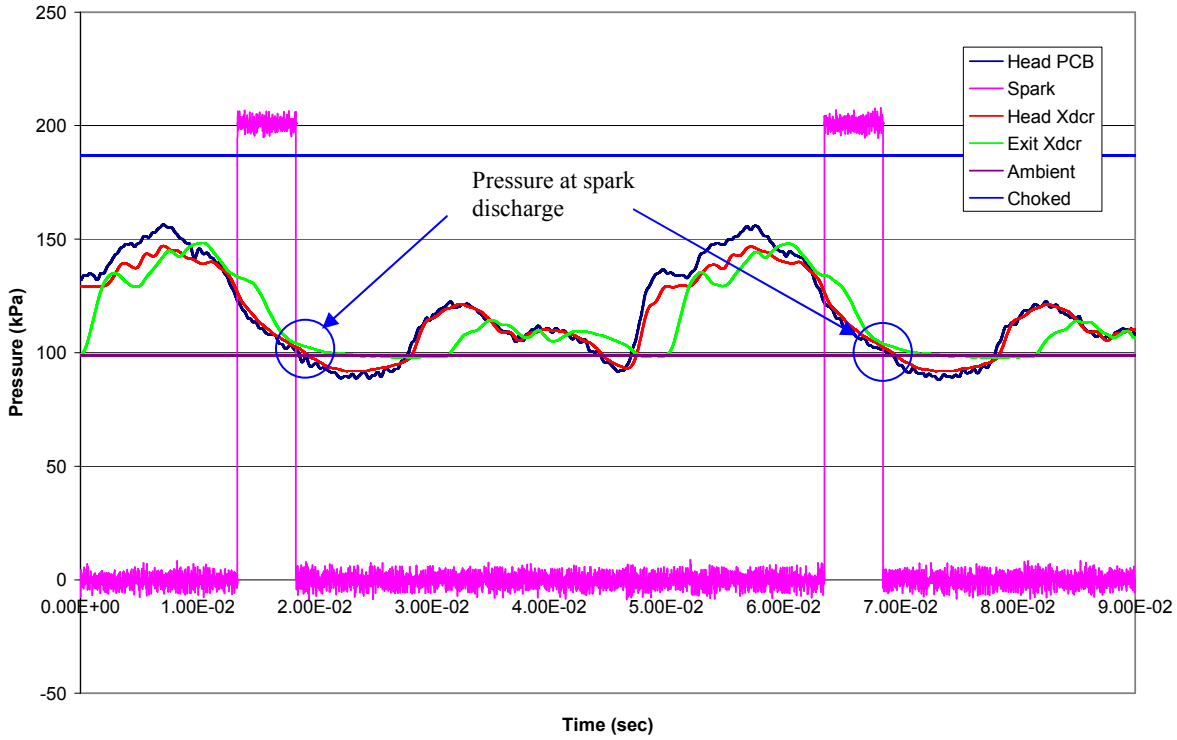

Figure 25. Cold flow spark discharge pressure ($D_2/D_1 = 0.675$, Spark Delay = 5, FF = 2)

Figure 25 above is a sample pressure transducer output trace for a cold flow test with the pressure at spark drop points highlighted. For the cold flow tests, the spark pulse was discharging, but voltage was not applied to the actual spark plug to produce ignition, nor was the hydrogen fuel flowing. As presented earlier, each pressure trace intersects the spark trace at a specific pressure. The resulting pressure is a function of the tube nozzle orifice diameter at the tube exit, a factor affecting blown down time of the tube,

the initial pressure at fill based on fill fraction, and the pressure at the time of spark discharge. The pressure of interest for reference to ignition time corresponds roughly to the tube head pressure trace at the instant of spark discharge. The PCB dynamic pressure transducer in the cylinder head and the 100 psia absolute pressure transducer at the tube head measured approximately identical pressure.

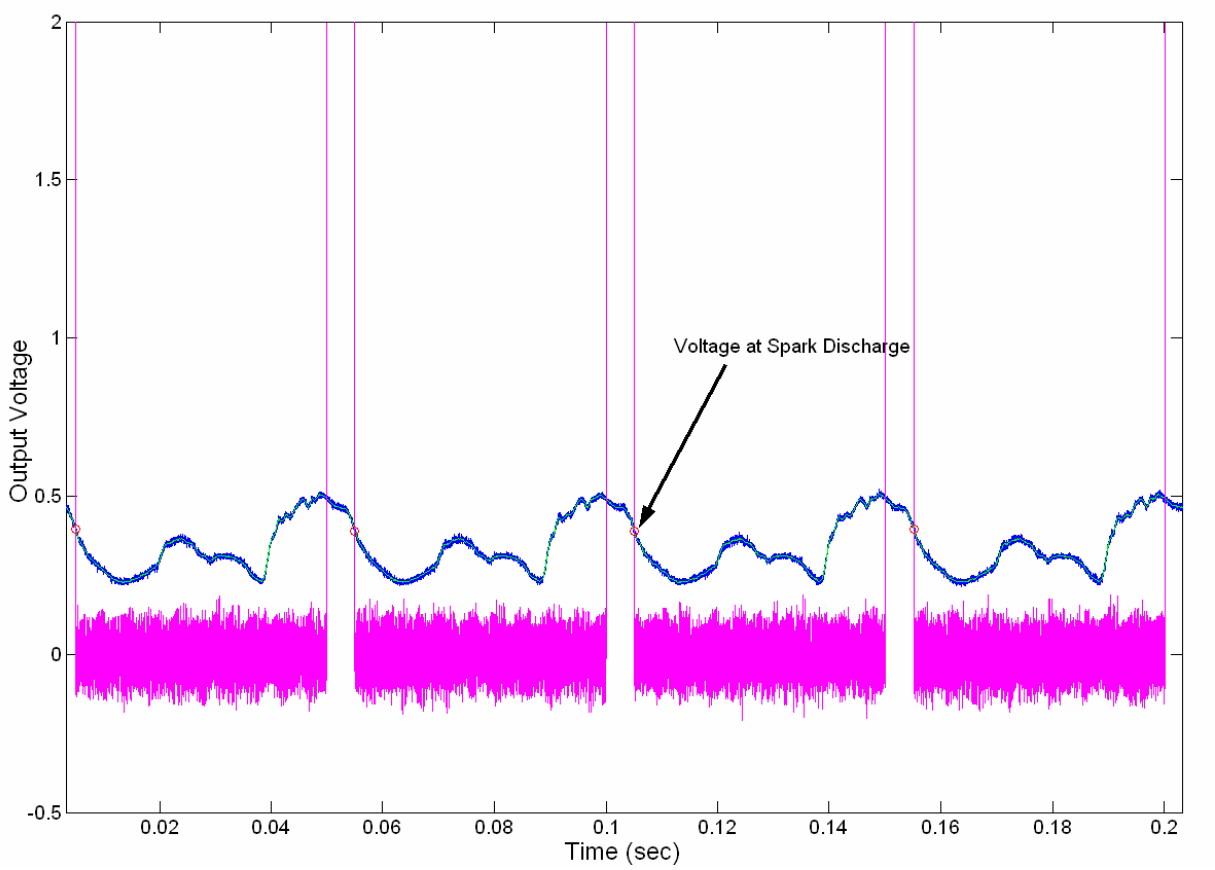

Figure 26 - Tube head voltage versus time signal output trace

For each measured pressure trace at the tube head the output signal is processed with a filter and examined at spark discharge for a total of eight cycles using the MATLAB computer code to produce Figure 26 is provided in the appendix. The program reads the raw data output from an Excel spreadsheet created by the user from the original data output file, and determines the intersection of the spark discharge and the tube head

voltage output trace for each cycle. The values of the eight cycles are averaged, the standard deviation determined and corrected for pressure based on the initial static pressure measurements at ambient conditions, and corrected for absolute pressure by the appropriate scale factor of 33.33 psia/volt (229.83 kPa/volt) for the Sensotec (Model TJE/0713-10JA) pressure transducers used. The values for the averaged ignition pressure and standard deviation are averaged and tabulated in Table 5 below. As tabulated in Table 5 the standard deviation shows only a small variance in pressure at ignition based on the pressure transducer output. Because hydrogen was not flowing during the cold flow pressure tests, the upstream manifold pressure is lower corresponding to a lower pressure at spark discharge.

Table 5. Pressure Correction at Ignition for Volumetric Flow (spark delay = 0)

Nozzle Size	Cold Flow Tube Head Ignition Pressure (kPa)	Standard Deviation (kPa)	FF	Air Only Manifold Pressure (kPa)	Air & Fuel Manifold Pressure (kPa)	Pressure Difference (kPa)	Corrected Ignition Pressure (kPa)
0.85	102.8668	0.1327	2	44.80944138	57.98966992	13.18022854	137.0912189
0.75	115.0163	0.33	2	47.96067641	62.98677028	15.02609387	149.7337798
0.675	126.3223	0.2504	2	52.82821649	69.04704032	16.21882383	157.3090655
0.6	140.5872	0.2164	2	59.66526467	78.60739397	18.9421293	169.2594257
0.5	164.9605	0.2736	2	75.16822988	99.1604215	23.99219162	194.9505341
Estimated:	196			100			
0.85	110.7648	0.5961	2.5	61.29715719	83.01969574	21.72253854	164.2968609
0.75	126.581	0.4756	2.5	65.17992598	92.03930173	26.85937576	179.692918
0.675	140.7022	0.2993	2.5	70.46952173	101.2465591	30.77703732	190.6944478
0.6	158.1217	0.1888	2.5	78.85402924	113.3387618	34.48473254	205.1431293
0.5	188.1103	0.2439	2.5	99.08386768	135.1803474	36.09647969	231.2411133
Estimated:	237			140			
0.85	119.7144	0.3974	3	77.67233678	104.5175705	26.84523373	183.4856927
0.75	140.2283	0.5865	3	83.89037365	114.9855457	31.095172	199.9824188
0.675	158.6041	0.3949	3	91.79659185	125.1310308	33.33443892	212.6078198
0.6	178.1579	0.1967	3	100.7157188	137.254599	36.53888014	227.6948174
0.5	214.472	0.3444	3	126.6290436	156.5140545	29.88501088	251.661966
Estimated:	256			160			
0.85	129.3894	0.3199	3.5	92.49999499	125.1433331	32.64333813	200.5797027
0.75	153.0809	0.5616	3.5	99.98418509	134.753285	34.76909994	214.9975986
0.675	174.6573	0.1933	3.5	110.3663796	143.4798285	33.11344895	226.9557409
0.6	198.8622	0.4011	3.5	123.9279535	153.6916208	29.76366733	240.9491467
0.5	241.8032	0.5118	3.5	154.3148726	169.9026785	15.58780589	263.1634556
Estimated:	277			180			

Given that the manifold pressure for each nozzle size and fill fraction is known for both the hot and cold ignition tests using snapshot data from the engine control panel, it is possible to establish a relationship of the tube exit nozzle orifice diameter to the manifold pressure. Figure 27 is a comparison of the manifold pressures for each nozzle size for both the hot ignition and cold flow tests. Each data point represents a snapshot value at approximately the time the data for each 0.8 sec interval was measured during testing. Establishing a relationship between manifold pressure and detonation tube exit nozzle orifice diameter for the hot ignition tests, and a relationship between the cold flow tests versus nozzle orifice diameter, provided a method of correction given the pressure difference at spark discharge with no hydrogen flowing.

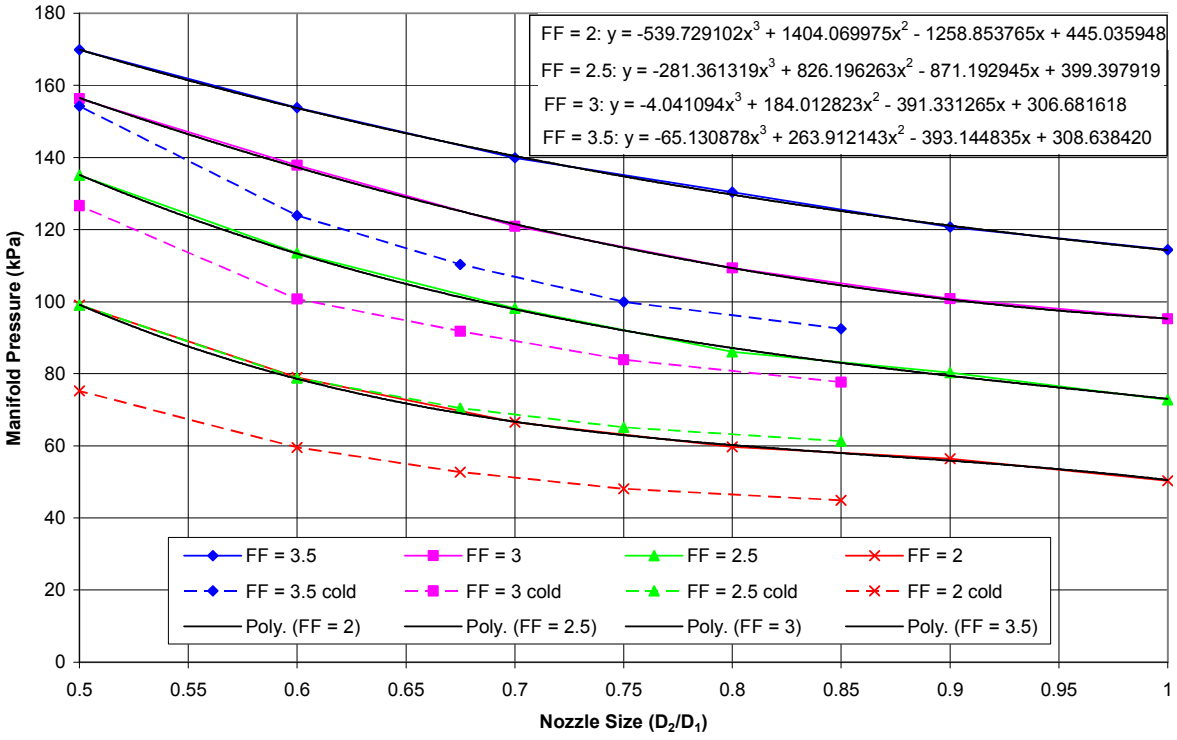

Figure 27. Engine manifold pressure versus nozzle size (cold and hot flow comparison)

The relationship between manifold pressure and tube nozzle orifice diameter for the cold flow tests are also presented in Figure 27. Establishing curve fits for the snapshot value of manifold pressures for each nozzle size and fill fraction provided a relationship for the full range of nozzle sizes tested to include the ability to predict the pressure versus nozzle size relationship for those nozzle sizes not tested.

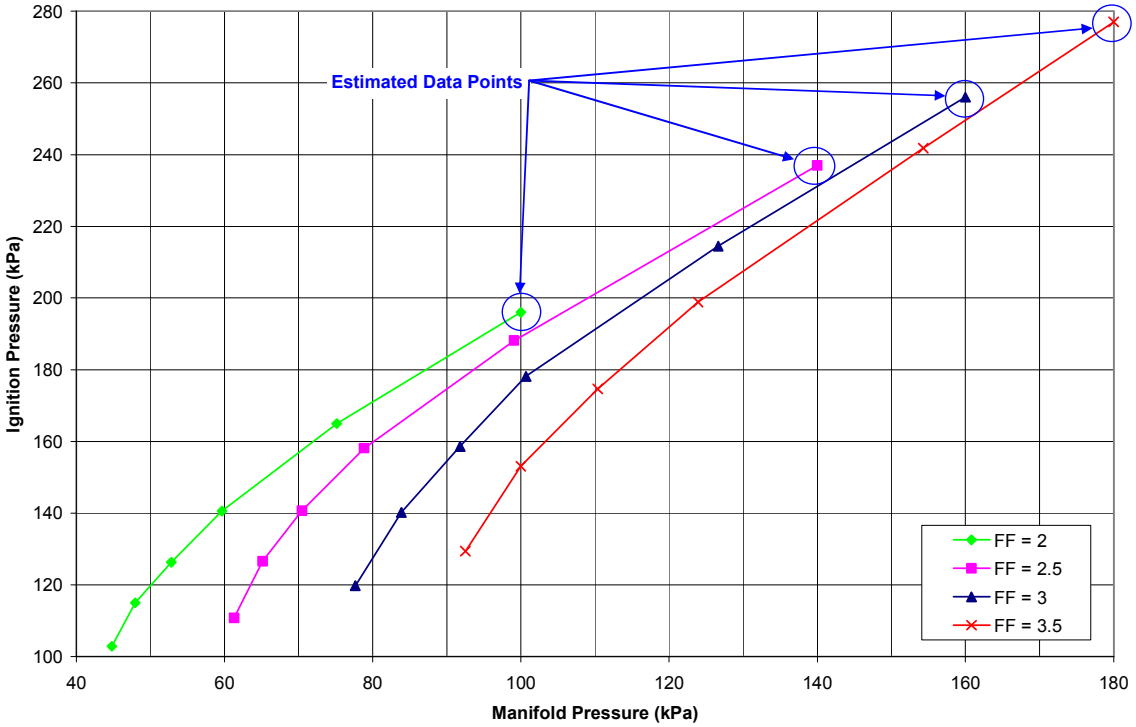

Figure 28. Manifold pressure versus ignition pressure correction chart

From the relationship between detonation tube nozzle orifice exit it is possible to establish a relationship between the upstream manifold pressure and the ignition pressure for each fill fraction as shown in Figure 28. The manifold pressure readings for the ignition tests were higher with the addition of the hydrogen fuel flow in comparison to the cold flow tests where only air was flowing during the pressure readings. Figure 28 represents the relationship between the measured upstream manifold pressure and the

downstream tube pressure across the poppet valve in the cylinder head for any gas flow and is a function of the lift and duration of the valve dynamics only as presented by equations (41) to (49). Given that the manifold pressure was higher than most all the pressure readings taken during the cold flow testing, the higher ranges of manifold pressure versus ignition pressure had to be estimated by forecasting the data trend. From examination of the data trends as provided in Figure 28 the forecasted value was based on a relative comparison of the data trends at higher fill fractions. The approximate slope of the higher fill fraction data trends provided a reasonable estimate of the lower fill fraction data trends. The forecasted data trend can be assumed to hold valid for all unchoked flow across the poppet valve during engine operation. At the highest forecasted pressure of 180 kPa for a fill fraction of 3.5, the ratio of upstream to downstream pressure (approximately 100 kPa at ambient) slightly exceeds the choked pressure ratio across the poppet valve given by equation (48) and is a limiting factor on the PDE engine performance and operation as is discussed later in the experimental results.

Using the relationship of manifold pressure versus ignition pressure determined from Figure 28, the corrected ignition pressure, or pressure at spark discharge from the cold flow ignition tests can be determined. Thus for each nozzle size as tested during the hot flow ignition testing the higher manifold pressure can be related to an adjusted ignition pressure. Figure 29 shows a plot of the corrected pressure at ignition for each nozzle size tested during the hot flow ignition tests.

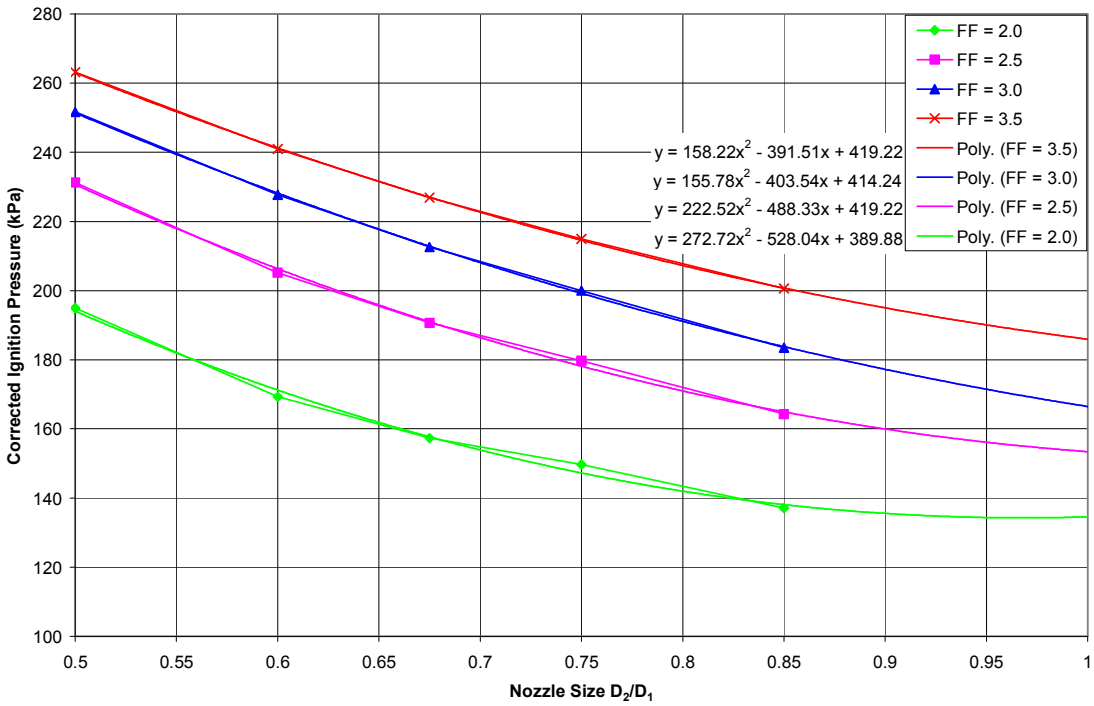

Figure 29. Corrected ignition pressure at tube head versus nozzle size for baseline test conditions (FF = 2, Spark Delay = 0, $\phi = 1$)

VI. Experimental Results and Analysis

Baseline Test Conditions versus Varying Nozzle Orifice Exit Diameter

The experimentally observed results of choking the free stream stagnation pressure using nozzle orifice sizes of varying diameters and using hydrogen as a fuel in the pulse detonation engine are presented. At the baseline test conditions of a fill fraction of 2, ignition delay of 0 and equivalence ratio equal to 1, the effects of varying the orifice exit are shown in Figure 30. A trendline through the data points in Figure 30 reveals an optimal orifice size of approximately 65 to 70% of the detonation tube diameter for this experimental setup. As the nozzle diameter decreases to approximately 0.5 or 50% of the tube diameter, the mass flow rate at the nozzle exit begins to fluctuate and the ignition time increases again.

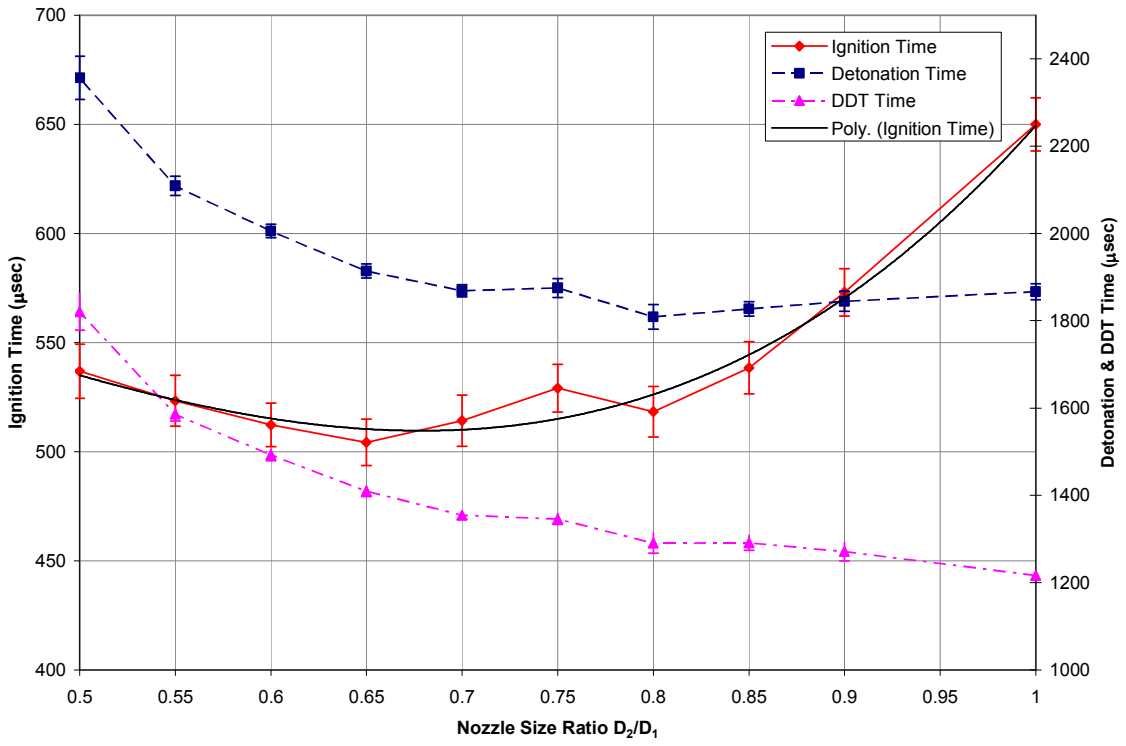

Figure 30. Ignition, detonation & DDT time versus nozzle size (FF = 2, ϕ = 1, spark delay = 0)

The overall detonation time in Figure 30 decreases to a minimum at approximately 0.8 D_2/D_1. A notable bump or increase in ignition time occurs at 0.75 D_2/D_1. Additional testing at the same reference point under similar test conditions suggests the data trend at 0.75 D_2/D_1 can be attributed to a engine flow system instability associated with restricting the nozzle exit of the detonation tube as it could not be duplicated.

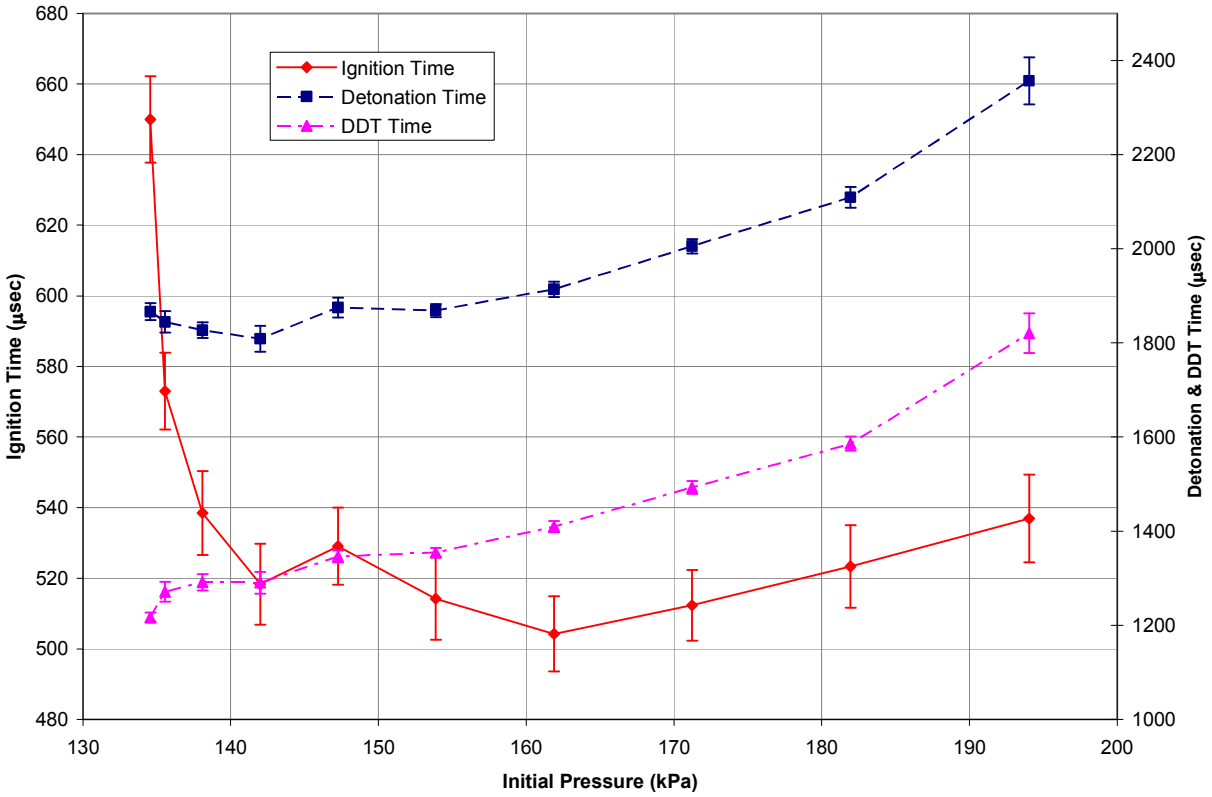

Figure 31. Ignition, detonation & DDT time versus initial spark pressure (FF = 2, ϕ = 1, spark delay = 0)

Detonation and DDT times are both plotted with ignition time in Figure 30. Detonation time is the total time from spark discharge until a detonation (C-J speed) is recorded and includes both ignition and DDT times. Subtracting the ignition time from

the total detonation time provides the DDT or deflagration to detonation transition time. The DDT time appears to increase slowly until approximately 70% tube diameter where a more rapid increase in DDT occurs as the nozzle diameter decreases. The detonation time gradually decreases until approximately 80% tube diameter before increasing. The decreasing trend in detonation time for nozzle sizes from 1 to 0.8 can be attributed to the relatively larger decrease in ignition time.

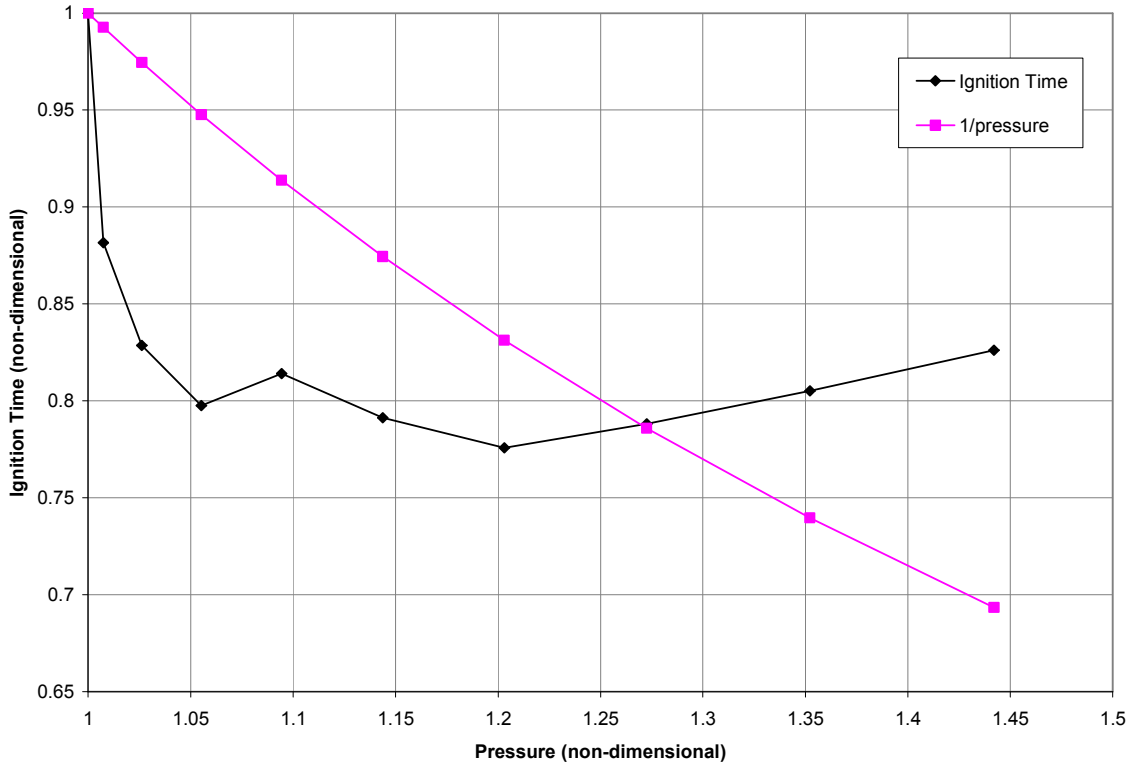

Figure 32. Non-dimensional pressure versus non-dimensional ignition time (FF = 2, ϕ = 1, spark delay = 0)

A plot of ignition time versus initial pressure is shown in Figure 31. The pressure at ignition was determined from the plot of corrected nozzle size versus initial pressure in Figure 29. The reaction order for hydrogen and air is considered to be approximately 1.0 as given by n in equation (24). A plot of non-dimensional pressure versus non-

dimensional ignition time in Figure 32 illustrates a relative comparison to theory given by equation (24) where ignition time varies inversely with pressure. As the nozzle size is decreased the pressure at ignition increases with the expectation that the ignition time would continue to decrease instead of decrease to a minimum at 0.75 D_2/D_1 and increase again at 0.5 D_2/D_1.

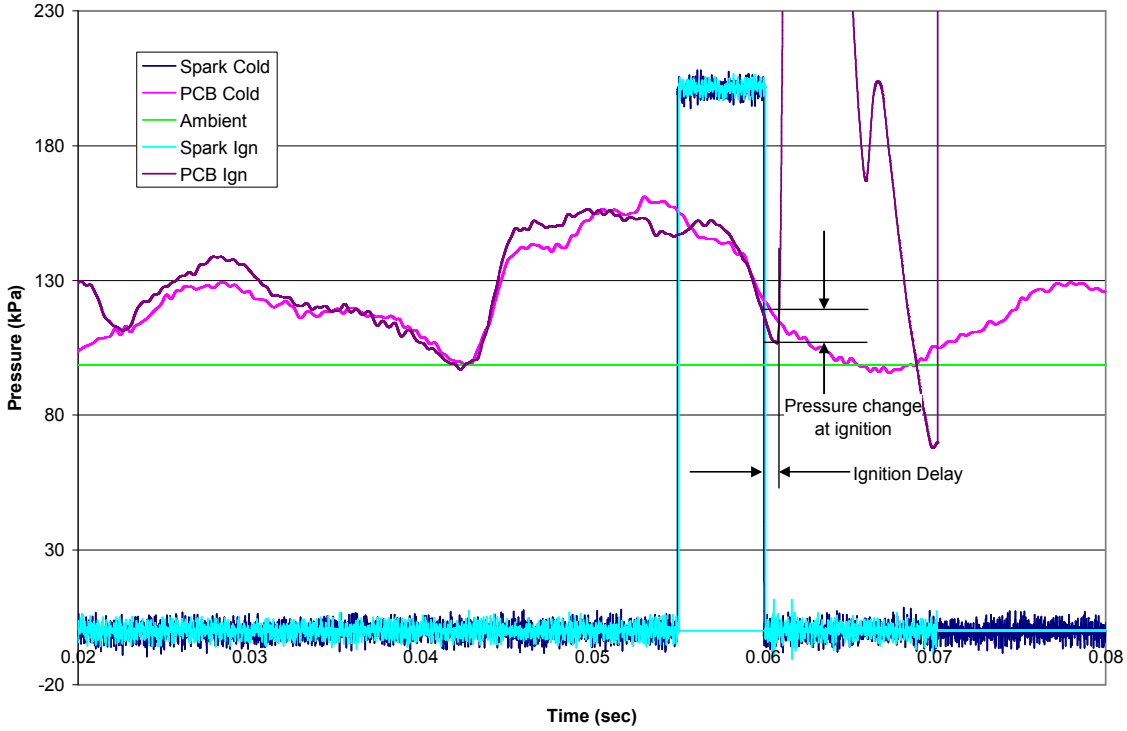

Figure 33. Superimposed ignition and cold flow cylinder head pressure traces with pressure change at ignition delay depicted (0.75 D_2/D_1, FF = 2, spark delay = 0, $\phi = 1$)

The flow dynamics, changing pressure conditions upstream in the manifold, and flow conditions across the poppet valves at the head of the detonation tube all have an effect on the ignition time. Figure 33 is a plot of the PCB cylinder head pressure trace for both the ignition and cold flow tests at the test conditions of 0.75 nozzle size, fill fraction of 2, ignition delay of 0 and equivalence ratio of 1. The pressure traces reveal the similarity of cold flow to actual ignition test conditions and illustrate a graphic depiction

of the slope of the pressure decrease after the fill valve closes. The slope of the pressure decrease after fill is a function of the blow down time and resulting expansion after the fill valve closes and varies depending upon initial fill fraction and manifold pressure and also nozzle orifice size at the nozzle exit.

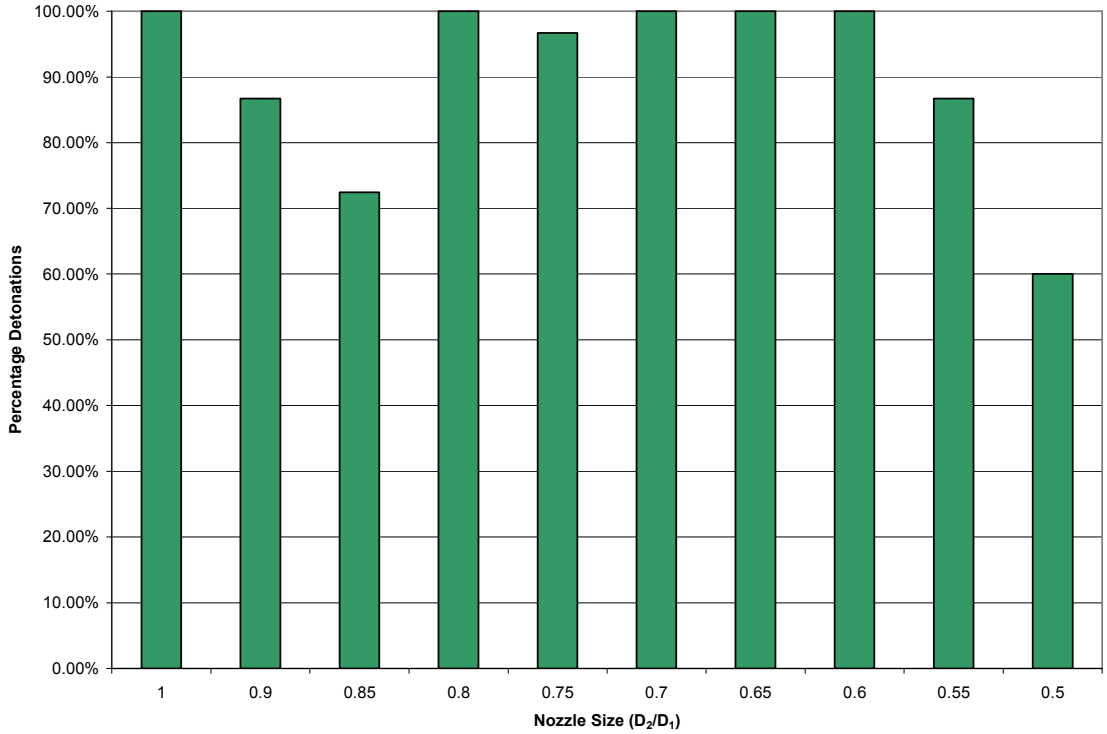

Figure 34. Percentage of detonations occurring with nozzle variation (spark delay = 0, Fill Fraction = 2)

The percentage of detonations is also important in examining the quality of data measured. Figure 34 shows the percentage of recorded detonations for each nozzle size. Approximately 15 cycles per run at 2 runs each produced at total of 30 samples. As the nozzle size began to decrease to 0.5 D_2/D_1 the effect of choking at the nozzle exit are apparent. A decrease in percentage of detonations can also be observed to decrease to a minimum at 0.85 D_2/D_1. Additional data taken and documented later in this chapter

indicates the data trend can be possibly attributed to pressure fluctuations varying the equivalence ratio upstream of the fill valves in the main fill manifold.

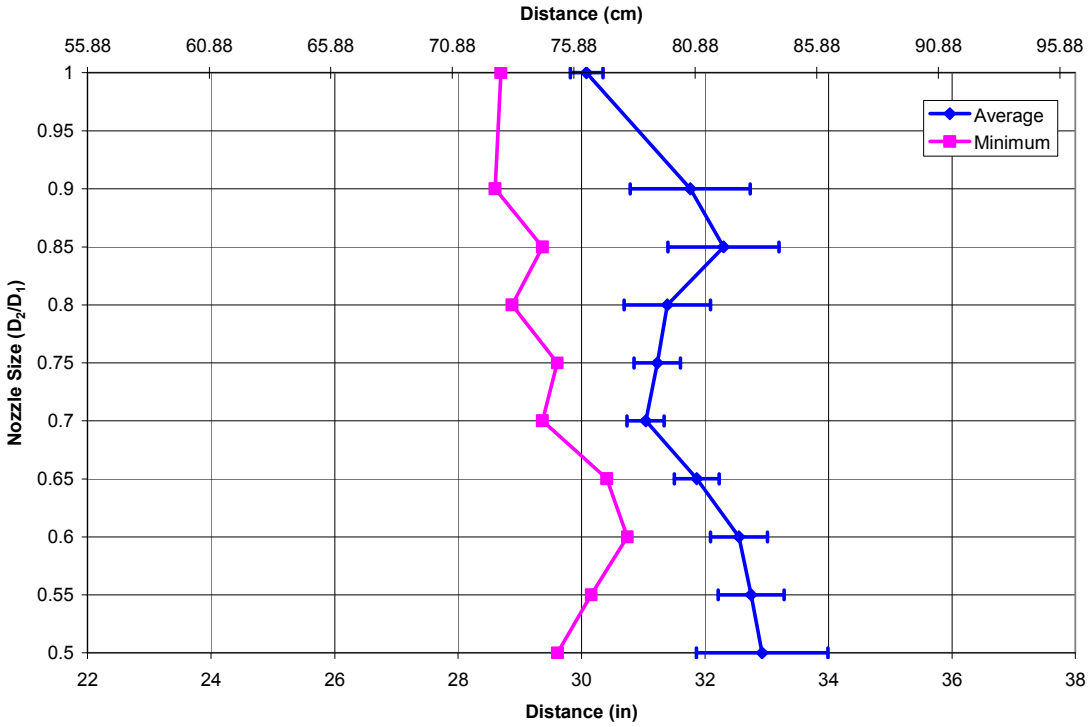

Figure 35. Detonation distance versus nozzle size (FF = 2, spark delay = 0, $\phi = 1$)

Detonation distance is also important and presented below. Intent in this study was to reduce DDT time and distance by increasing the detonation tube pressure. Figure 35 represents a plot of axial distance down the length of the detonation tube referenced from the cylinder head where detonations are recorded versus a change in nozzle size. The plot is presented for a left to right moving detonation wave traveling axially down the length of the tube. The effects of nozzle size on DDT distance are to slightly increase the overall DDT distance from 1.0 to 0.5 D_2/D_1. The average and minimum recorded DDT distances are plotted for comparison.

Variation of Equivalence Ratio

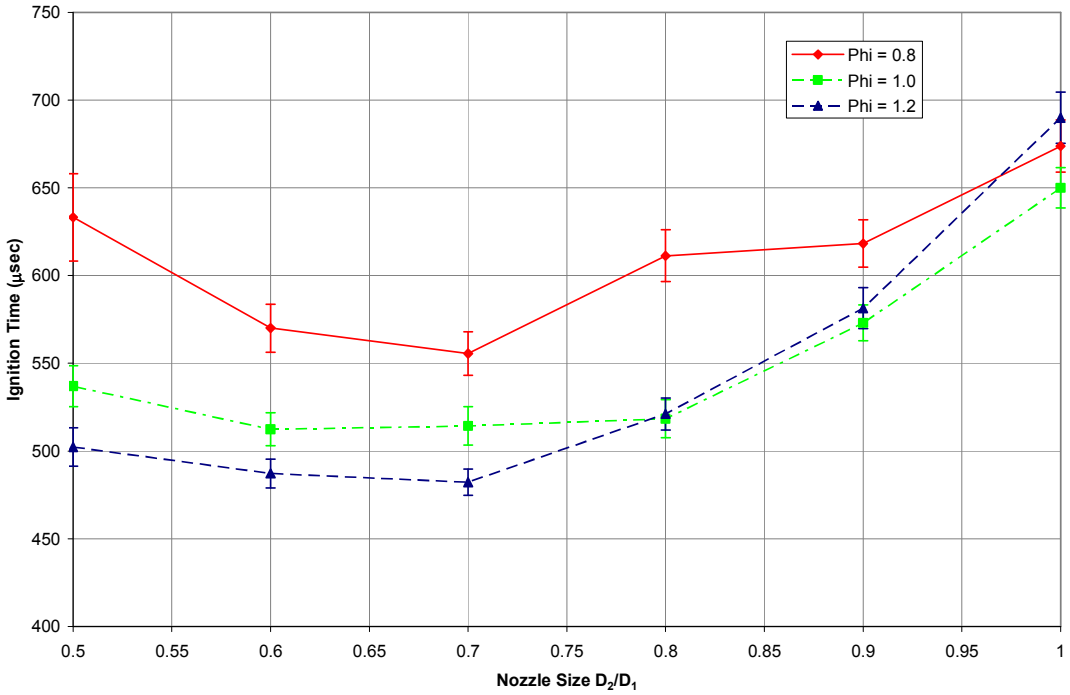

Figure 36. Ignition time versus nozzle size with varying equivalence ratio (FF = 2, spark delay = 0)

The effects of varying the equivalence ration versus nozzle orifice size were examined using equivalence ratios of 0.8, 1.0, and 1.2. Each equivalence ratio was independently varied from the baseline test conditions of fill fraction of 2, equivalence ratio of 1, and ignition delay of 0. The results are plotted in Figure 36 and illustrate that increased equivalence ratio has the potential for decreased ignition time below nozzle orifice sizes of 0.8 D_2/D_1. Equivalence ratios above 1.2 were not examined. A lower equivalence ratio results in fewer molecular collisions between fuel and air and decreased ignition times. As in the case of the equivalence ratio of 1 the minimum ignition time corresponds to roughly 0.7 D_2/D_1 or roughly 70% of the tube diameter.

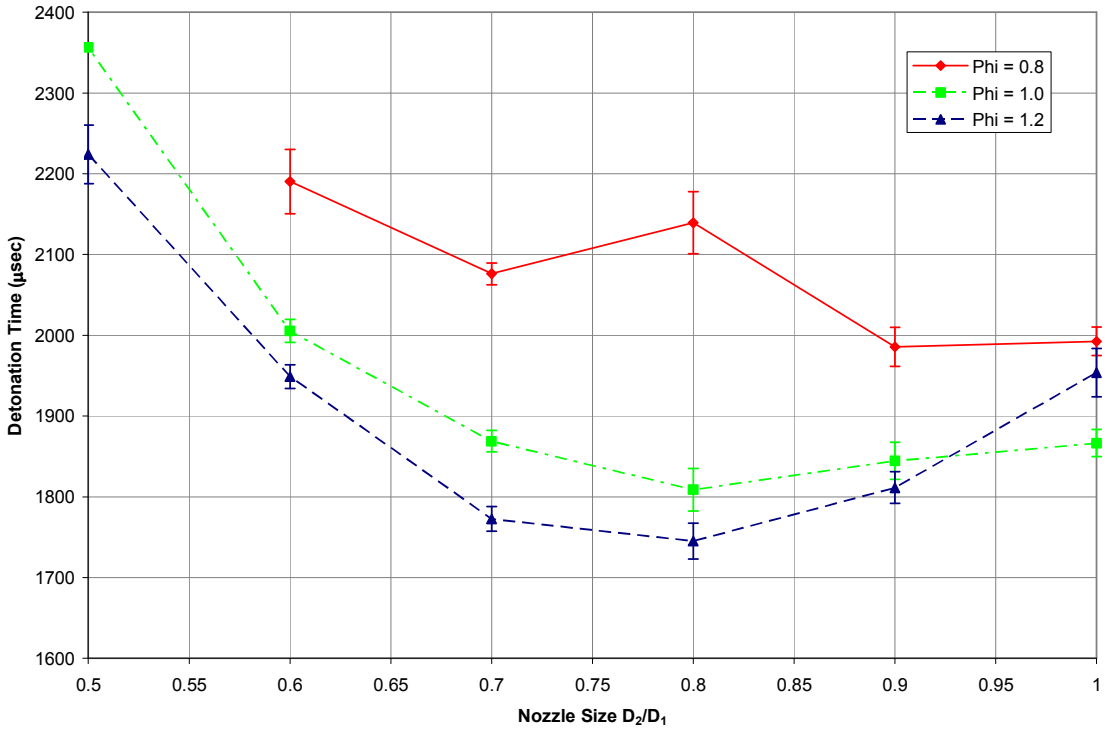

Figure 37. Detonation time versus nozzle with variation of equivalence ratio (FF = 2, spark delay = 0)

Detonation and DDT times for a variation of equivalence ratio are plotted in Figure 37 and Figure 38. Of note in both figures is that both the detonation and DDT times are reduced at approximately 0.8 D_2/D_1 or 80% nozzle size for the case of equivalence ratio 1.2 when compared to equivalence ratio 1.0 which increases for all nozzle ratios 0.5 to 1.0 D_2/D_1. The variation of equivalence ratio indicates the significance of filling the tube with the proper proportion of fuel and air at ignition. As the mixture or equivalence ratio is leaned, fewer molecular collisions occur decreasing the potential for initiating and sustaining a reaction after spark discharge, increasing the ignition time. A plot of ignition time versus initial pressure is shown below in Figure 39.

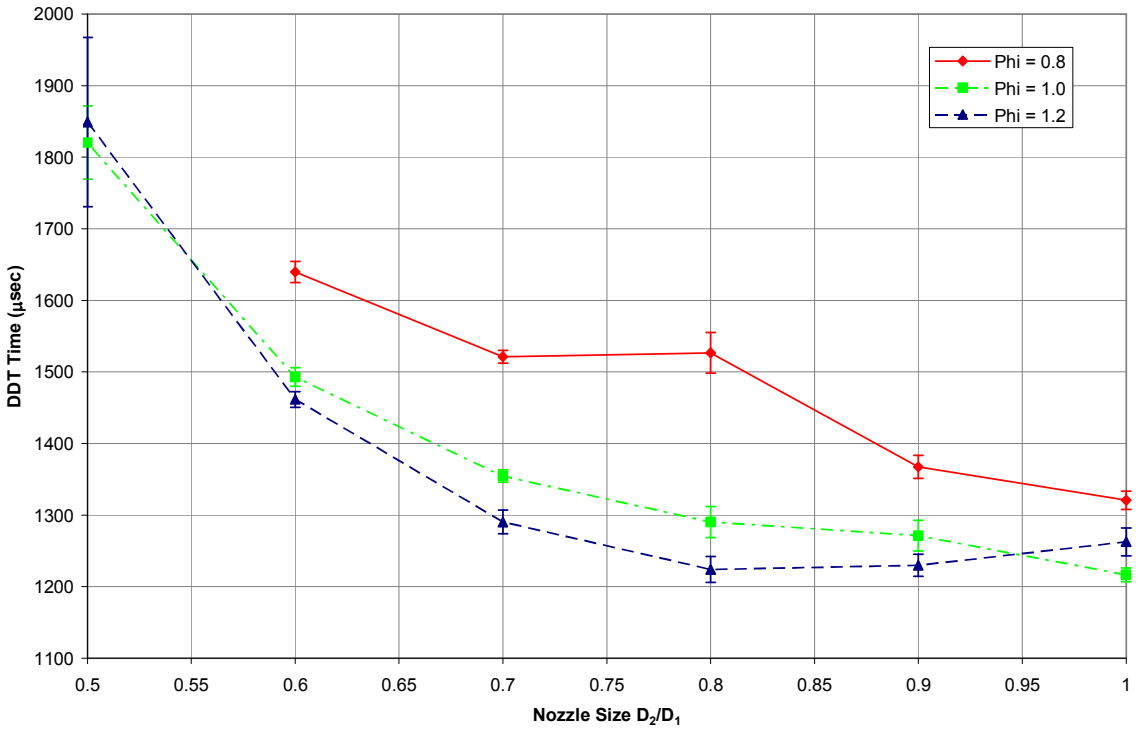

Figure 38. DDT time versus nozzle size with equivalence ratio variation (FF = 2, spark delay = 0)

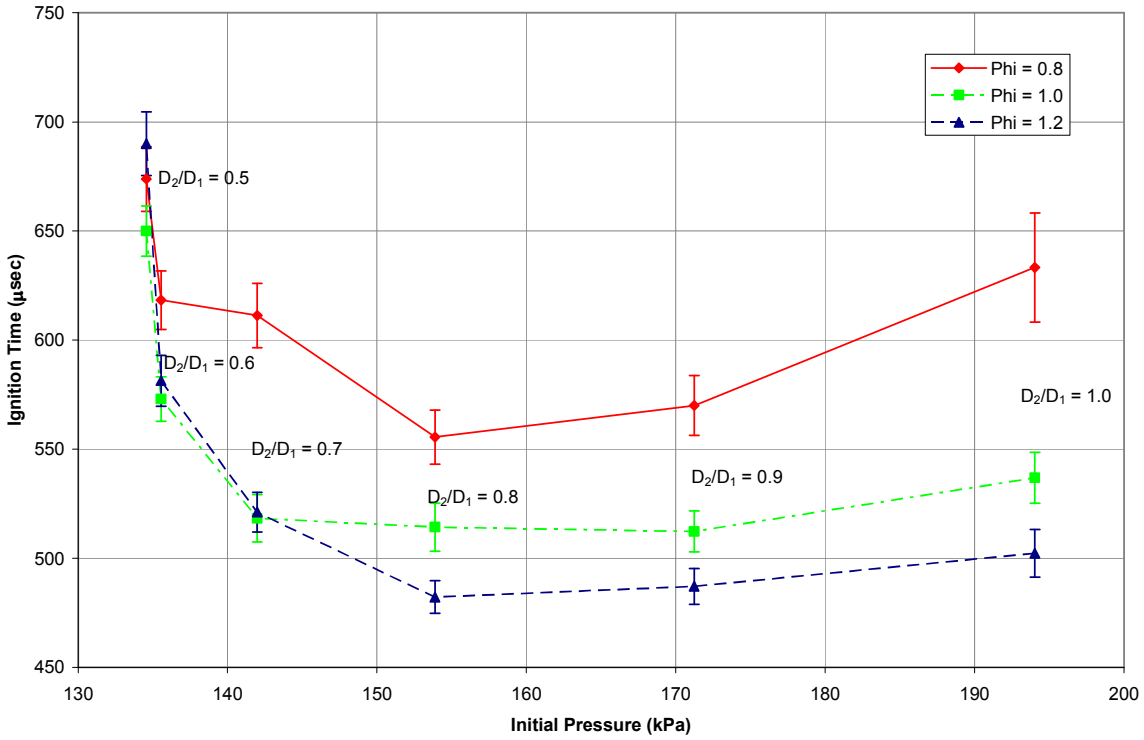

Figure 39. Ignition time versus initial pressure with varying equivalence ratio (FF = 2, ϕ = 1, spark delay = 0)

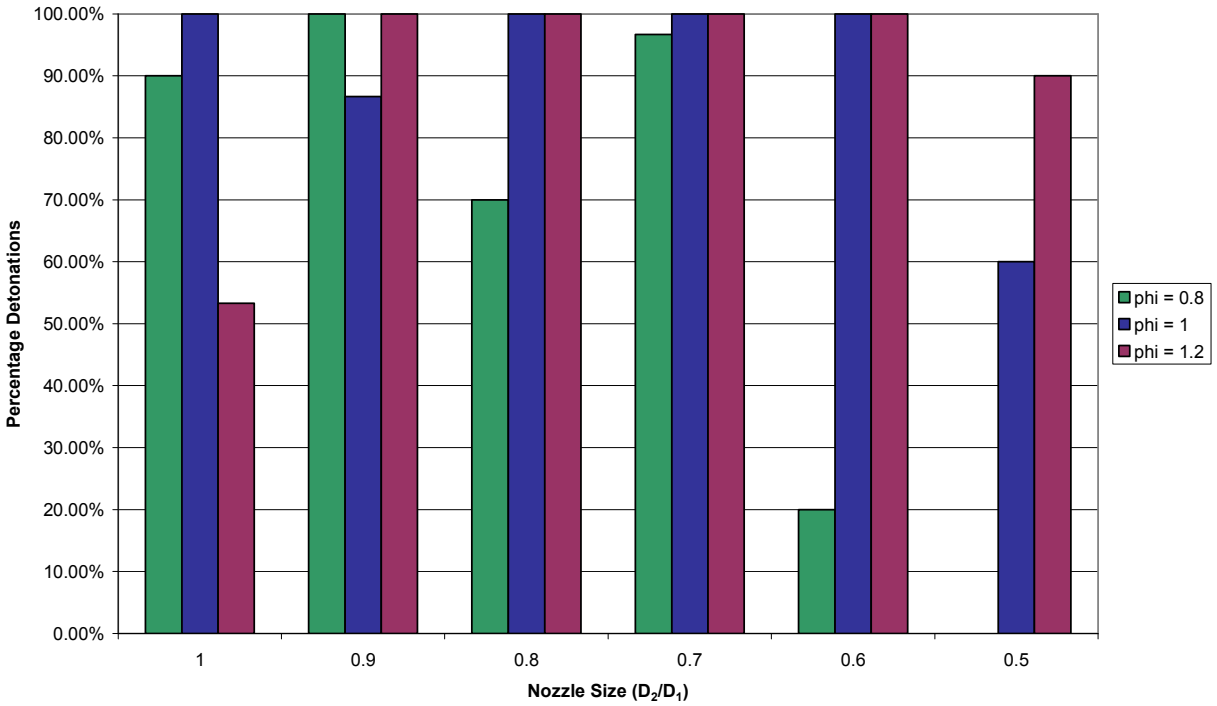

Figure 40. Percent detonations occurring with variation of equivalence ratio (spark delay = 0, Fill Fraction = 2)

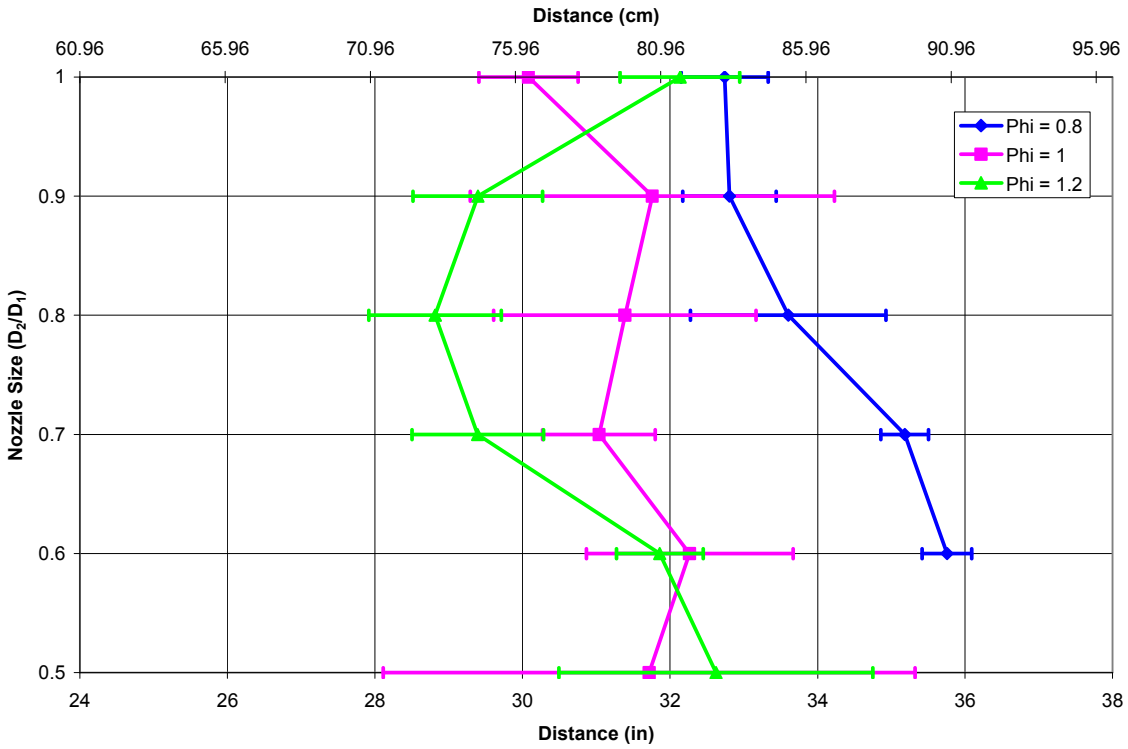

Figure 41. Average detonation distance versus nozzle size with variation of equivalence ratio (FF = 2, spark delay = 0)

The percentage of recorded detonations is also presented in Figure 40 and illustrates how decreasing or leaning the equivalence ratio serves to decrease the overall performance. Increasing the equivalence ratio produces more detonations and as shown in Figure 40 and produces a relatively shorter detonation distance as shown in Figure 41.

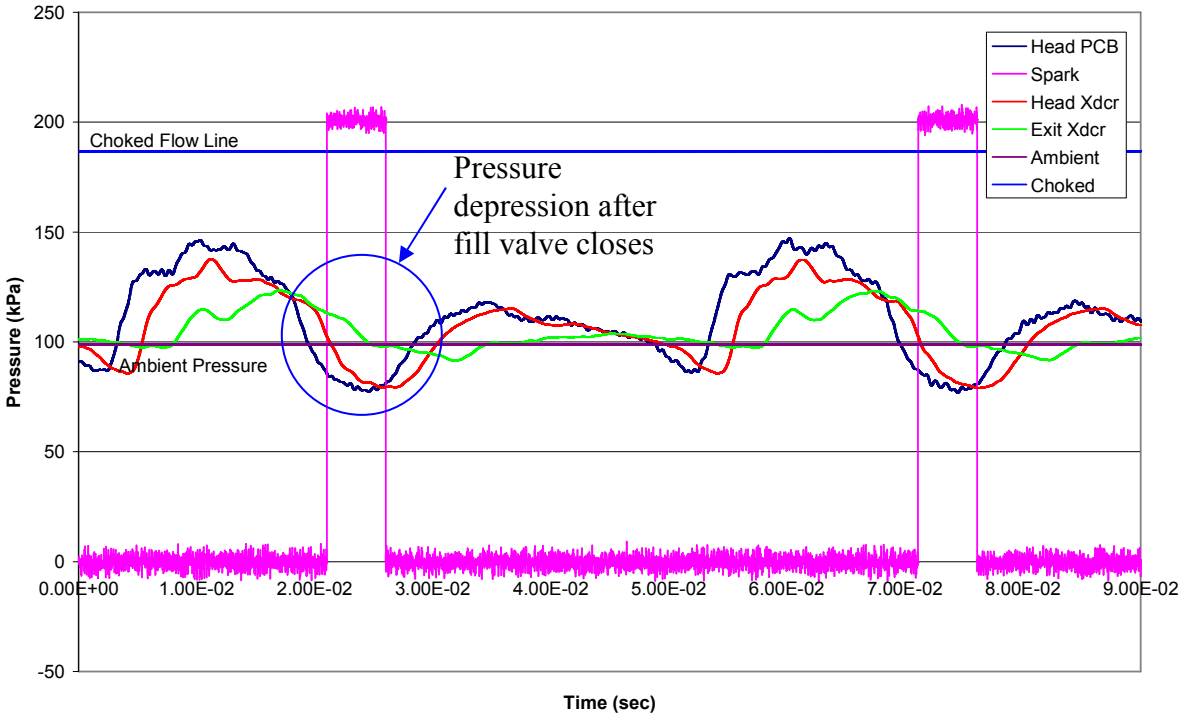

Figure 42. Pressure depression after fill valve closes (Cold Flow-No Ignition, D_2/D_1 = 0.85, spark delay = 5, FF = 2)

Variation of Initial Spark Time

The effects of varying the spark time are examined next. As the spark time is varied the pressure in the detonation tube is allowed to vary after closing of the fill valve. After the fill valve is closed the momentum of air continues to flow axially down the length of the detonation tube with an associated momentum. The pressure drops at the head of the tube from the resulting expansion wave and the flow from the exit of the tube

is slowed by the developing depression at the head of the tube, and after a brief period less than 0.01 sec, the pressure increases again. A plot of the pressure trace for the case of the open tube shows the resulting pressure depression at the head of the tube after the fill valve closes and how it has the potential for a large effect on ignition time (Figure 42). With no nozzle or restriction at the exit of the detonation tube more momentum and a large flow rate from the detonation tube exists and the potential for a larger expansion at the head of the tube occurs. A nozzle restriction at the tube exit slows the flow rate momentum from the tube exit and the associated pressure drop and expansion at the head of the detonation tube.

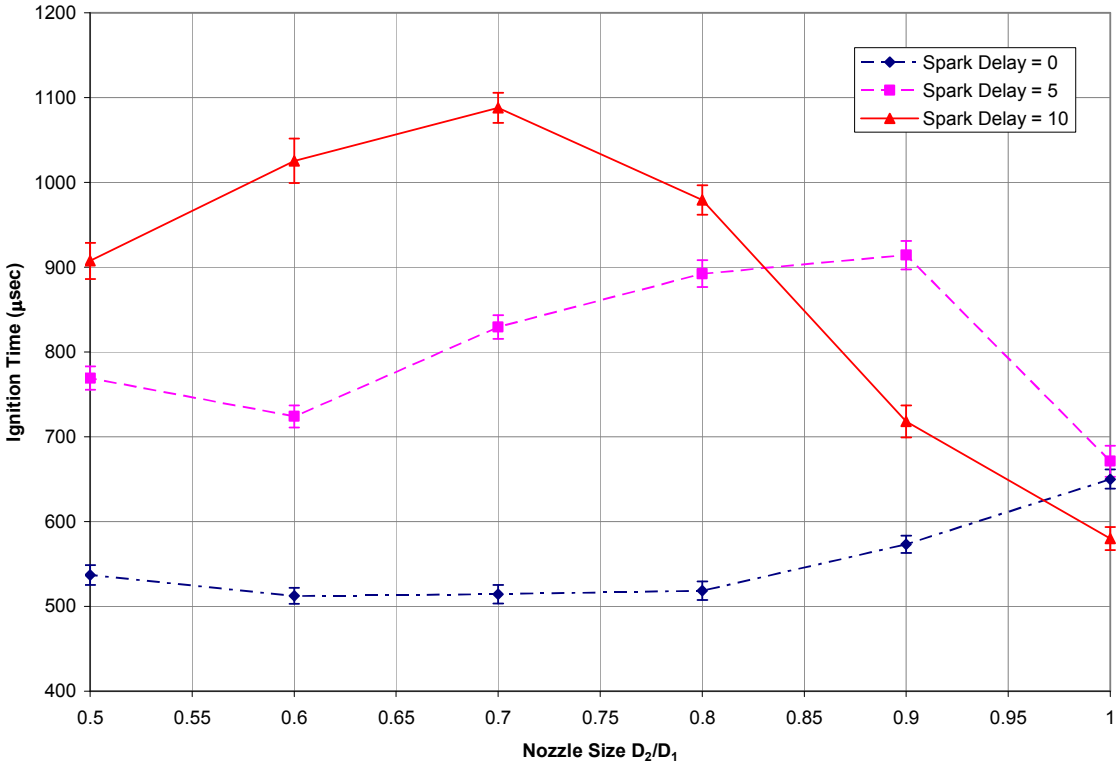

Figure 43. Ignition time versus nozzle size with varying spark delays (FF = 2, $\phi = 1$)

The resulting pressure drop after the fill valve closes can be observed to diminish as the flow is further restricted by decreasing the nozzle size also decreasing the momentum of the flow in the cold flow tests. The nozzle restriction at the tube exit has the overall effect of increasing the transient pressure at fill on the tube but also restrains the mass flow rate inhibiting the pressure depression and expansion at the head of the detonation tube. The dynamics of filling the tube varies as the nozzle size is reduced at the tube exit affecting ignition, detonation and DDT time. In all cases with restricted flow at the nozzle exit it can be observed as shown in Figure 43 that a spark delay of 0 provides the most optimal ignition initiation time. For a fuel to gain the most benefit the effects of increased pressure on the fill pulse it must have the potential to ignite rapidly before the detonation tube can blow down to ambient pressure after the fill valve is closed on the fill portion of the PDE cycle. This becomes a prime consideration when considering liquid fuels other than gaseous hydrogen or acetylene. Liquid fuels can have characteristically longer ignition times from droplet evaporation and require more ignition energy to initiate combustion. If the ignition process is of sufficient length the detonation tube will blow down and pressure will reduce closer to ambient before ignition actually occurs or even reduce below ambient or initial pressure in the case of the open non-restricted detonation tube.

The effects of spark delay on both detonation time and DDT time are presented below. Examination of both with a variation in nozzle size reveals the importance of initiating the spark as immediately as possible in the case of a restricted detonation tube.

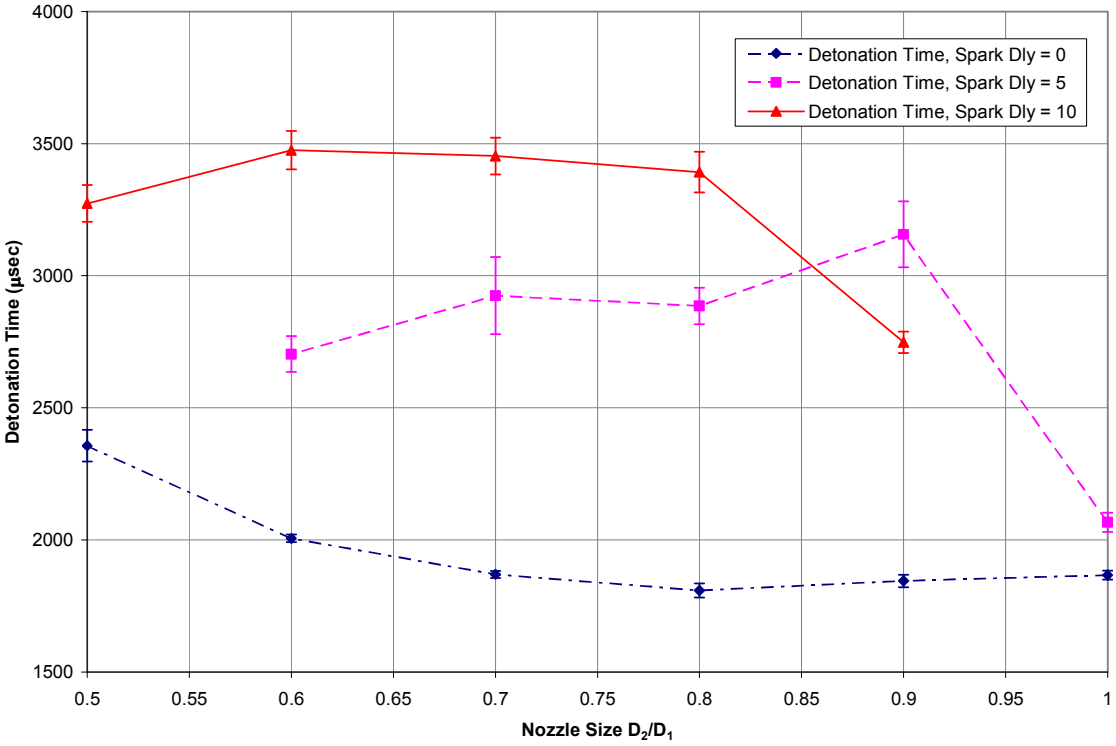

Figure 44. Detonation time versus nozzle size with spark delay variation (FF = 2, $\phi = 1$)

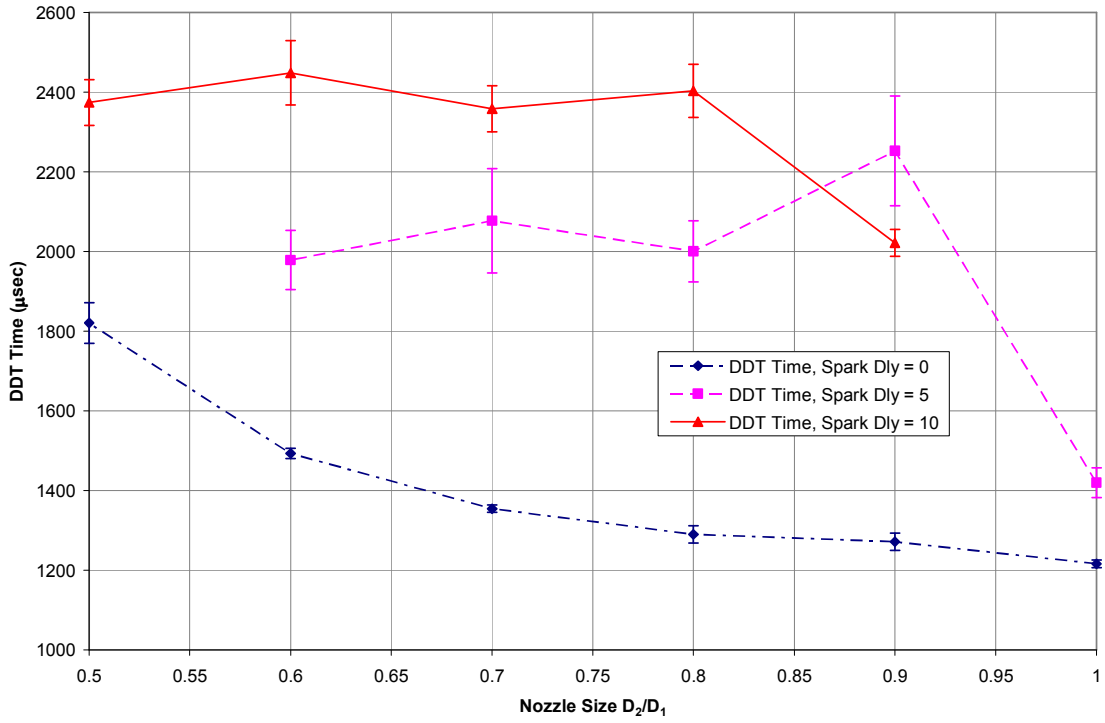

Figure 45. DDT time versus nozzle size with spark delay variation (FF = 2, $\phi = 1$)

For both detonation time and DDT time a spark delay greater than zero allows the tube to blow down to ambient and with the detonation distance further from the head of the detonation tube. In both cases of detonation and DDT time with spark delays greater than zero a less than optimal performance condition results when the detonation tube exit is restricted.

The effects of ignition (spark) delay on the percentage of recorded detonations and detonation distance are shown below in Figure 46 and Figure 47. The effects of ignition delay are quite significant. The number of recorded detonations decreases significantly with any preset spark delay greater than zero. After the fill valve closes considerable blow down of the pressure in the detonation tube occurs inhibiting ignition. The same can be observed in the case of detonation distance and time with a recognizable decrease in both.

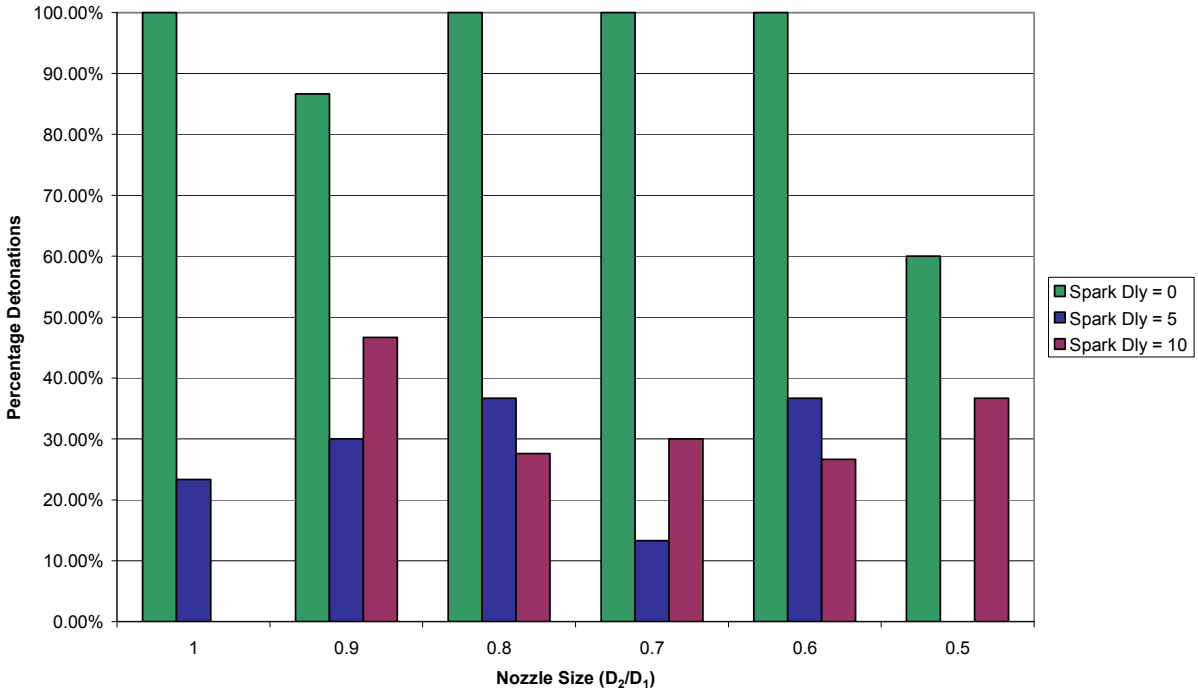

Figure 46. Percent detonations occurring with variation of spark delay ($\phi = 1$, FF = 2)

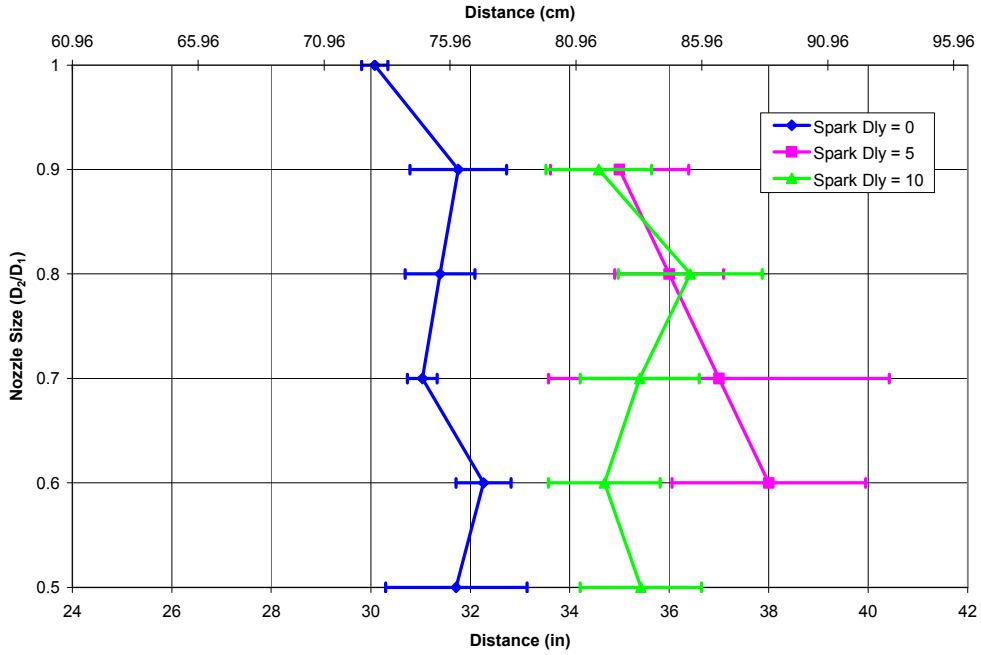

Figure 47. Average detonation distance versus nozzle size with variation of spark delay (FF = 2, $\phi = 1$)

Fill Fraction Variation

The effects of increasing the fill fraction and decreasing the nozzle size were examined and associated performance benefits were observed. Figure 48 is a plot of ignition time versus fill fraction. As can be observed in the figure a minimum ignition time corresponds to approximately 0.7 D_2/D_1. Ignition time plotted against initial pressure as in Figure 49 also shows that ignition time is reduced to a minimum for approximately 0.7 D_2/D_1.

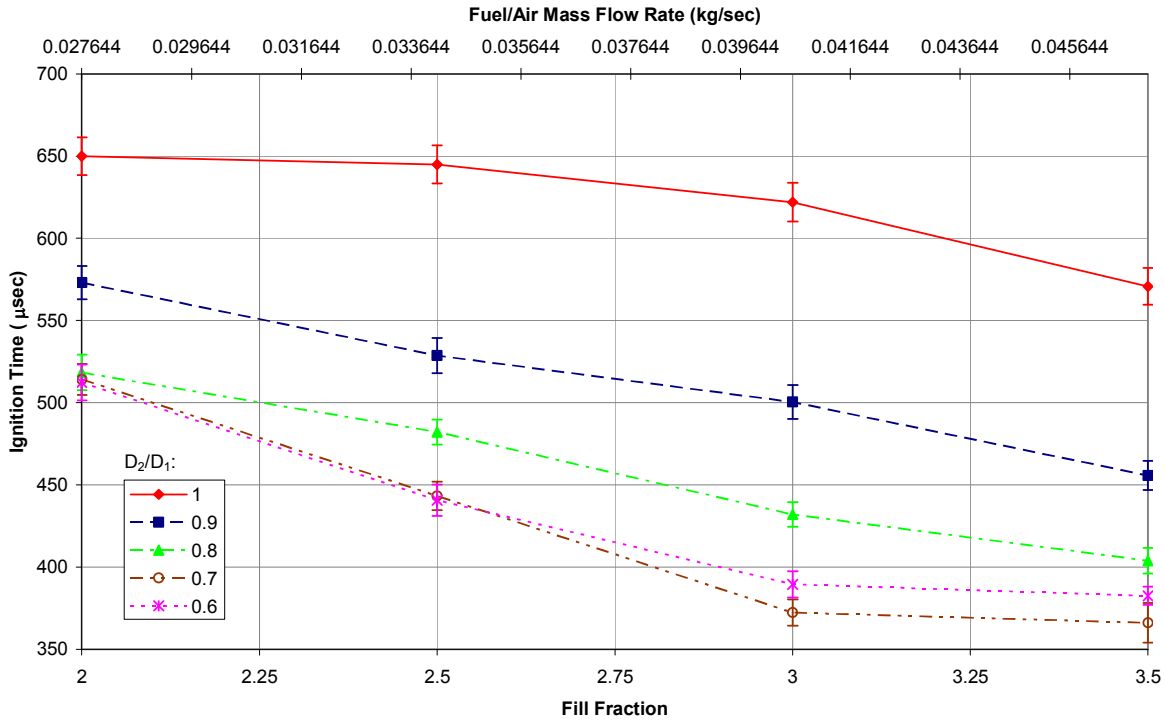

Figure 48. Ignition time versus fill fraction with nozzle size variation, D_2/D_1 ($\phi = 1$, spark delay = 0)

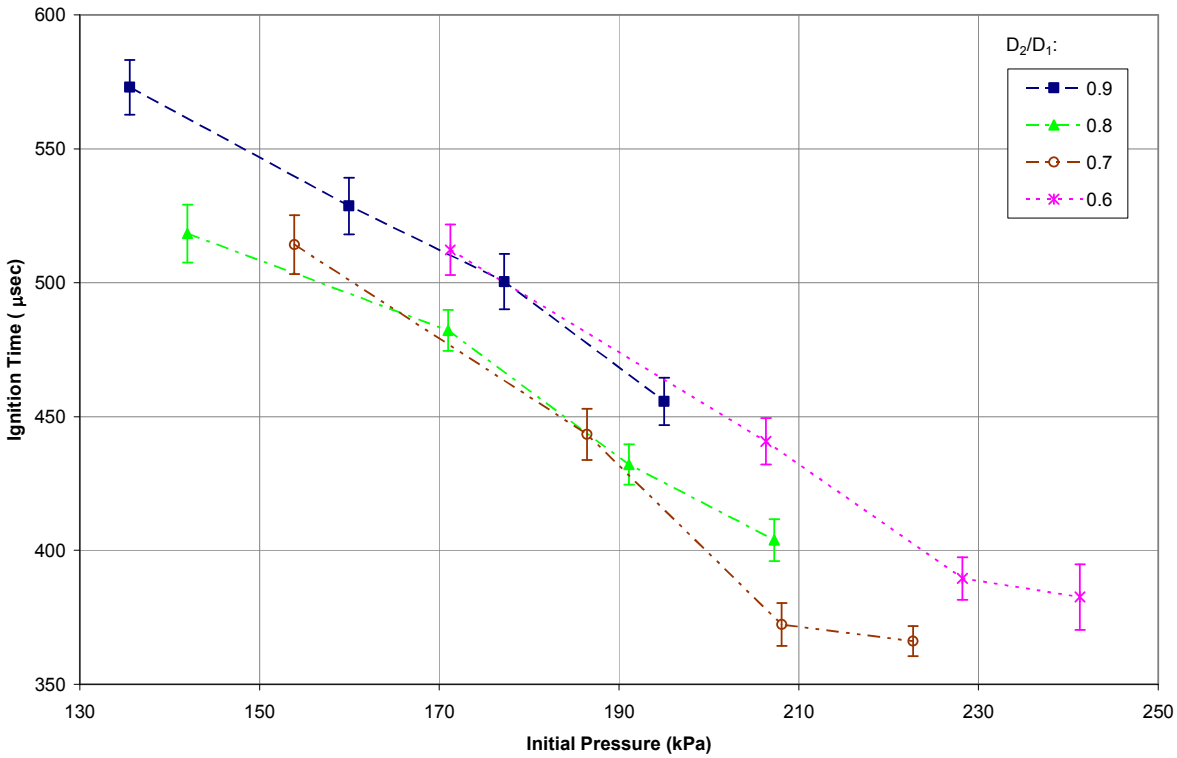

Figure 49. Ignition time versus initial pressure (Tube head) with varying nozzle sizes, D_2/D_1 ($\phi = 1$, spark delay = 0)

Plots of both detonation and DDT time for a variation in fill fraction are shown in Figure 50 and Figure 51. A general decrease in overall detonation time to a minimum at approximately 0.8 D_2/D_1 can be observed. The overall trend with DDT time for a variation in nozzle size with increasing fill fraction is a general increase in DDT time as nozzle size decreases. The trend toward an increase in DDT time becomes more pronounced as nozzle size is decreased below 0.8 D_2/D_1 indicating much of the decrease in overall detonation time can be attributed to the effects of pressure on the ignition time.

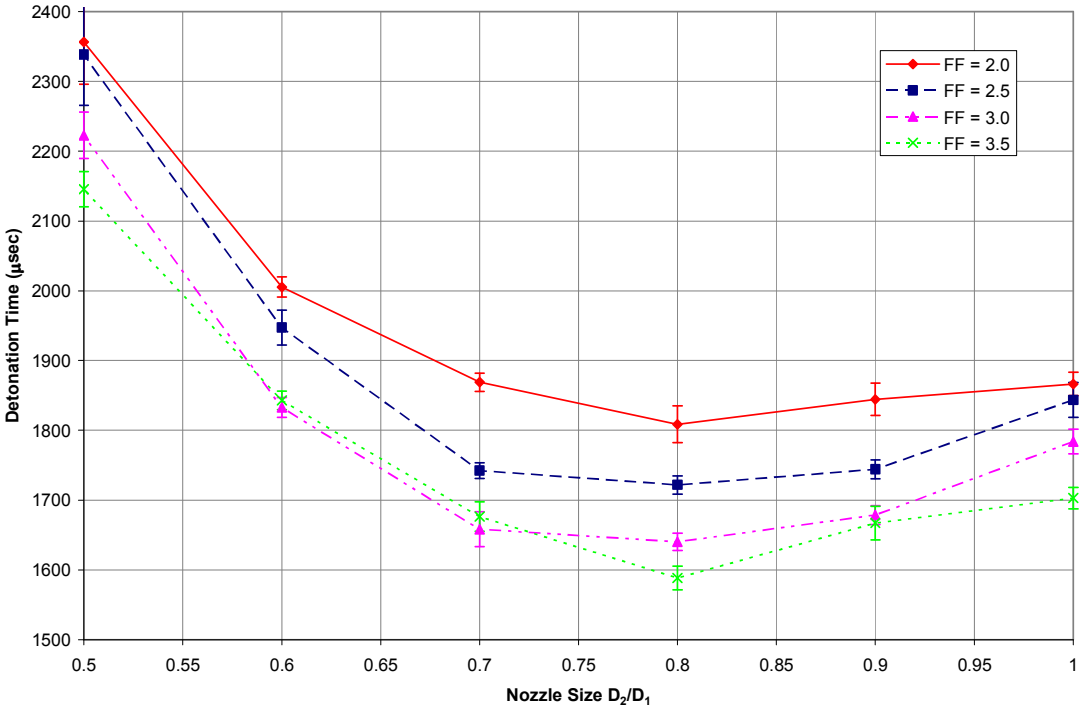

Figure 50. Detonation time versus nozzle size with varying fill fraction ($\phi = 1$, spark delay = 0)

Similar to the baseline test condition an increase in fill fraction variation also shows an increase in DDT time as nozzle size is decreased as shown in Figure 51. The percentage of detonations in Figure 52 is quite consistent until approximately 0.5 D_2/D_1

where the flow conditions at the nozzle exit become a factor. Figure 53 illustrates the recorded detonation distance with a variation in fill fraction. In general the overall trend is to reduce the detonation distance. The higher fill fraction at 3.5 has a large variation and data scatter due to some of the instabilities associated with restricting the nozzle exit of the PDE. In general the fill fraction corresponding to 3 produces the most predictable and minimal detonation distances. Higher fill fractions and smaller nozzle sizes generate more back pressure on the system and create more instability during operation as is discussed in the next section.

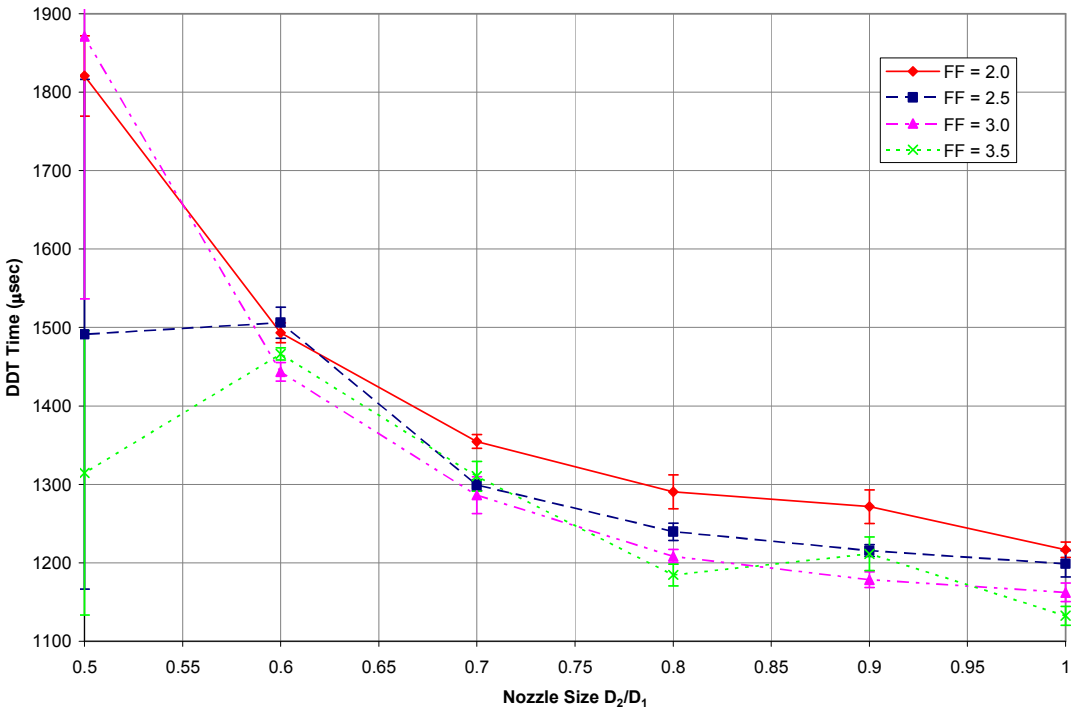

Figure 51. DDT time versus nozzle size with varying fill fraction ($\phi = 1$, spark delay = 0)

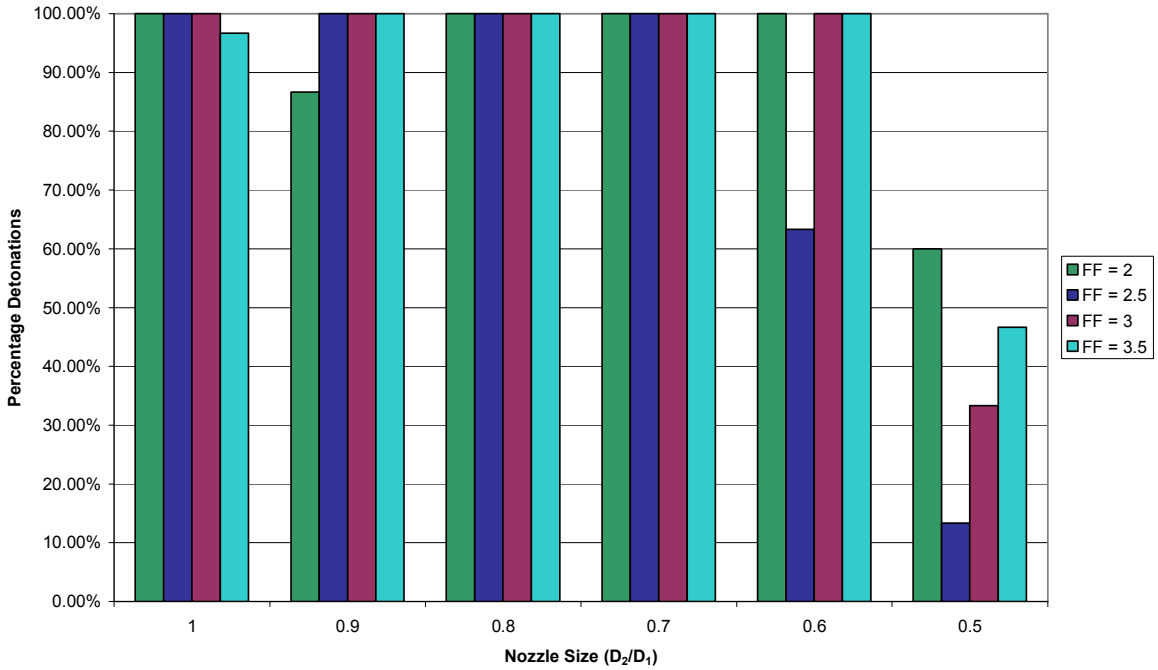

Figure 52. Percentage detonations occurring with variation of Fill Fraction (spark delay = 0, $\phi = 1$)

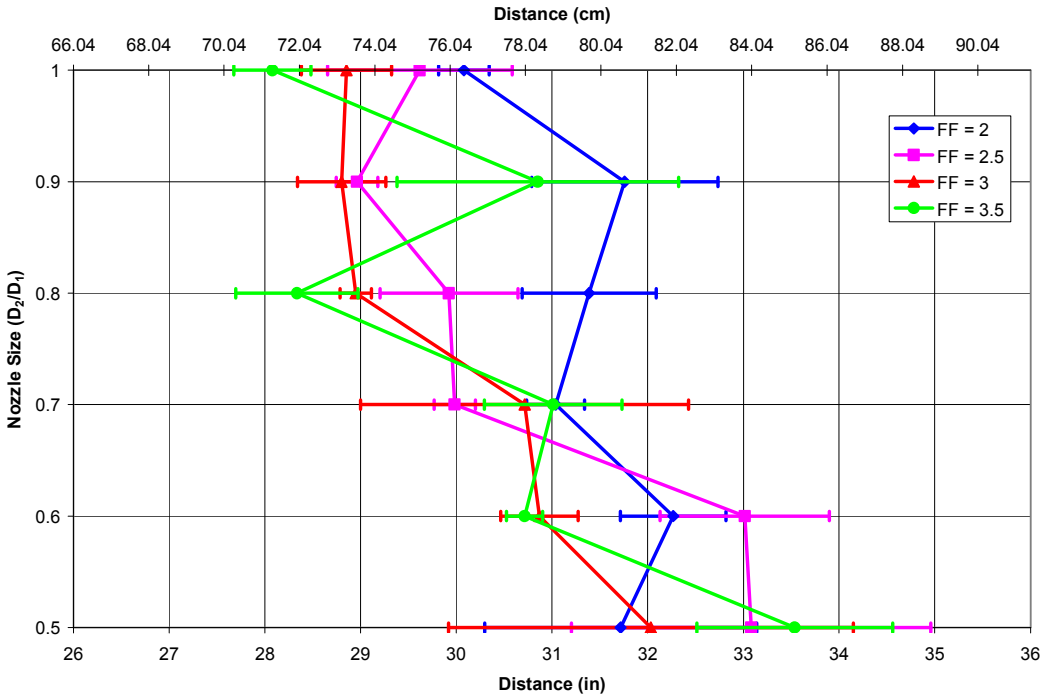

Figure 53. Average detonation distance versus nozzle size with fill fraction variation (spark delay = 0, $\phi = 1$)

VII. Conclusions and Recommendations

Conclusions

A major problem associated with attaching a nozzle restriction to the exit of the pulse detonation tube is overall system stability with regard to air and fuel flow once the combustion process begins. The measurements taken during the cold flow tests to examine pressure data were taken at identical preset engine test conditions to that of the hot ignition tests prior to spark discharge. The pulse detonation engine generates thrust by the large mass flux from the exit of the pulse detonation tube. After the spark is turned on, the engine begins firing, and the large mass flux exits the detonation tube, the tube is evacuated to a pressure below ambient. In the case of a detonation tube with no nozzle restriction at the exit, the pressure depression after the tube is fired is equalized more rapidly through the reverse flow of air back into the detonation tube and the flow from the purge pulse at the head of the tube before the fill valve again opens to flow the fuel and air mixture. The tube pressure equalizes quickly enough to allow for the fill valve to open again on the fill cycle allowing the fuel and air mixture to flow into the tube across the open poppet valve at an unchoked pressure ratio on the next fill cycle.

As the tube exit is further restricted by the nozzle orifice attached to the exit of the tube, the time to equalize the pressure after firing occurs over a larger period of time. Because the tube pressure is lower when the fill valve again opens the fill poppet valve at the head of the detonation tube chokes and decreases the mass flow rate across the valve.

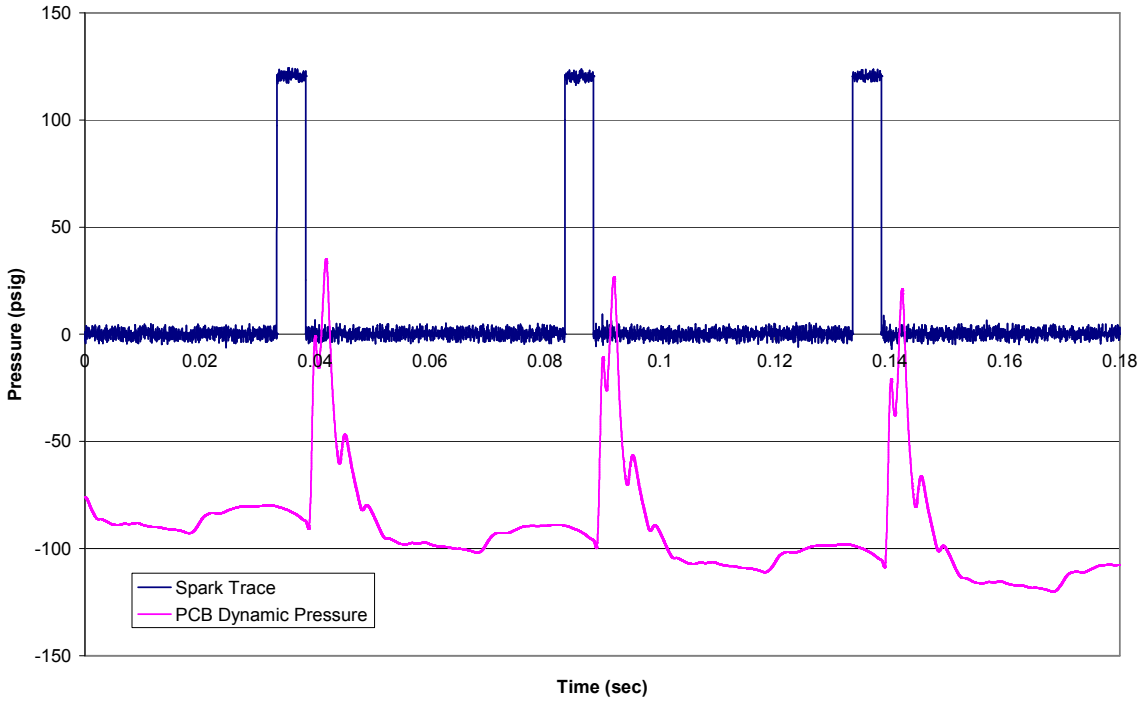

Figure 54 - PCB dynamic pressure transducer trace (D_2/D_1 = 0.6, spark delay = 0, FF = 2)

This phenomenon can be observed in an overall drop of the PCB dynamic pressure trace over the interval the data was taken in this research as represented by Figure 54. The pressure decreases after the spark is initiated as can be shown by the PCB dynamic pressure trace. The engine misfires on a single cycle to equalize the pressure in the detonation tube and then either back fires or continues to run at an unsteady and cyclic pulsing to again repeat the process. As the fill valve at the head of the tube becomes choked the mass flow rate becomes entirely dependent on the upstream manifold pressure and the tube begins partially fill with a loss of performance at the smaller nozzle orifice sizes as can be indicated by both the increase in ignition and DDT time below approximately 0.7 D_2/D_1 in most all cases presented above in the experimental results section.

A nozzle orifice restriction has demonstrated some potential performance benefits, mostly in reducing ignition time though back pressure from the nozzle at the tube exit can have a large effect on the flow conditions upstream, varying the equivalence ratio and flow dynamics through the valve. Increasing the free stream pressure inside the detonation tube shows less benefit associated with reducing DDT time and distance. A very small window of time is available following the fill pulse in the PDE cycle in which to extract performance benefits associated with increased pressure. DDT time appeared in most cases to not exhibit any appreciable performance benefits from the effects of increasing pressure. The less promising performance effects of pressure on DDT can be primarily attributed to the fact that the blow down time of a pulse detonation tube after the fill portion of the cycle occurs very rapidly. Following the peak pressure after the fill portion of the PDE cycle the tube pressure decreases or decays more rapidly with a steeper slope for a larger orifice size and decreases more slowly with decreasing nozzle size diameter providing a longer time period in which the tube pressure relaxes or blows down to ambient pressure. In comparison to the overall pressure rise from the combustion and subsequent detonation wave, only a very brief time period is available with which to extract any associated performance benefit. The nozzle exit can generally be restricted until the flow at the nozzle exit restricts the detonation tube backflow after firing, enough to inhibit the fill valve from remaining at an unchoked flow condition during operation. As the fill valve at the head of the detonation tube reaches a choked flow condition the mass flow rate across the valve becomes entirely dependent on upstream pressure, the mass flow rate begins to fluctuate and the associated back pressure

can have a large influence on the flow of the fuel/air mixture at tube fill. Filling the detonation tube on the fill cycle with the appropriate and uniformly mixed fuel/air mixture on the fill cycle is essential to achieving maximum thrust and performance from the detonation tube. As can be shown from the tests of varying the equivalence ratio the ignition time can be strongly influenced by the fuel/air mixture ratio.

While this research study was effective at illustrating the ability of a choked nozzle exit to reduce ignition time it has also pointed out the significance of the effects of back pressure from the nozzle exit on overall detonation performance. A brief multi-tube study consisting of two detonation tube was also performed and revealed that smooth and uniform flow to the detonation tube is important in controlling critical performance parameters such as equivalence ratio. The results of which are included in the appendix. The ignition time was reduced in the multi-tube study at a data point known to have deviated from ignition theory where a variance in ignition time varies in proportion to the inverse of pressure. The study showed only a reduction in equivalence ratio variance suggests the not that the problem was eliminated entirely. Adequate design of a fuel/air supply system is essential for practical PDE operation to ensure the critical parameter of equivalence ratio is properly measured and controlled.

A problem associated with the choked condition at the nozzle exit when using the PDE as a propulsive device for aerospace applications is that the ambient air pressure drops as an ascent in altitude made, hypothetically making the fill valve at the tube head more susceptible to a choked flow condition. For the PDE to use a nozzle at the detonation tube exit or even ascend in altitude to a lower pressure the engine control

system must be able to adjust the upstream pressure across the fill valve to operate at choked flow condition to ensure adequate mass flow rate to continue to fill the detonation tube to capacity before ignition.

A major problem to be overcome that was not examined in this report is the need to also control shock reflections with any kind of nozzle attachment to the end of a pulse detonation tube. In very high frequency PDE applications a shock reflection propagating backwards in the detonation tube has the potential to interfere with the purge and fill flow dynamics associated with the pulse detonation engine cycle.

Cooling of the pulse detonation tube and associated components becomes of significance when using a nozzle as a flow restriction device. Any restriction results in reduction and altered flow characteristic to some extent of the detonation tube. Cooling of the detonation tube is essential for continued operation of the PDE to remain below material thermal structural limits but also to control hot spots that can develop in the detonation tube. A fuel such as hydrogen is relatively easy to ignite and detonate in contrast to a liquid fuel such as JP-8. Thermal heating of the detonation tube would be of some benefit to aid in droplet evaporation and decreased ignition time however exceedingly high temperatures at point sources within the detonation tube also offer the potential for alternate sources of ignition. If a point source of ignition at a location some distance from the head of the detonation tube ignites the fuel air mixture while filling the tube, the potential exists for a combustion wave to initiate and travel in both directions, either of which will create a detonation and one combustion wave traveling in the opposite direction to that desired.

Most notable in all the experimental data was the more optimal ignition condition of zero spark delay. Though the spark is initiated in an expansion wave the associated pressure is still at a maximum after the fill valve closes. A fuel such as hydrogen with relatively low ignition time offers more potential to take advantage of the increased pressure on the fill pressure pulse immediately after the fill valve closes. A liquid hydrocarbon fuel with a longer ignition time would be less advantageous to benefit from the increased pressure on the fill pressure pulse. An advantage can be observed with using a nozzle and a spark delay greater than zero is used in that the characteristic pressure dip or depression following closure of the fill valve diminishes from the reduces mass flow rate and associated momentum from the exit of the detonation tube.

Some amount of mechanical pre-compression is possible using a nozzle restriction at the exit of the pulse detonation tube and has been shown to affect primarily the ignition time with less effect on the DDT time. The unsteady nature of the pulse detonation engine does not readily lend itself to a simple optimal nozzle design or analytical flow model with which to readily estimate its performance. In considering any nozzle restriction at the exit of a pulse detonation tube the unsteady flow dynamics through the detonation tube present a continually changing set of loss coefficients and flow parameters based on the mass flow with which to determine performance. Experimentation and research to examine the effects of impulse performance from a single detonation tube has been documented and has shown associated performance benefits. Multi-cycle pulse detonation presents an entirely unique problem in that the PDE must still operate within a cycle of filling, firing and purging the tube with the only

potential for a variation in pressure available from the compressible nature of the fuel/air mixture.

Recommendations

Future research similar to that undertaken in this research must have an adequate method on measuring a controlling a uniformly distributed flow of fuel and air mixture. As can also be noted by engine flow conditions presented in the appendix, acquiring data at a steady state condition is essential to proper measurement of engine performance. A notable trend is a decrease in upstream manifold fuel pressure after ignition due in part to the reduction in downstream pressure in the detonation tube at fill when the valve opens. Control of upstream fuel and air flow conditions are essential to properly measure and predict performance of the PDE. The detonation tube pressure must be equalized when run with a nozzle restriction on the tube exit in multi-cycle operation to prevent choking of the fill valve, the fill valve must be operated at a choked condition. A robust fuel/air supply system for testing under identical conditions of choked flow with accurate measurement of key engine parameters is essential to future research on nozzle and choke flow studies of the PDE.

While a Schelkin spiral has been proved quite effective at reducing DDT time the research performed herein was aimed at isolating the effects of pressure to the extent possible. A combination of a Schelkin spiral and optimal nozzle orifice size could ultimately produce a minimum detonation tube length but was beyond the scope of this research. A recommendation for future testing would be to examine the effects of a combination of some length of a Schelkin spiral and nozzle combination to reduce the

DDT time. Given that the results of this research showed potential performance benefits at approximately 70% nozzle restriction a worthwhile research effort might entail examining the effects of thrust with a converging-diverging nozzle with a similar exit area to tube diameter restriction. A CFD study to examine optimal nozzle dimensions for a PDE nozzle would offer another avenue for continued research on the PDE. Still yet another interesting option for research would be to examine larger tube diameters than used in this research for comparison to the nozzle to tube diameter ratio of which a minimum ignition time corresponded to an orifice to tube diameter of approximately 70%.

It is quite clear from this study that a nozzle orifice or any kind of flow restrictor with a diameter less than the detonation tube diameter will have to be designed with consideration for the choked flow and resulting shock that occurs at the detonation tube exit. The detonation that proceeds down the detonation tube interacts with the nozzle restriction in addition to the shock produced at the nozzle exit from the choked flow. The benefits from restricting the nozzle flow have been noted in this report but solution of the problems associated with restricting the flow will require some form of a PDE design solution to the existing configuration. The tube must be filled to a maximum pressure without interference effects of ambient pressure, choked flow at the fill valve, or shock reflections from the nozzle exit.

For any success using a nozzle attached to the end of a pulse detonation tube the associated difficulties described and documented herein of filling, firing, and purging must be overcome. This research has hopefully contributed to a greater understanding of

the effects of adding a flow restriction nozzle to the exit of a pulse detonation tube and contributed to greater knowledge of pulse detonation engine research in an effort to overcome the inherent difficulties and capitalize on the associated benefits varying the detonation tube pressure using nozzle restrictions and also by varying the mass flow rate and associated upstream stagnation pressure.

Appendix A: Engine Performance for Hot Ignition Testing

Engine Fuel and Air Mass Flow Rate Hot-Ignition Tests

A plot of air and fuel mass flow rate versus nozzle size for varying fill fractions is plotted below for the ignition engine tests. Both mass flow rates were quite consistent across the spectrum of engine performance conditions and show that conditions upstream of the fill and purge valves were appropriately adjusted to maintain constant fill fraction and mass flow.

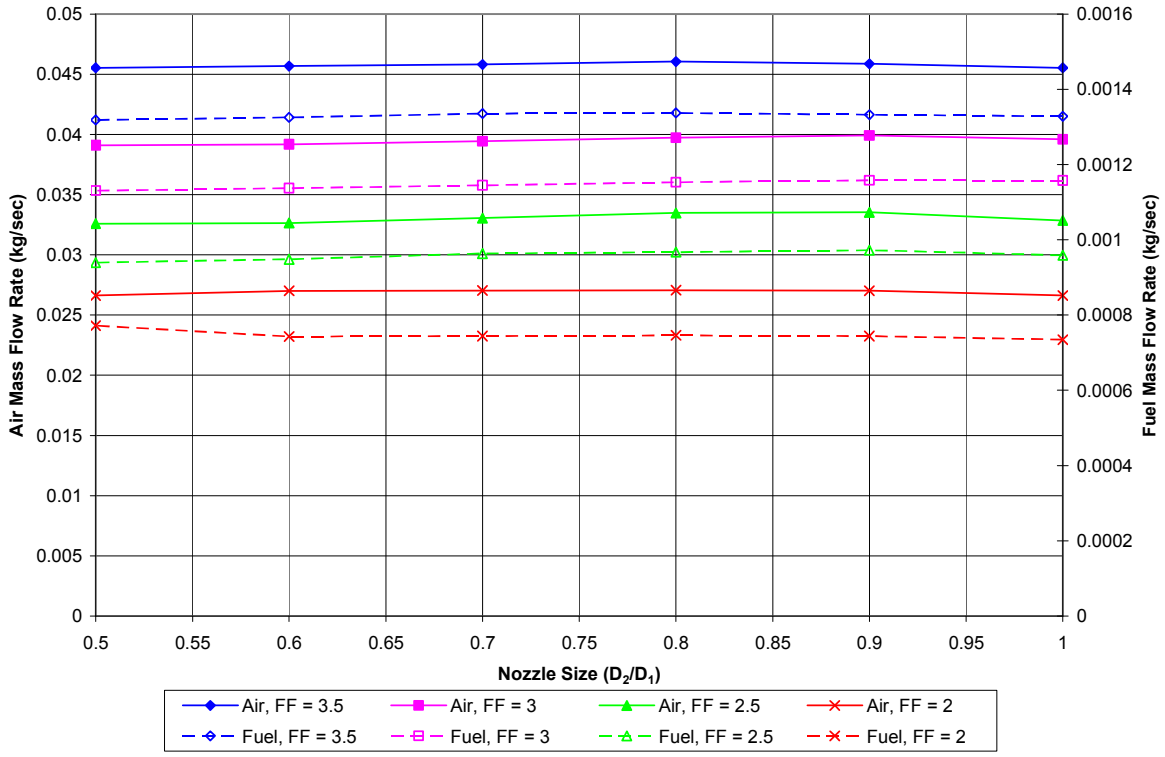

Figure 55 - Engine fuel and mass flow rate versus nozzle size for a variation in fill fraction

Hot-Ignition and Cold Flow Manifold Pressure Comparison

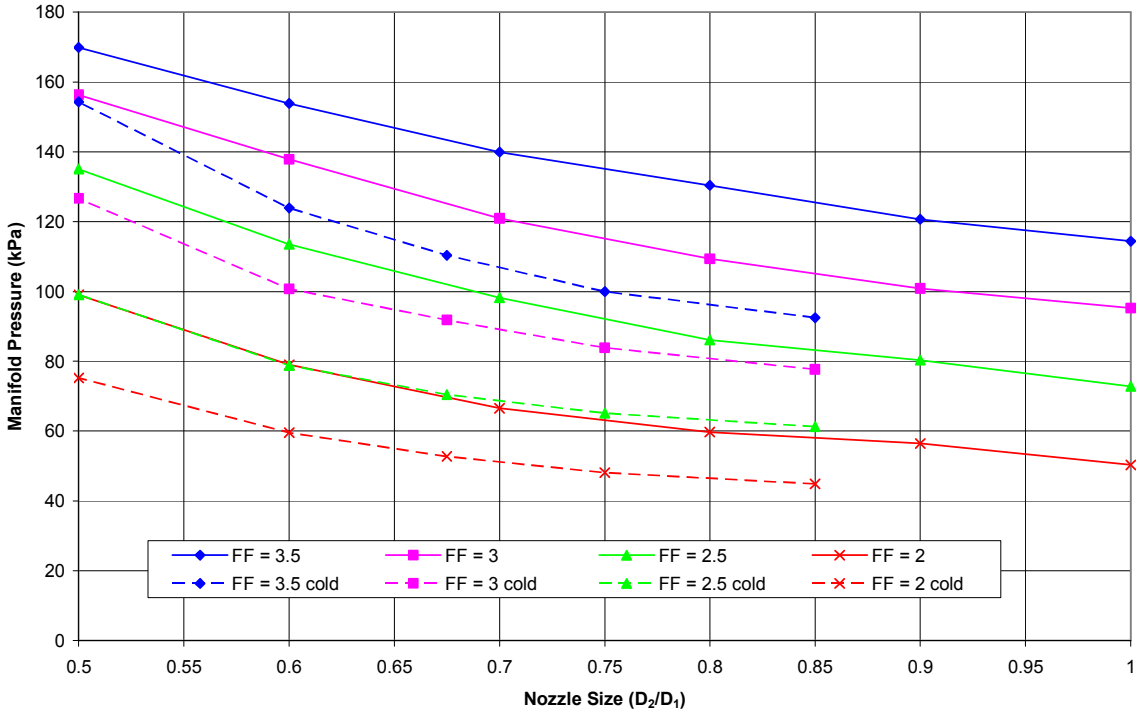

Figure 56 - Engine manifold pressure versus nozzle size comparison for cold flow and hot ignition engine runs

Figure 56 illustrates the manifold pressure differences upstream of the fill valves for the ignition and cold flow tests. For the cold flow pressure measurement tests the hydrogen was not flowing and contributed to a difference in manifold pressure for both the ignition and cold flow engine tests.

Hot-Ignition and Cold Flow Air Mass Flow Rate Comparison

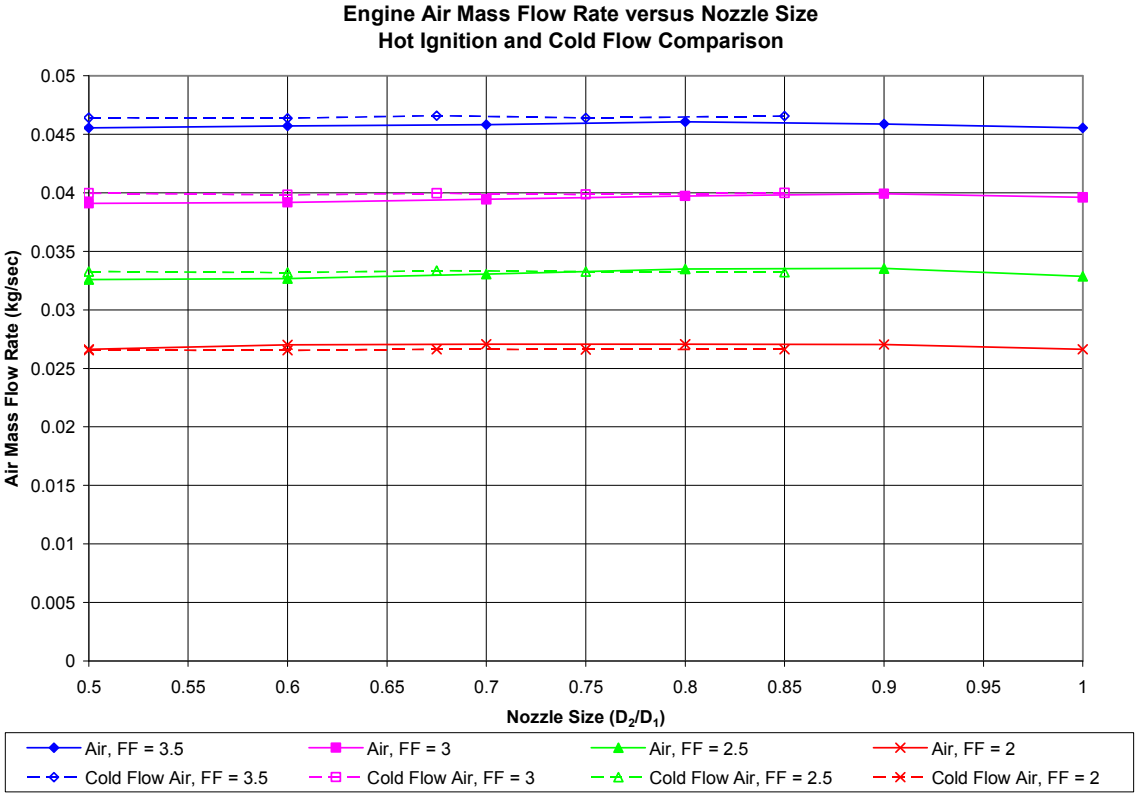

Figure 57 - Engine air flow rate versus nozzle size for comparison of ignition and cold flow tests

Engine air mass flow rates for both the ignition tests and cold flow are presented above. The above chart serves to illustrate the air mass flow rates were relatively close for both the ignition tests and cold flow (no ignition) tests. The difference in pressure in Figure 56 is due to the flow of hydrogen in the ignition tests that was not flowing in the cold flow pressure tests.

Appendix B: Initial PDE Nozzle Tests with 93 cm Detonation Tube

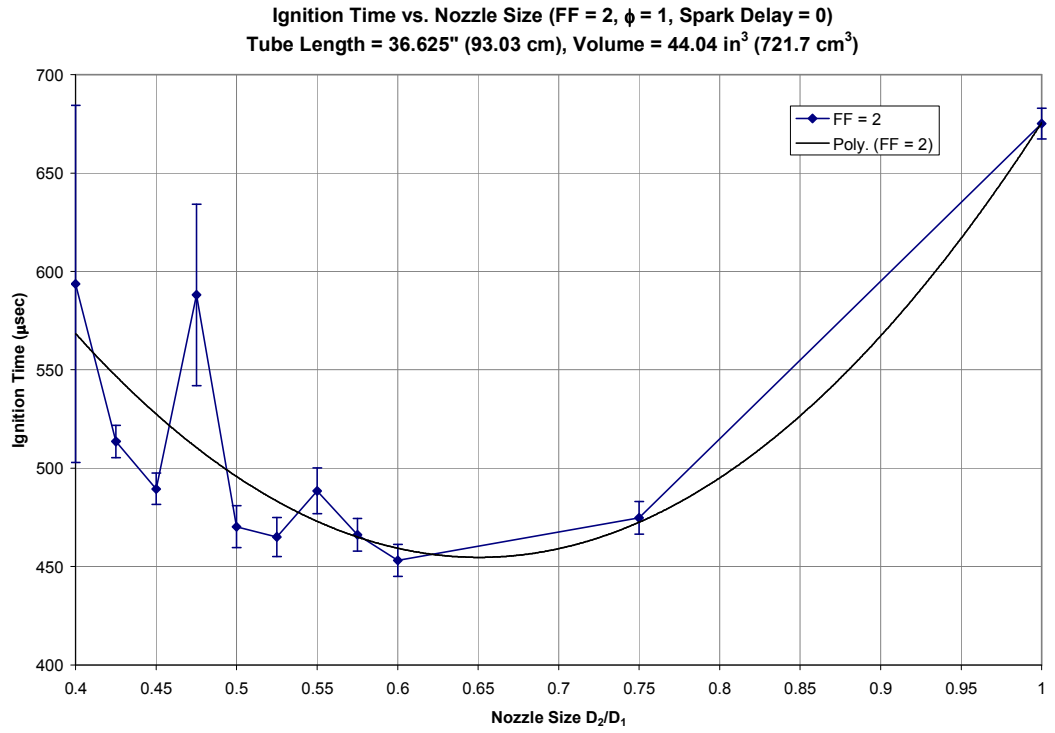

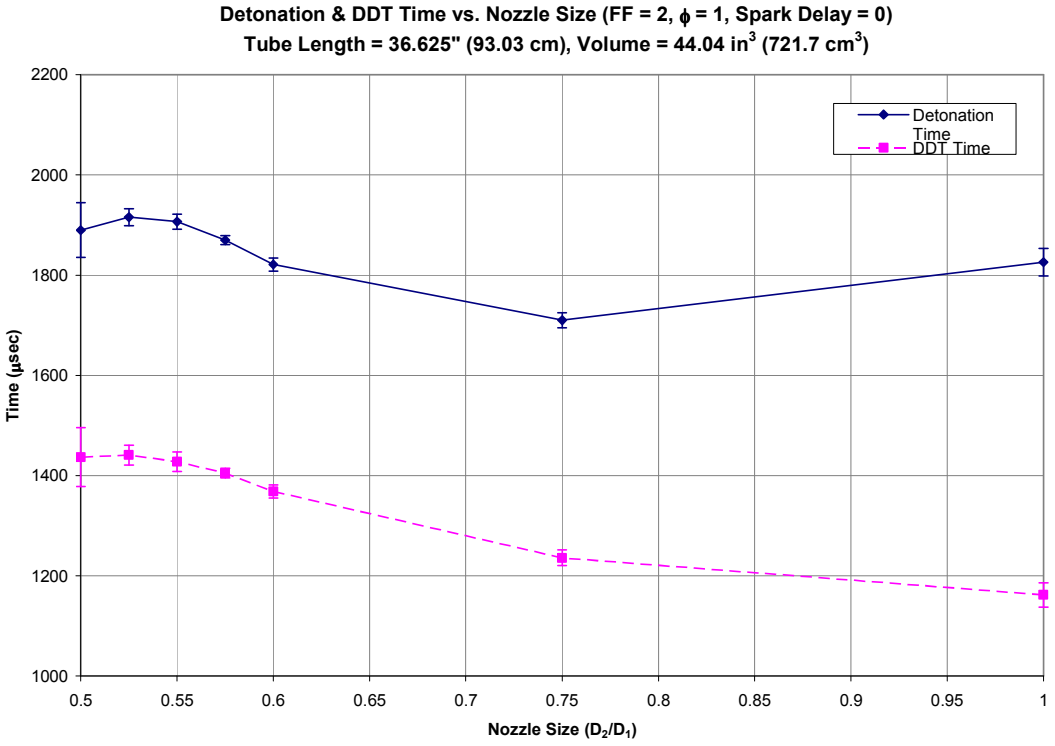

Appendix C: Single versus multi-tube test comparison at 0.65 D_2/D_1 nozzle size

All times in microsec (μsec)

# Tubes:	1	1	2	2
	Run3	Run4	Run5	Run6
	484	505	463	487
	551	480	515	461
	524	515	460	495
	512	474	477	440
	497	521	427	463
Run	517	520	475	480
Times:	491	495	508	489
	503	486	440	441
	501	498	447	479
	470	478	466	485
	521	522	512	468
	524	516	457	464
	500	474	449	478
	517	487	457	470
	558	538	396	417
Average:	511.3333	500.6	463.2667	467.8
Std Dev:	23.3136	20.52803	31.98765	21.3682

Average 1 Tube (Run 3&4)	Average 2 Tubes (Run 5&6)	Difference
505.9667	465.5333	40.43333

Appendix D: MATLAB code for pressure measurement at spark discharge

```
close all
clear all

Q = xlsread('Run2-2.xls');
[m,n] = size(Q)

k = n/5

t = []; c = [];  d = [];
ixmax = 3.9e5;
for i =1:k
        t = [t; Q(:,5*i-4)];
        c = [c; Q(:,5*i-2)];
        d = [d; Q(:,5*i-1)];
end
clear Q

        t = t(1:ixmax);
        c = c(1:ixmax);
        d = d(1:ixmax);

figure
plot(t,d,'b',t,c,'m')
zoom on

ix = 1+find(c(1:end-1)>2 & c(2:end)<2)
hold on
dsamp = d(ix)
plot(t(ix),dsamp,'ro')

dsamp_mean = mean(dsamp)
dsamp_std_dev = std(dsam
```

Appendix E: Cold Flow Pressure Trace Measurements

Appendix E is a summary of all measurements using the Sensotec 100 psia pressure transducers at the tube head and exit. Runs 2 through 37 are included. Run 1 was a test measurement with results duplicated at Run 2.

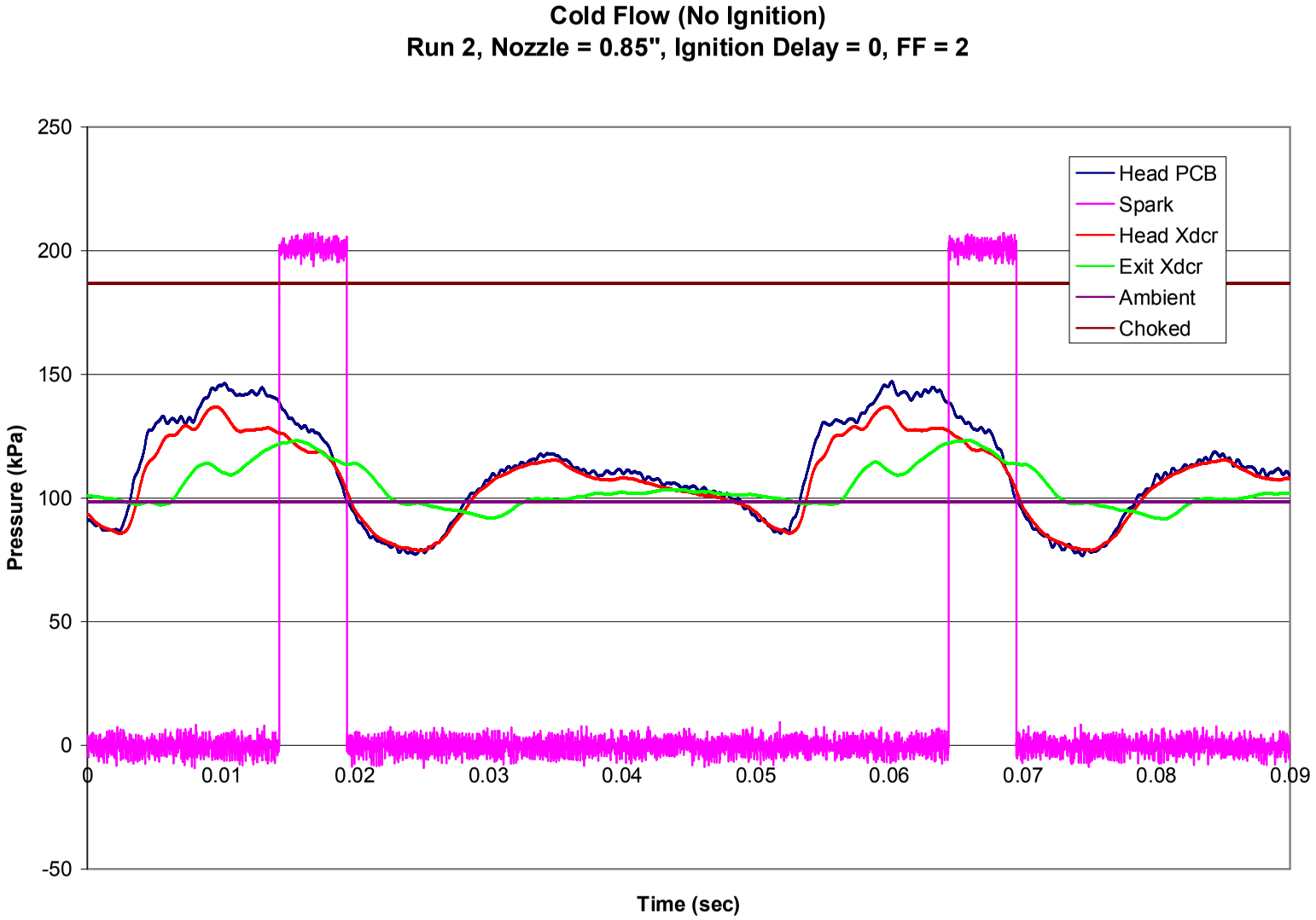
Cold Flow (No Ignition)
Run 2, Nozzle = 0.85", Ignition Delay = 0, FF = 2
Pressure (kPa)
250
200
150
100
50
0
-50
0
0.01
0.02
0.03
0.04
0.05
0.06
0.07
0.08
0.09
Time (sec)
Head PCB
Spark
Head Xdcr
Exit Xdcr
Ambient
Choked

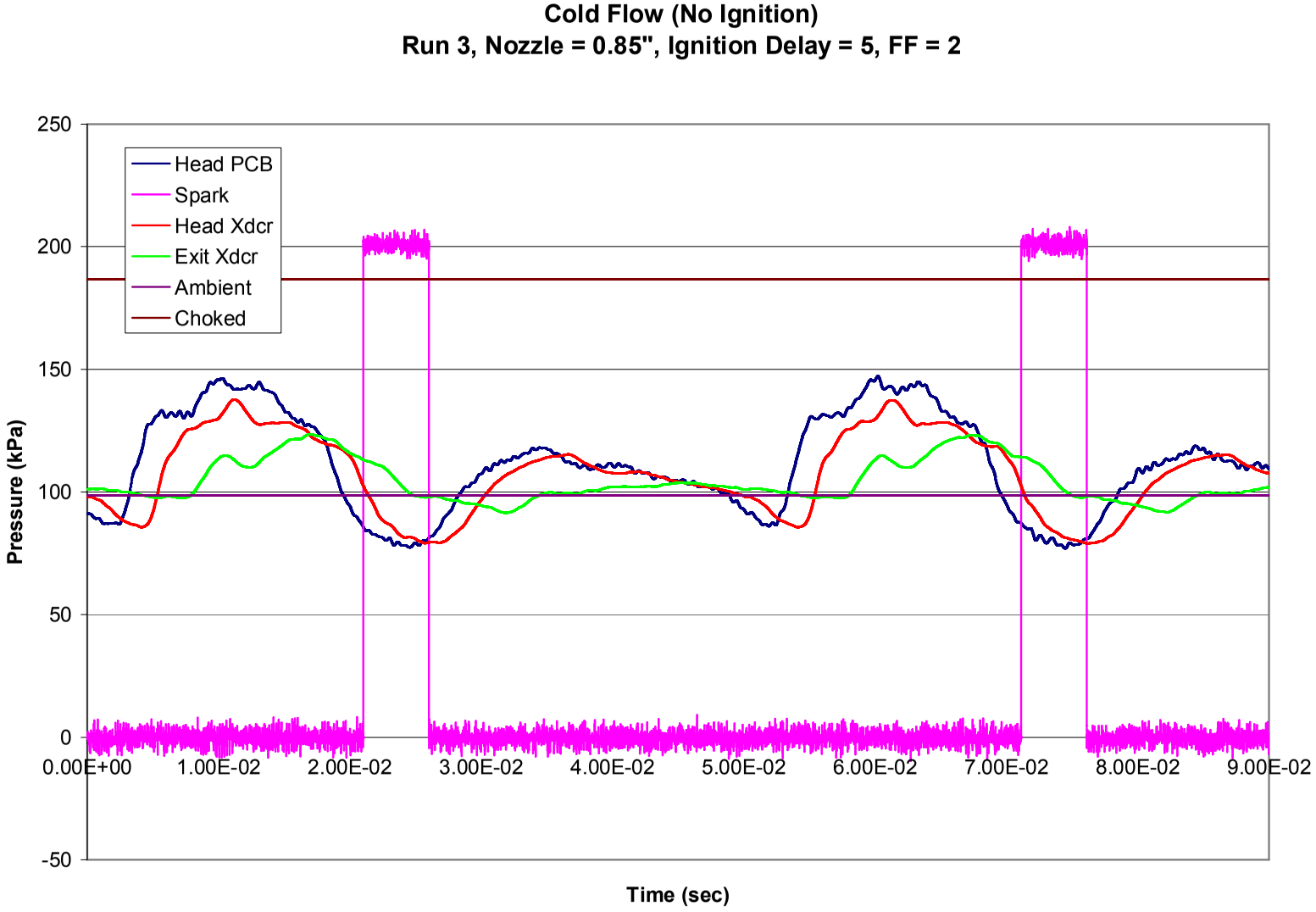
Cold Flow (No Ignition)
Run 3, Nozzle = 0.85", Ignition Delay = 5, FF = 2
Head PCB
Spark
Head Xdcr
Exit Xdcr
Ambient
Choked
Pressure (kPa)
250
200
150
100
50
0
-50
0.00E+00
1.00E-02
2.00E-02
3.00E-02
4.00E-02
5.00E-02
6.00E-02
7.00E-02
8.00E-02
9.00E-02
Time (sec)

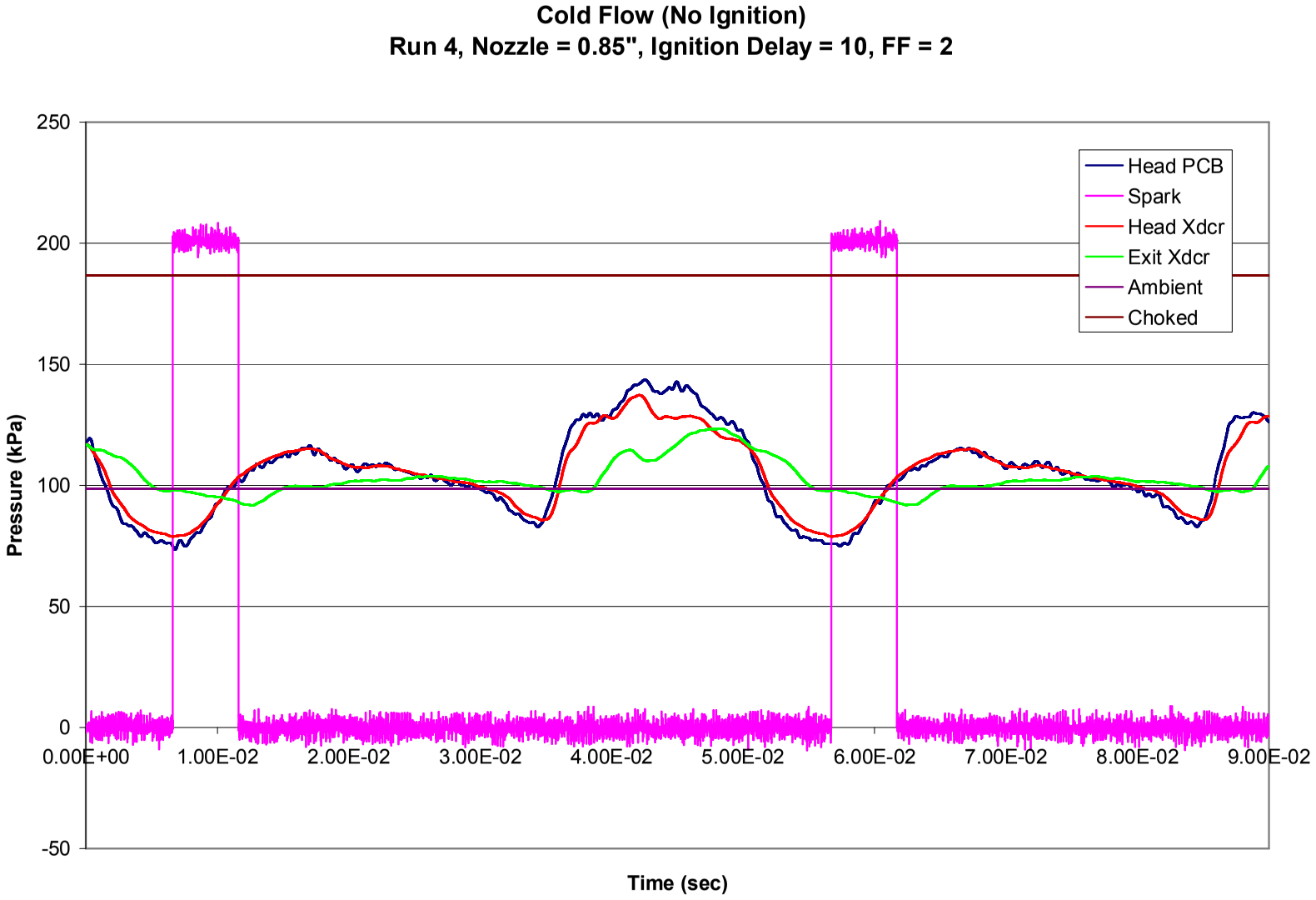
Cold Flow (No Ignition)
Run 4, Nozzle = 0.85", Ignition Delay = 10, FF = 2
Pressure (kPa)
250
200
150
100
50
0
-50
0.00E+00
1.00E-02
2.00E-02
3.00E-02
4.00E-02
5.00E-02
6.00E-02
7.00E-02
8.00E-02
9.00E-02
Time (sec)
Head PCB
Spark
Head Xdcr
Exit Xdcr
Ambient
Choked

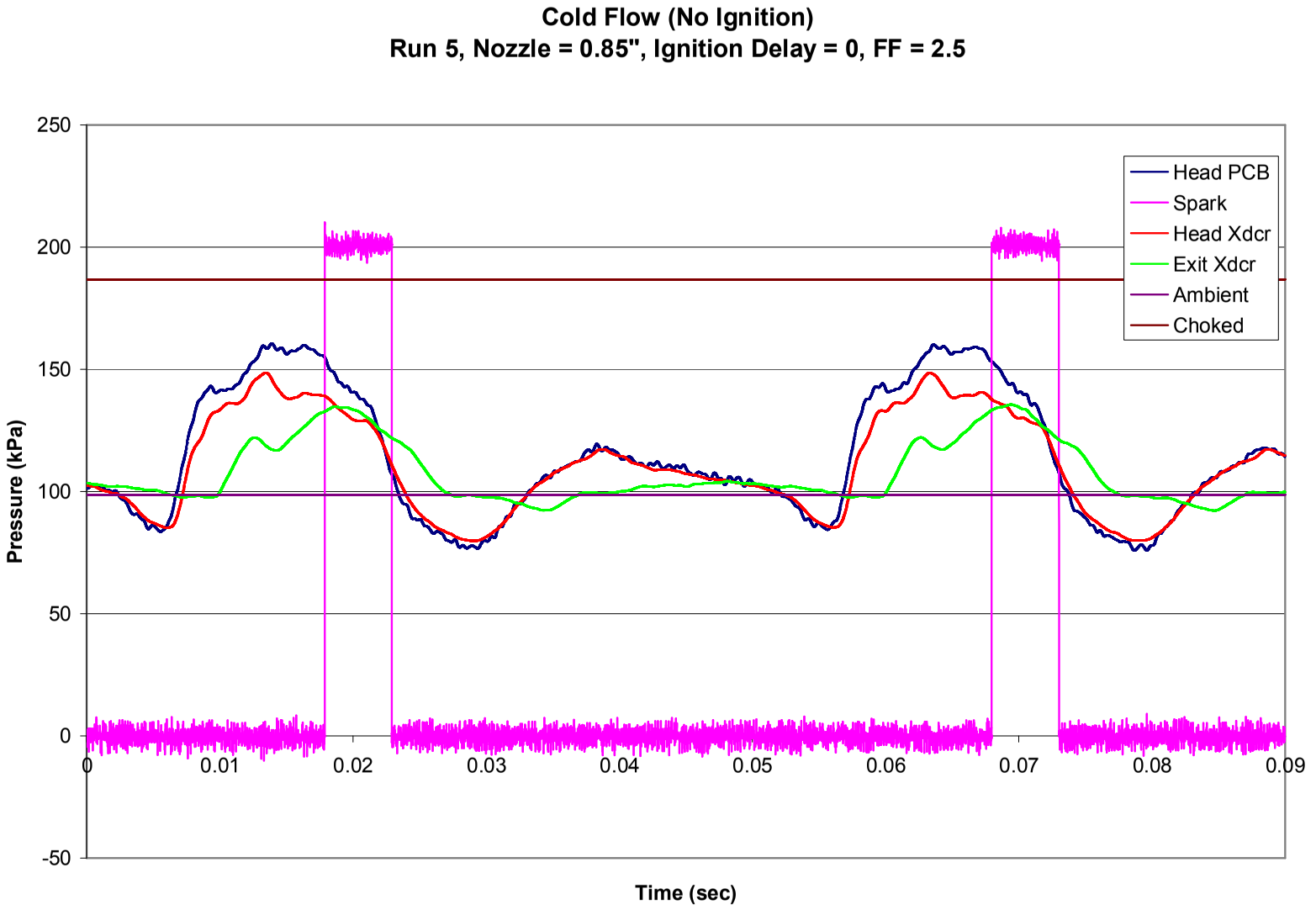
Cold Flow (No Ignition)
Run 5, Nozzle = 0.85", Ignition Delay = 0, FF = 2.5
Pressure (kPa)
250
200
150
100
50
0
-50
0
0.01
0.02
0.03
0.04
0.05
0.06
0.07
0.08
0.09
Time (sec)
Head PCB
Spark
Head Xdcr
Exit Xdcr
Ambient
Choked

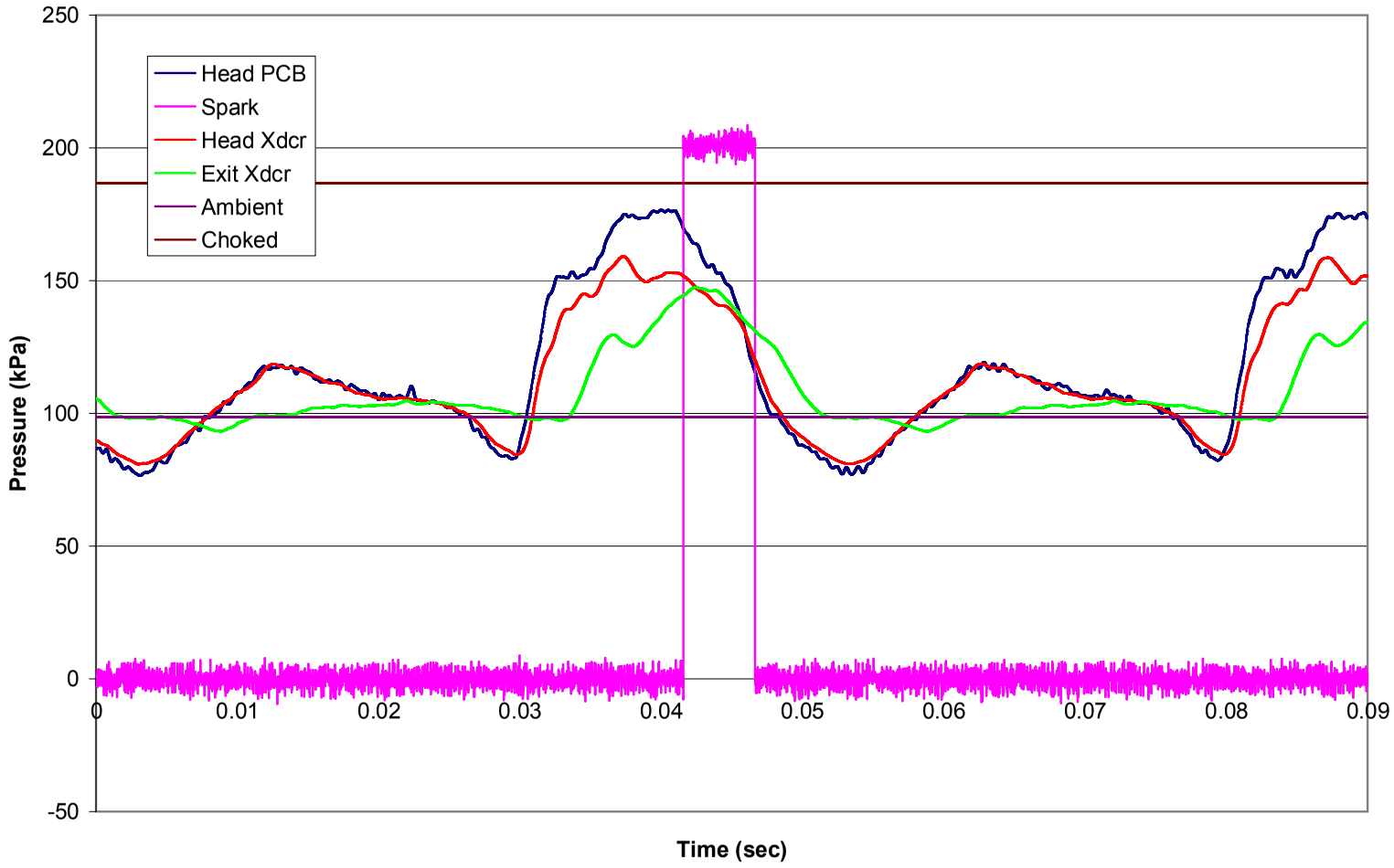
Cold Flow (No Ignition)
Run 6, Nozzle = 0.85", Ignition Delay = 0, FF = 3
Head PCB
Spark
Head Xdcr
Exit Xdcr
Ambient
Choked
Pressure (kPa)
250
200
150
100
50
0
-50
0
0.01
0.02
0.03
0.04
0.05
0.06
0.07
0.08
0.09
Time (sec)

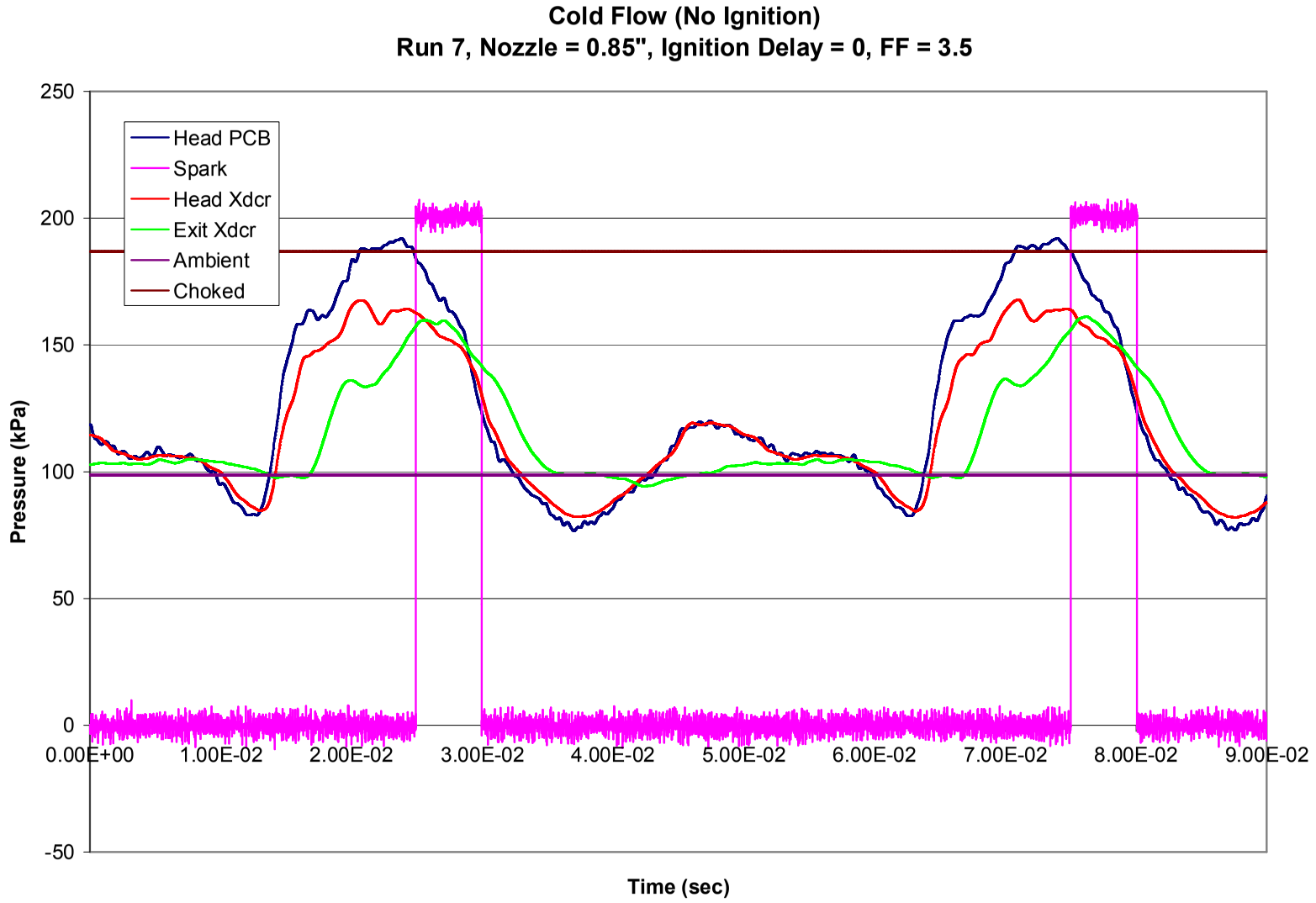
Cold Flow (No Ignition)
Run 7, Nozzle = 0.85", Ignition Delay = 0, FF = 3.5
Head PCB
Spark
Head Xdcr
Exit Xdcr
Ambient
Choked
Pressure (kPa)
250
200
150
100
50
0
-50
0.00E+00
1.00E-02
2.00E-02
3.00E-02
4.00E-02
5.00E-02
6.00E-02
7.00E-02
8.00E-02
9.00E-02
Time (sec)

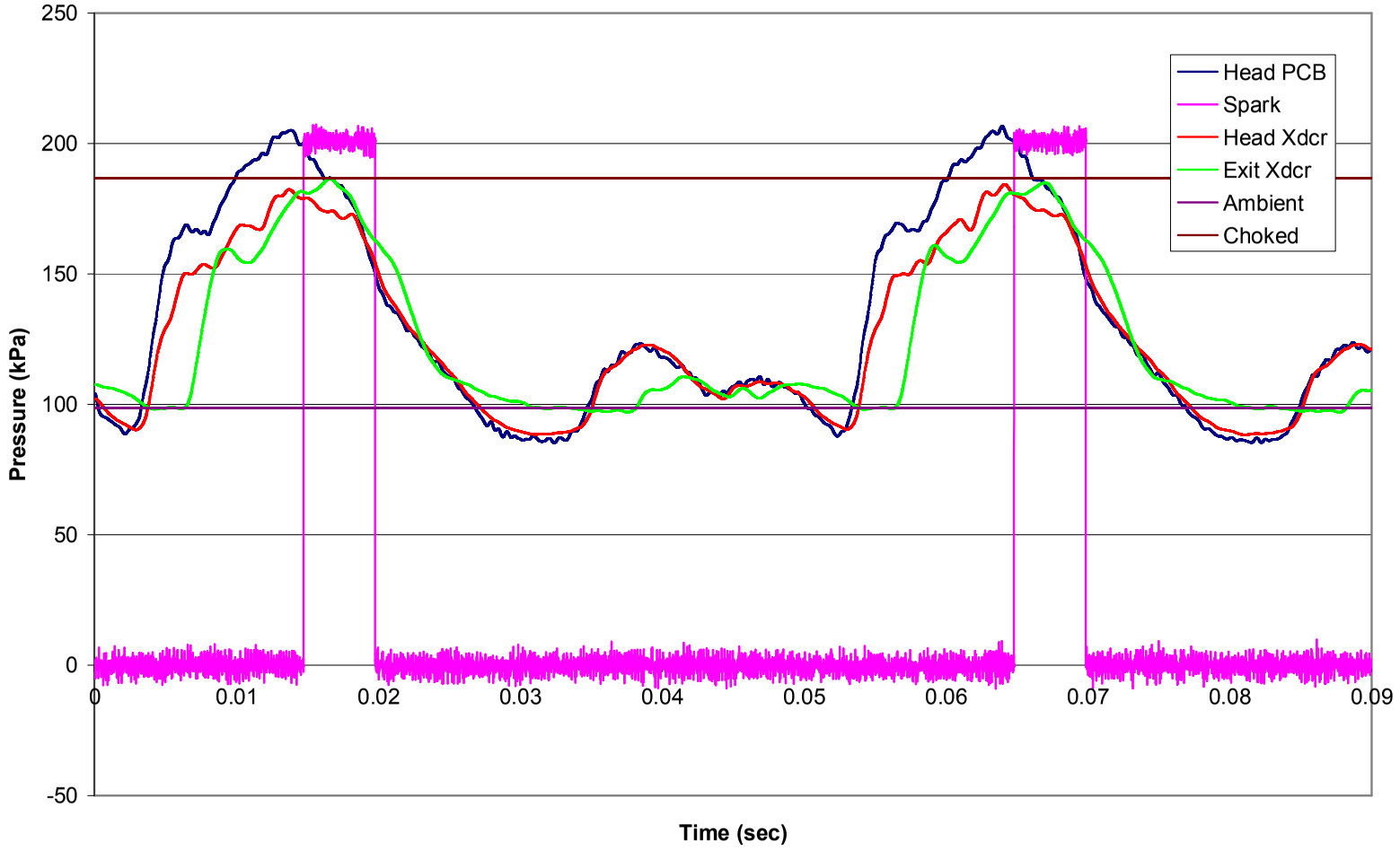
Cold Flow (No Ignition)
Run 8, Nozzle = 0.75", Ignition Delay = 0, FF = 3.5
Pressure (kPa)
250
200
150
100
50
0
-50
0
0.01
0.02
0.03
0.04
0.05
0.06
0.07
0.08
0.09
Time (sec)
Head PCB
Spark
Head Xdcr
Exit Xdcr
Ambient
Choked

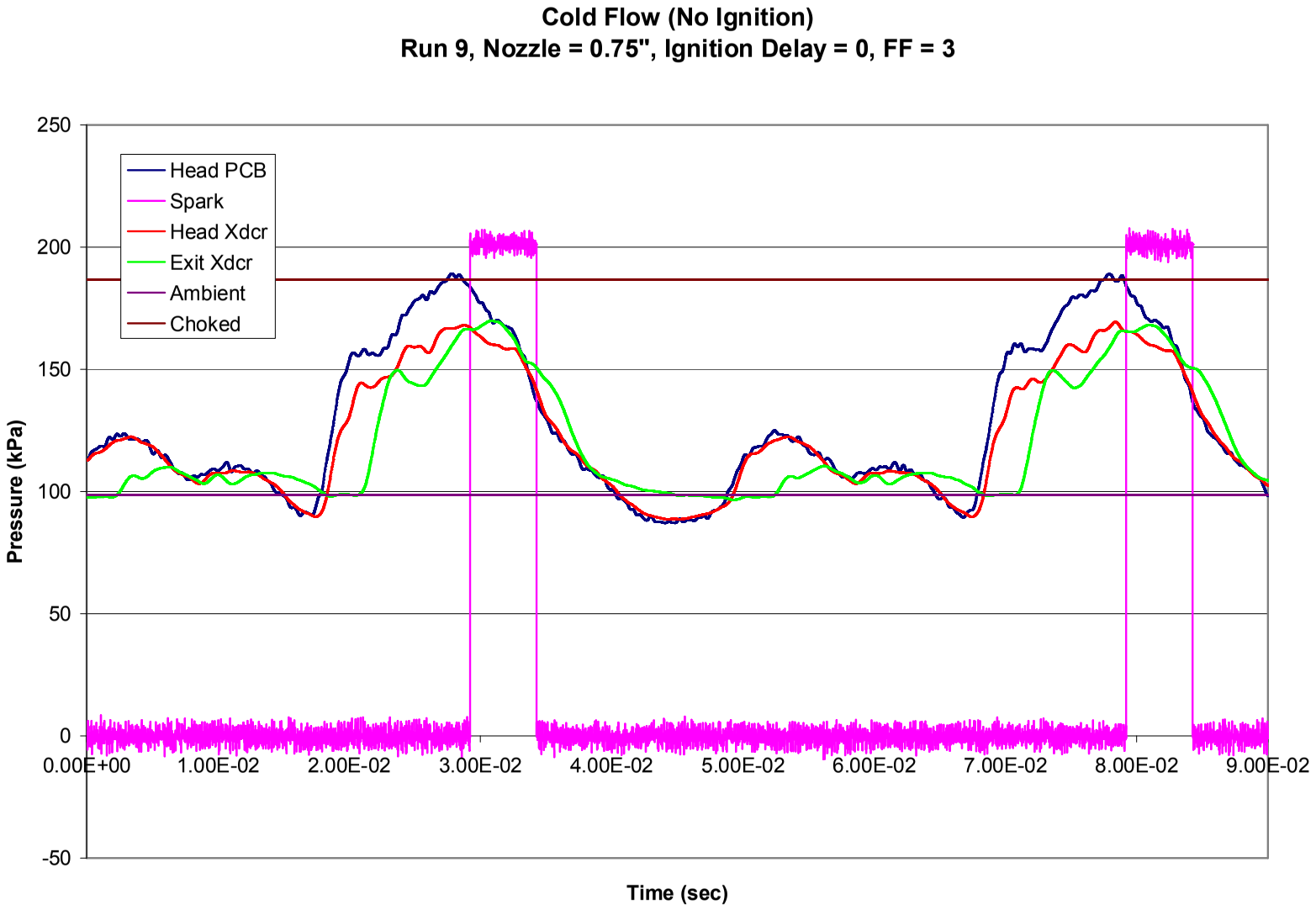
Cold Flow (No Ignition)
Run 9, Nozzle = 0.75", Ignition Delay = 0, FF = 3
Head PCB
Spark
Head Xdcr
Exit Xdcr
Ambient
Choked
Pressure (kPa)
250
200
150
100
50
0
-50
0.00E+00
1.00E-02
2.00E-02
3.00E-02
4.00E-02
5.00E-02
6.00E-02
7.00E-02
8.00E-02
9.00E-02
Time (sec)

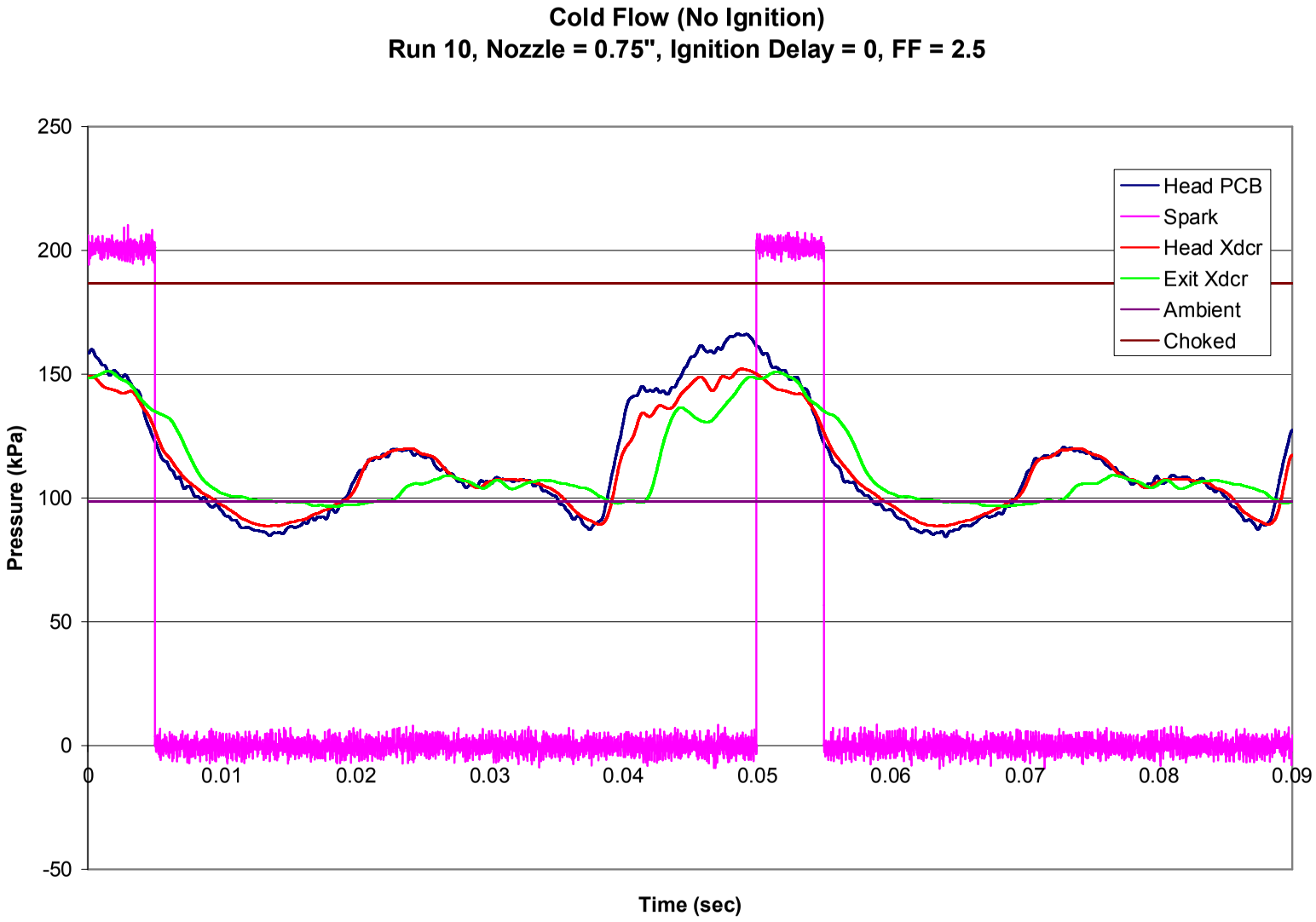
Cold Flow (No Ignition)
Run 10, Nozzle = 0.75", Ignition Delay = 0, FF = 2.5
Pressure (kPa)
250
200
150
100
50
0
-50
0
0.01
0.02
0.03
0.04
0.05
0.06
0.07
0.08
0.09
Time (sec)
Head PCB
Spark
Head Xdcr
Exit Xdcr
Ambient
Choked

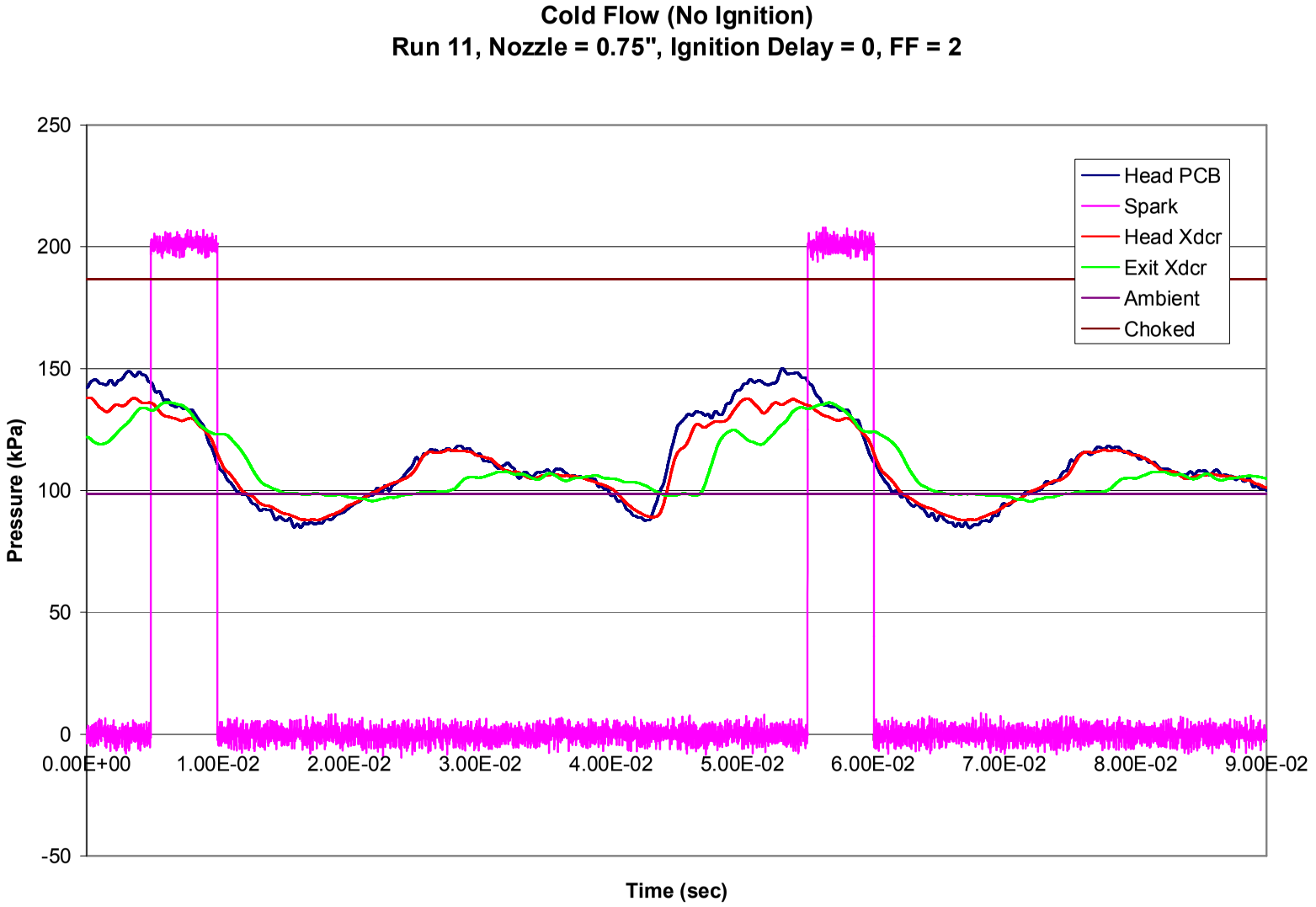
Cold Flow (No Ignition)
Run 11, Nozzle = 0.75", Ignition Delay = 0, FF = 2
Pressure (kPa)
250
200
150
100
50
0
-50
0.00E+00
1.00E-02
2.00E-02
3.00E-02
4.00E-02
5.00E-02
6.00E-02
7.00E-02
8.00E-02
9.00E-02
Time (sec)
Head PCB
Spark
Head Xdcr
Exit Xdcr
Ambient
Choked

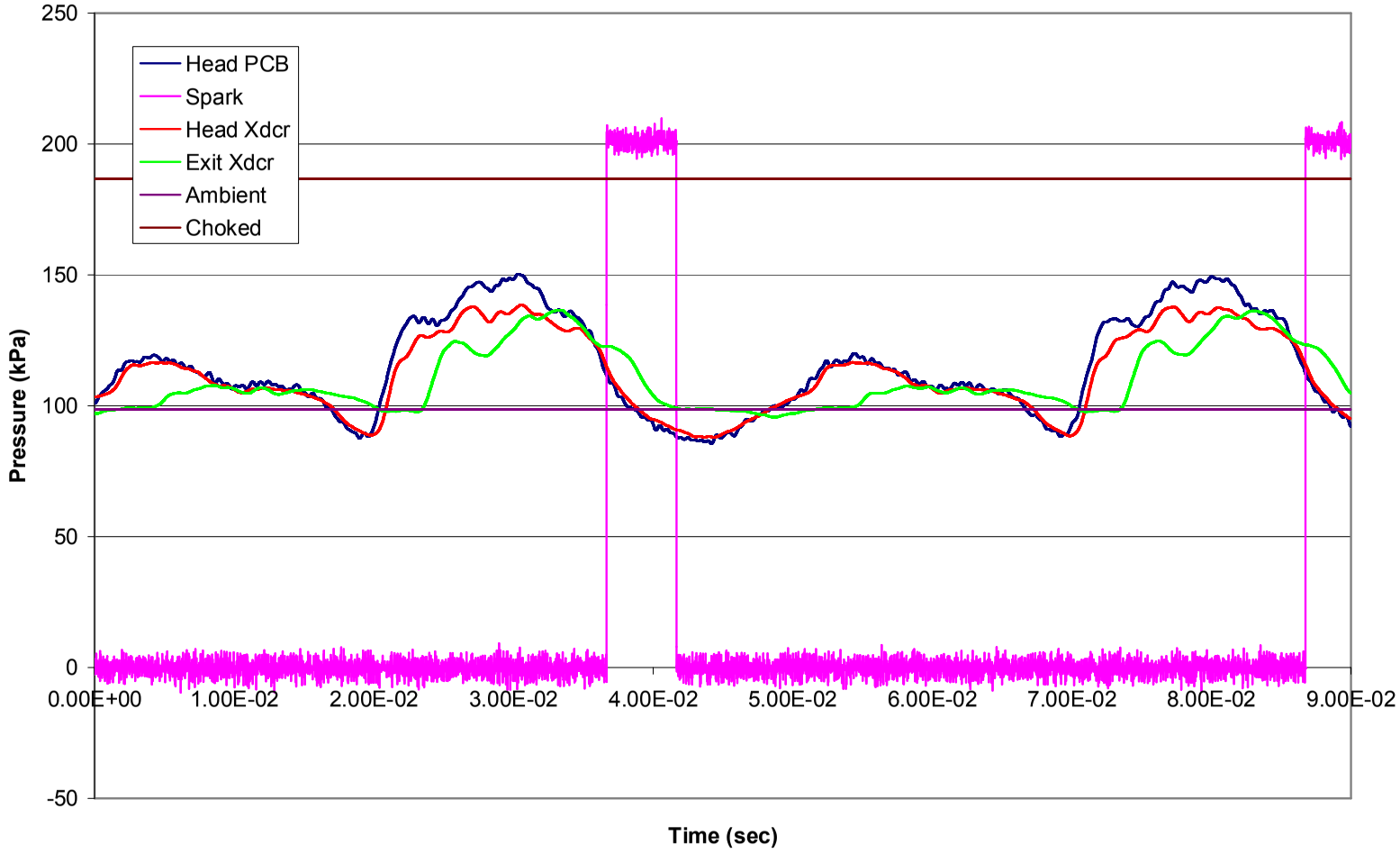
Cold Flow (No Ignition)
Run 12, Nozzle = 0.75", Ignition Delay = 5, FF = 2
Head PCB
Spark
Head Xdcr
Exit Xdcr
Ambient
Choked
Pressure (kPa)
250
200
150
100
50
0
-50
0.00E+00
1.00E-02
2.00E-02
3.00E-02
4.00E-02
5.00E-02
6.00E-02
7.00E-02
8.00E-02
9.00E-02
Time (sec)

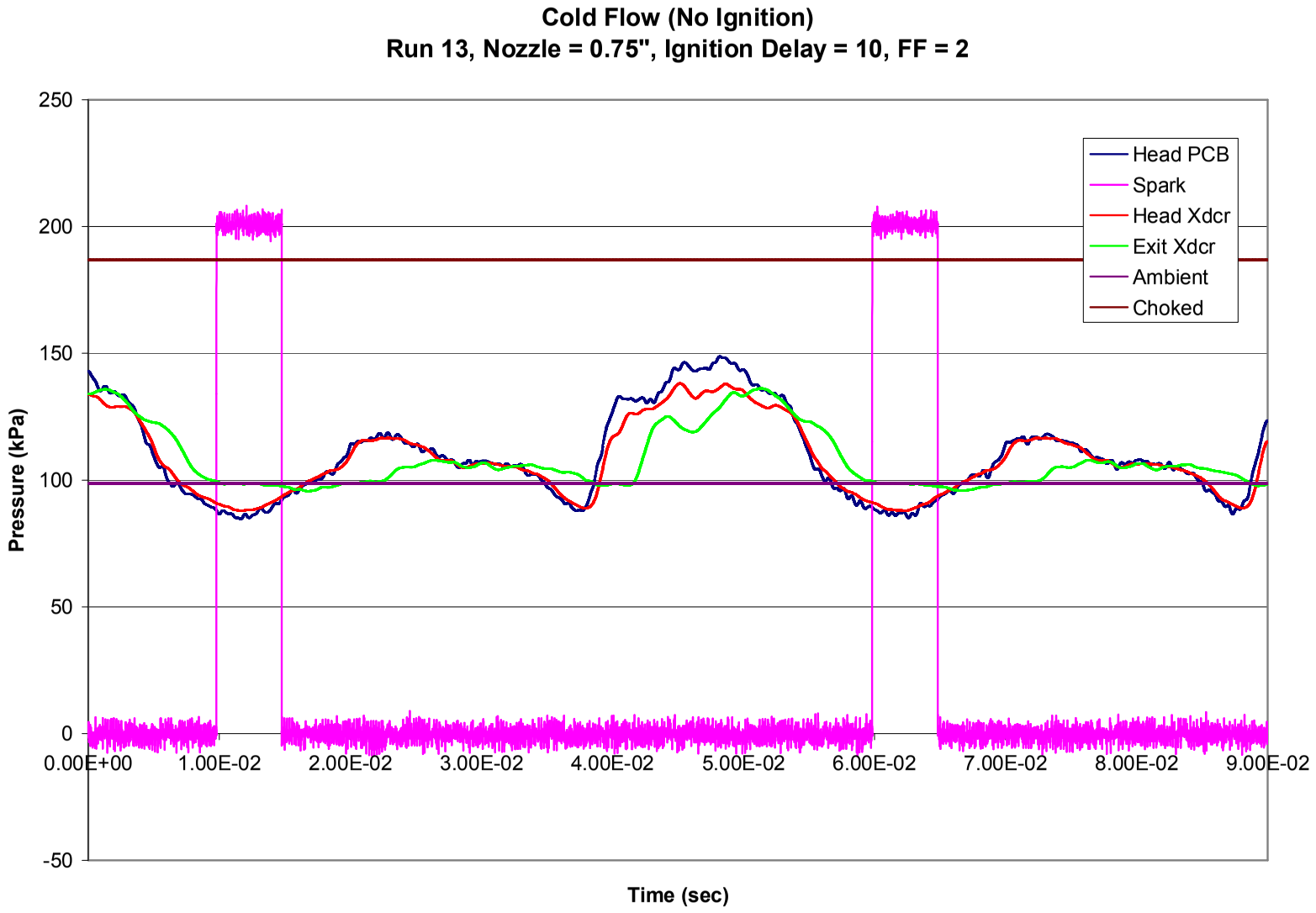
Cold Flow (No Ignition)
Run 13, Nozzle = 0.75", Ignition Delay = 10, FF = 2
Pressure (kPa)
250
200
150
100
50
0
-50
0.00E+00
1.00E-02
2.00E-02
3.00E-02
4.00E-02
5.00E-02
6.00E-02
7.00E-02
8.00E-02
9.00E-02
Time (sec)
Head PCB
Spark
Head Xdcr
Exit Xdcr
Ambient
Choked

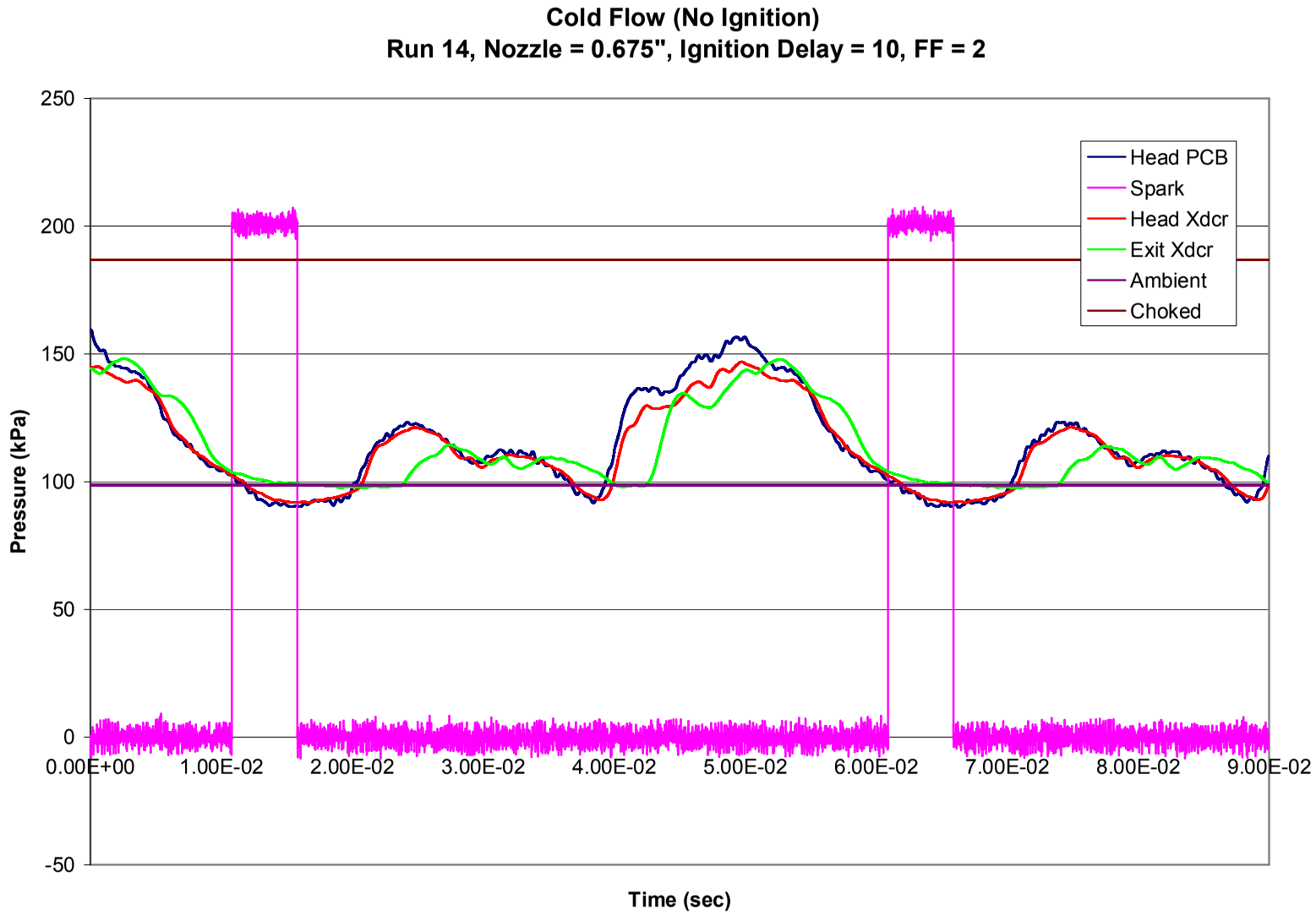
Cold Flow (No Ignition)
Run 14, Nozzle = 0.675", Ignition Delay = 10, FF = 2
Pressure (kPa)
250
200
150
100
50
0
-50
0.00E+00
1.00E-02
2.00E-02
3.00E-02
4.00E-02
5.00E-02
6.00E-02
7.00E-02
8.00E-02
9.00E-02
Time (sec)
Head PCB
Spark
Head Xdcr
Exit Xdcr
Ambient
Choked

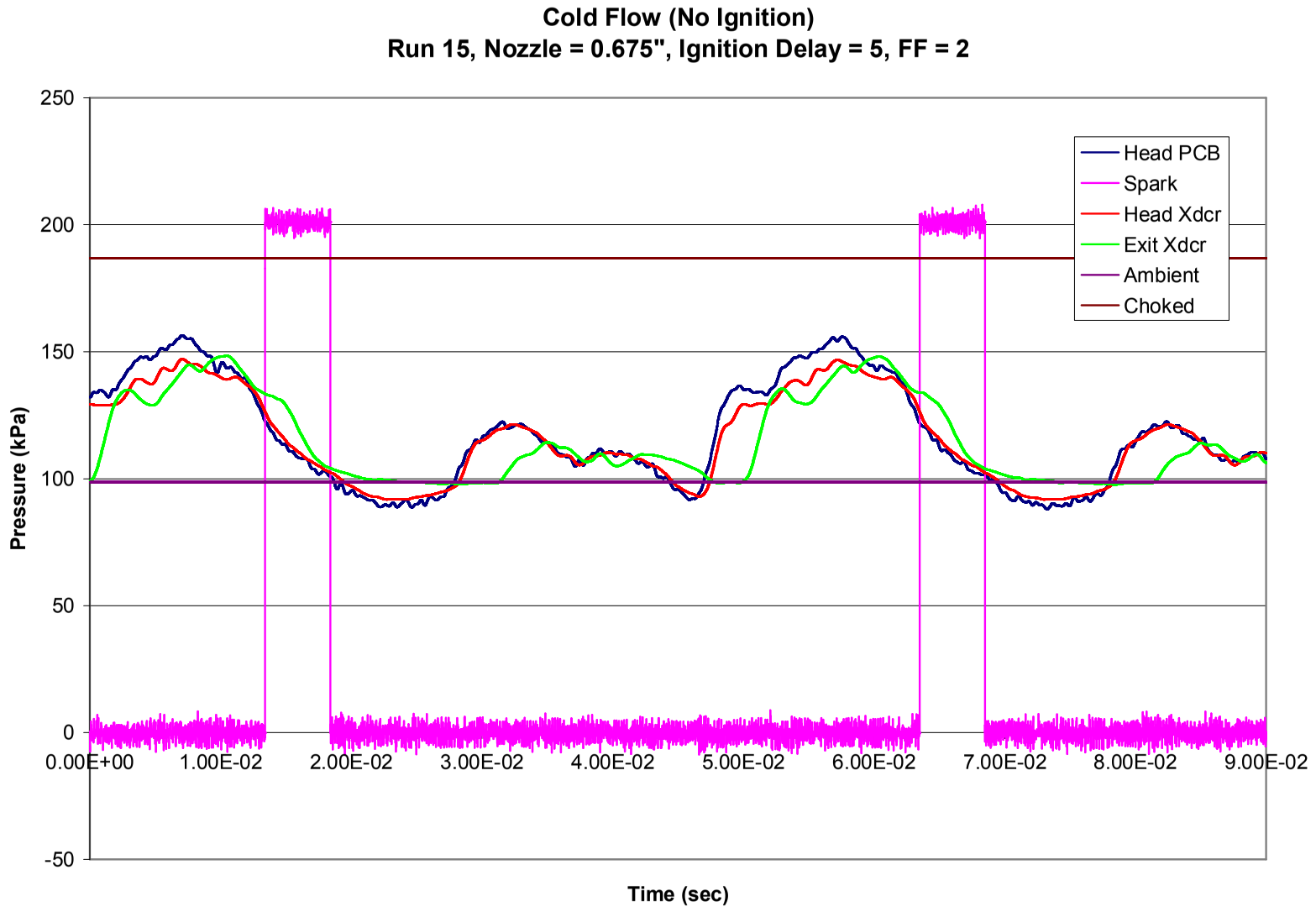
Cold Flow (No Ignition)
Run 15, Nozzle = 0.675", Ignition Delay = 5, FF = 2
Pressure (kPa)
250
200
150
100
50
0
-50
0.00E+00
1.00E-02
2.00E-02
3.00E-02
4.00E-02
5.00E-02
6.00E-02
7.00E-02
8.00E-02
9.00E-02
Time (sec)
Head PCB
Spark
Head Xdcr
Exit Xdcr
Ambient
Choked

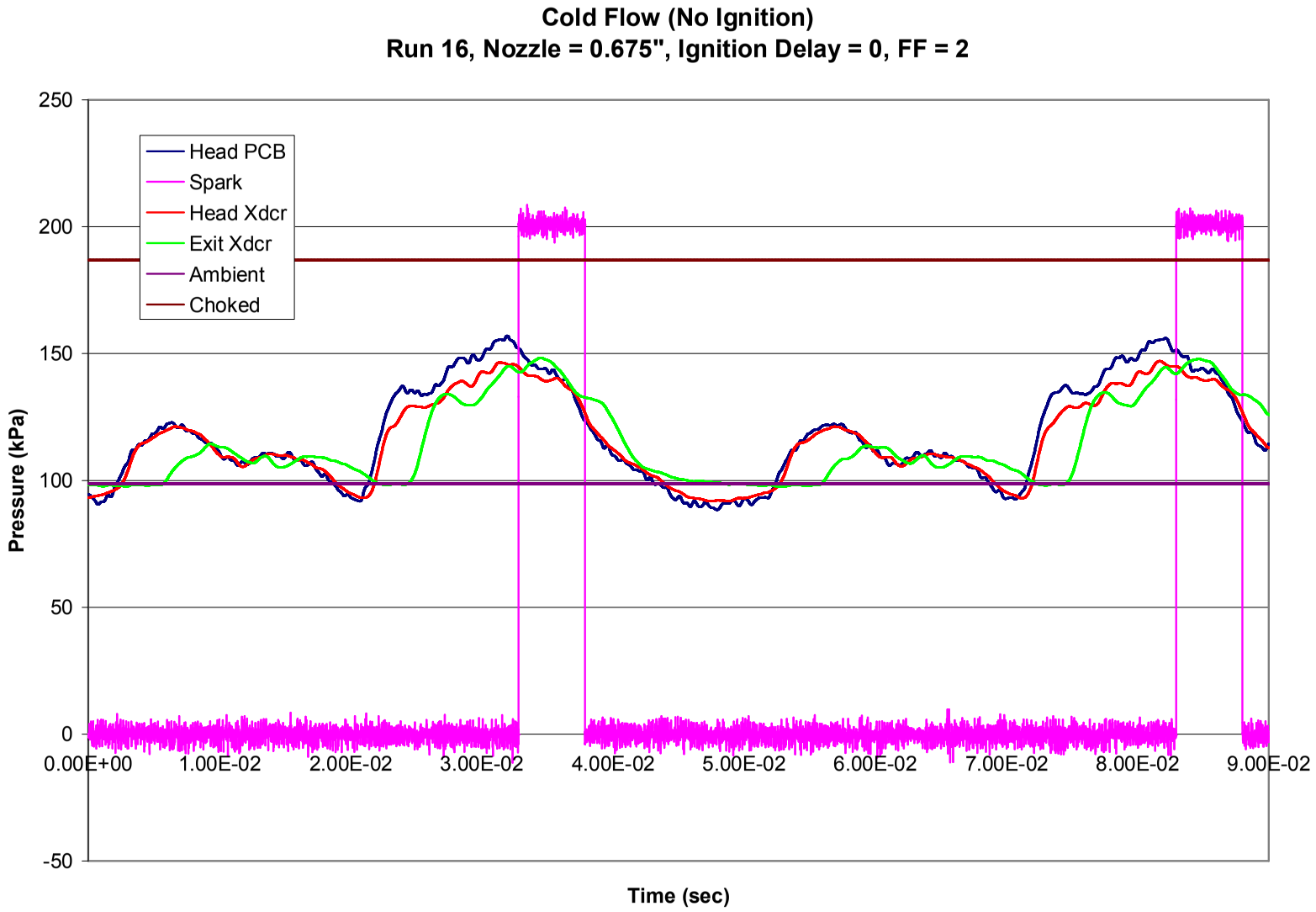
Cold Flow (No Ignition)
Run 16, Nozzle = 0.675", Ignition Delay = 0, FF = 2
Head PCB
Spark
Head Xdcr
Exit Xdcr
Ambient
Choked
Pressure (kPa)
250
200
150
100
50
0
-50
0.00E+00
1.00E-02
2.00E-02
3.00E-02
4.00E-02
5.00E-02
6.00E-02
7.00E-02
8.00E-02
9.00E-02
Time (sec)

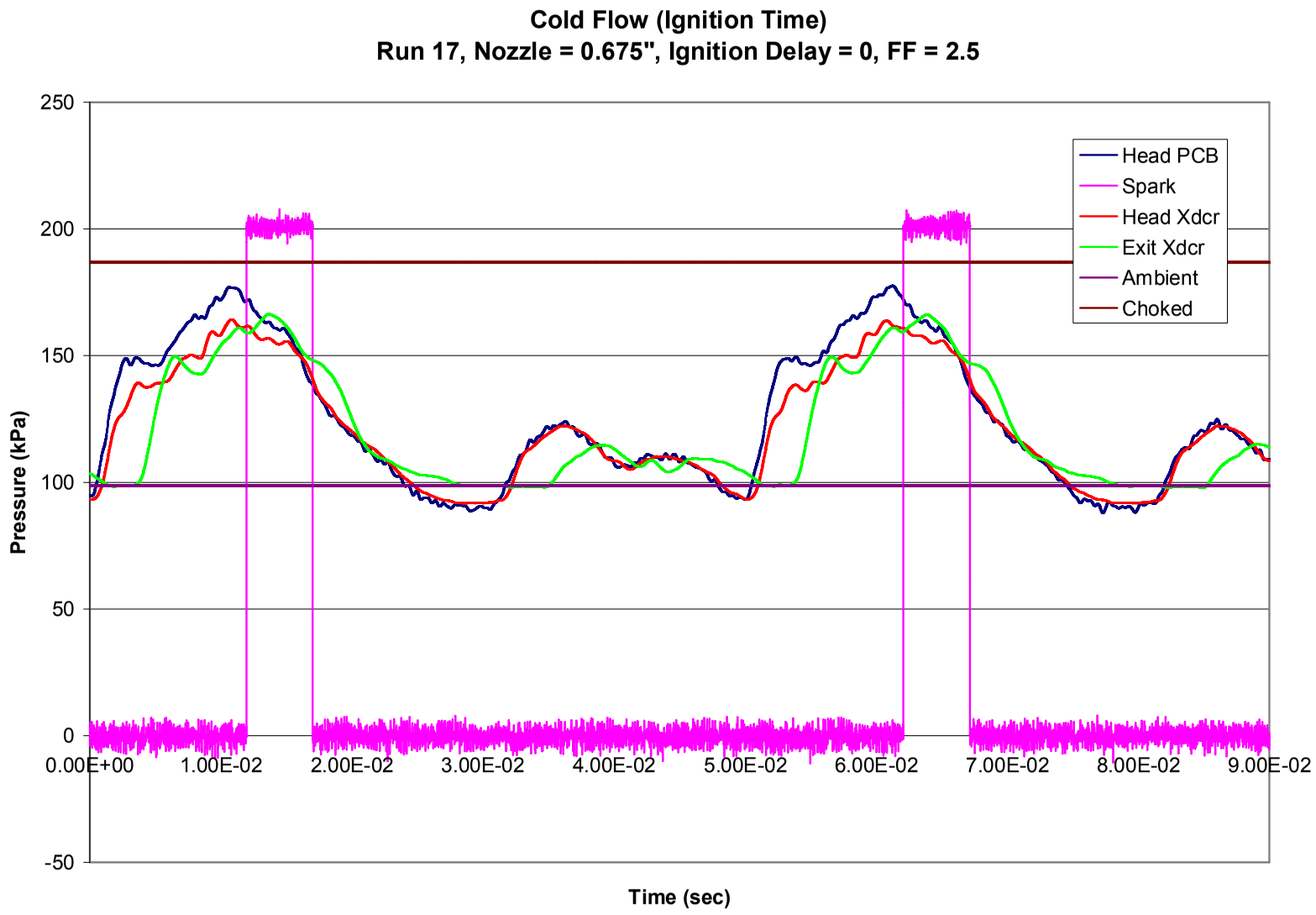
Cold Flow (Ignition Time)
Run 17, Nozzle = 0.675", Ignition Delay = 0, FF = 2.5
Pressure (kPa)
250
200
150
100
50
0
-50
0.00E+00
1.00E-02
2.00E-02
3.00E-02
4.00E-02
5.00E-02
6.00E-02
7.00E-02
8.00E-02
9.00E-02
Time (sec)
Head PCB
Spark
Head Xdcr
Exit Xdcr
Ambient
Choked

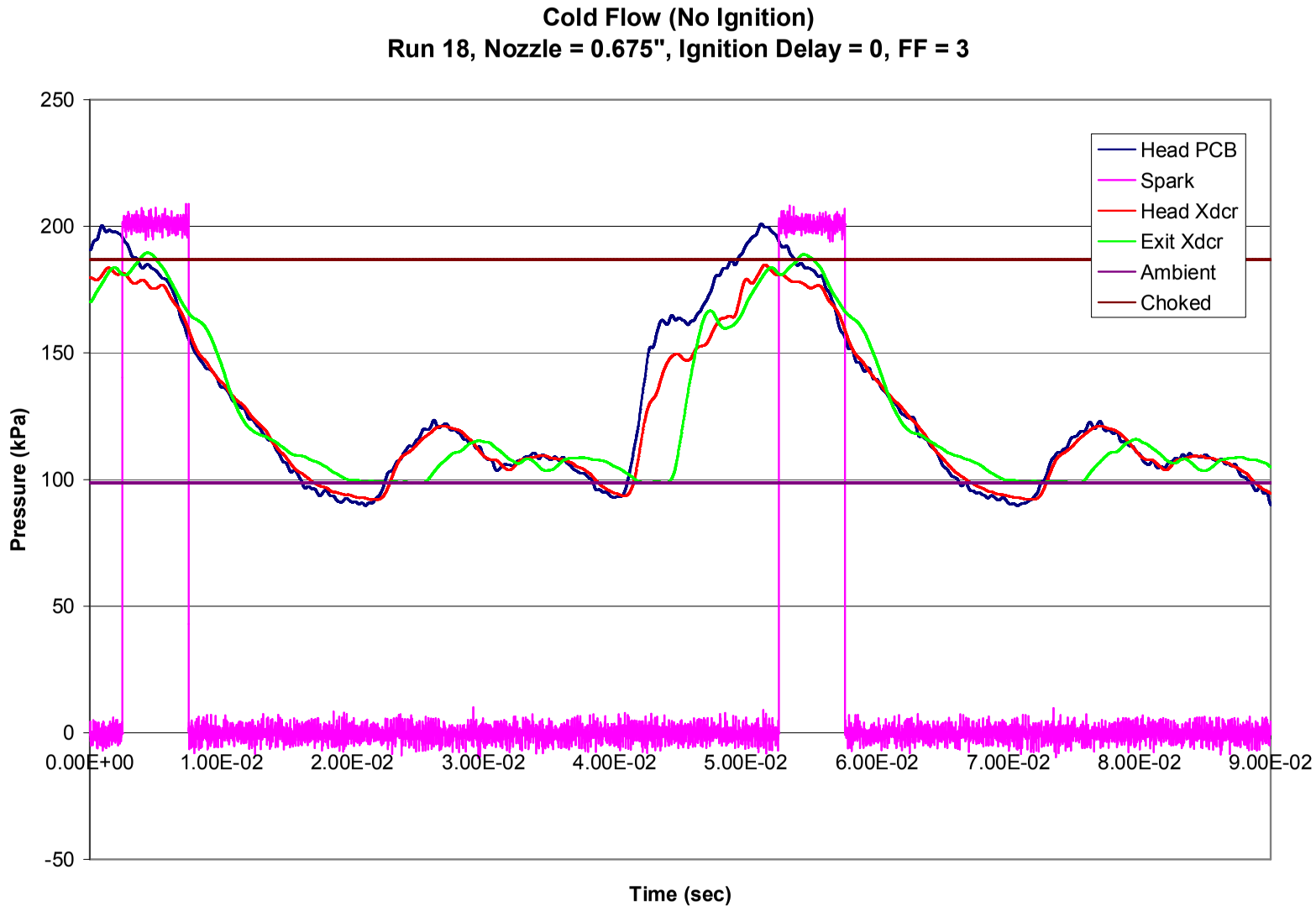
Cold Flow (No Ignition)
Run 18, Nozzle = 0.675", Ignition Delay = 0, FF = 3
Pressure (kPa)
250
200
150
100
50
0
-50
0.00E+00
1.00E-02
2.00E-02
3.00E-02
4.00E-02
5.00E-02
6.00E-02
7.00E-02
8.00E-02
9.00E-02
Time (sec)
Head PCB
Spark
Head Xdcr
Exit Xdcr
Ambient
Choked

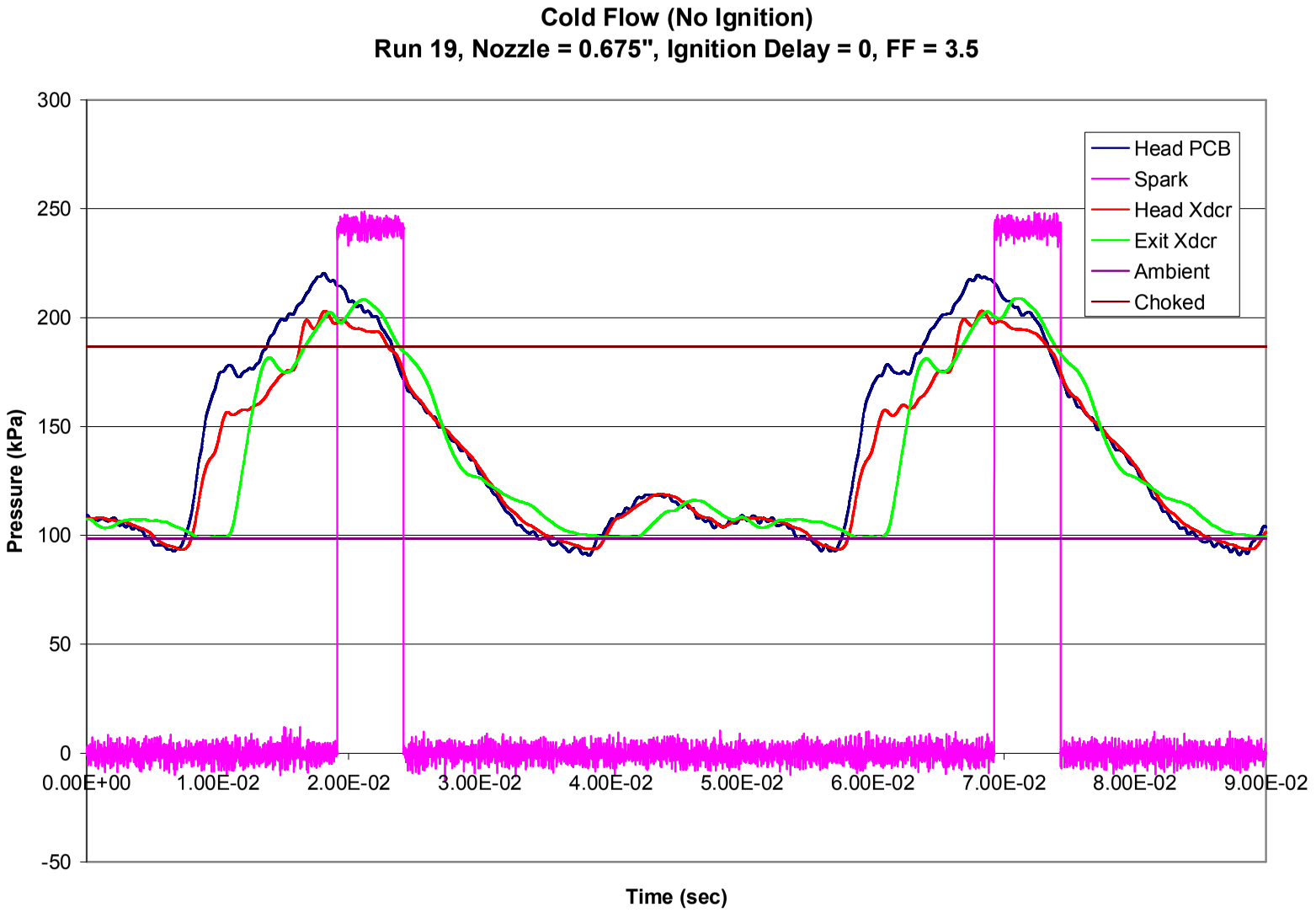
Cold Flow (No Ignition)
Run 19, Nozzle = 0.675", Ignition Delay = 0, FF = 3.5
Pressure (kPa)
300
250
200
150
100
50
0
-50
0.00E+00
1.00E-02
2.00E-02
3.00E-02
4.00E-02
5.00E-02
6.00E-02
7.00E-02
8.00E-02
9.00E-02
Time (sec)
Head PCB
Spark
Head Xdcr
Exit Xdcr
Ambient
Choked

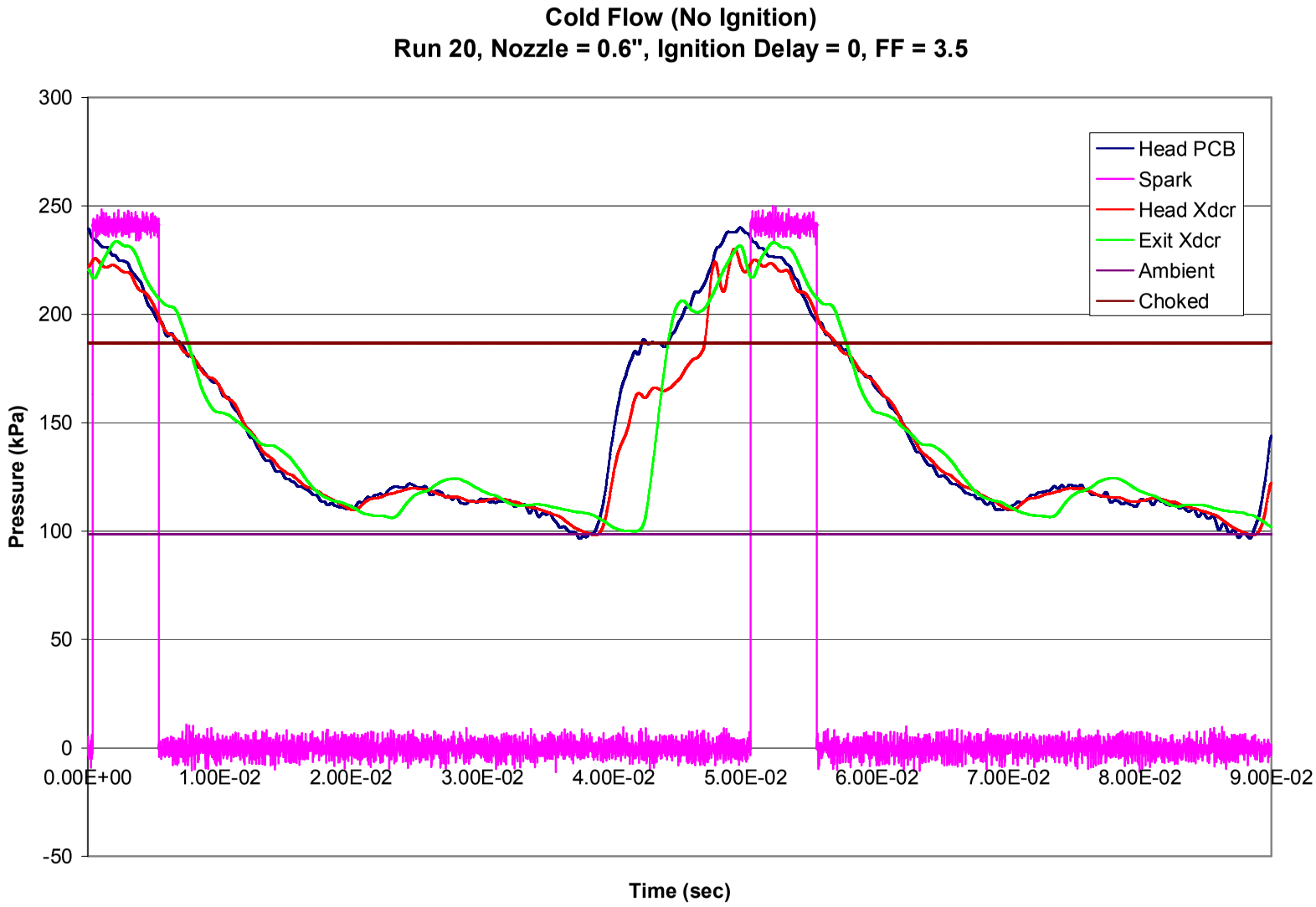
Cold Flow (No Ignition)
Run 20, Nozzle = 0.6", Ignition Delay = 0, FF = 3.5
Pressure (kPa)
300
250
200
150
100
50
0
-50
0.00E+00
1.00E-02
2.00E-02
3.00E-02
4.00E-02
5.00E-02
6.00E-02
7.00E-02
8.00E-02
9.00E-02
Time (sec)
Head PCB
Spark
Head Xdcr
Exit Xdcr
Ambient
Choked

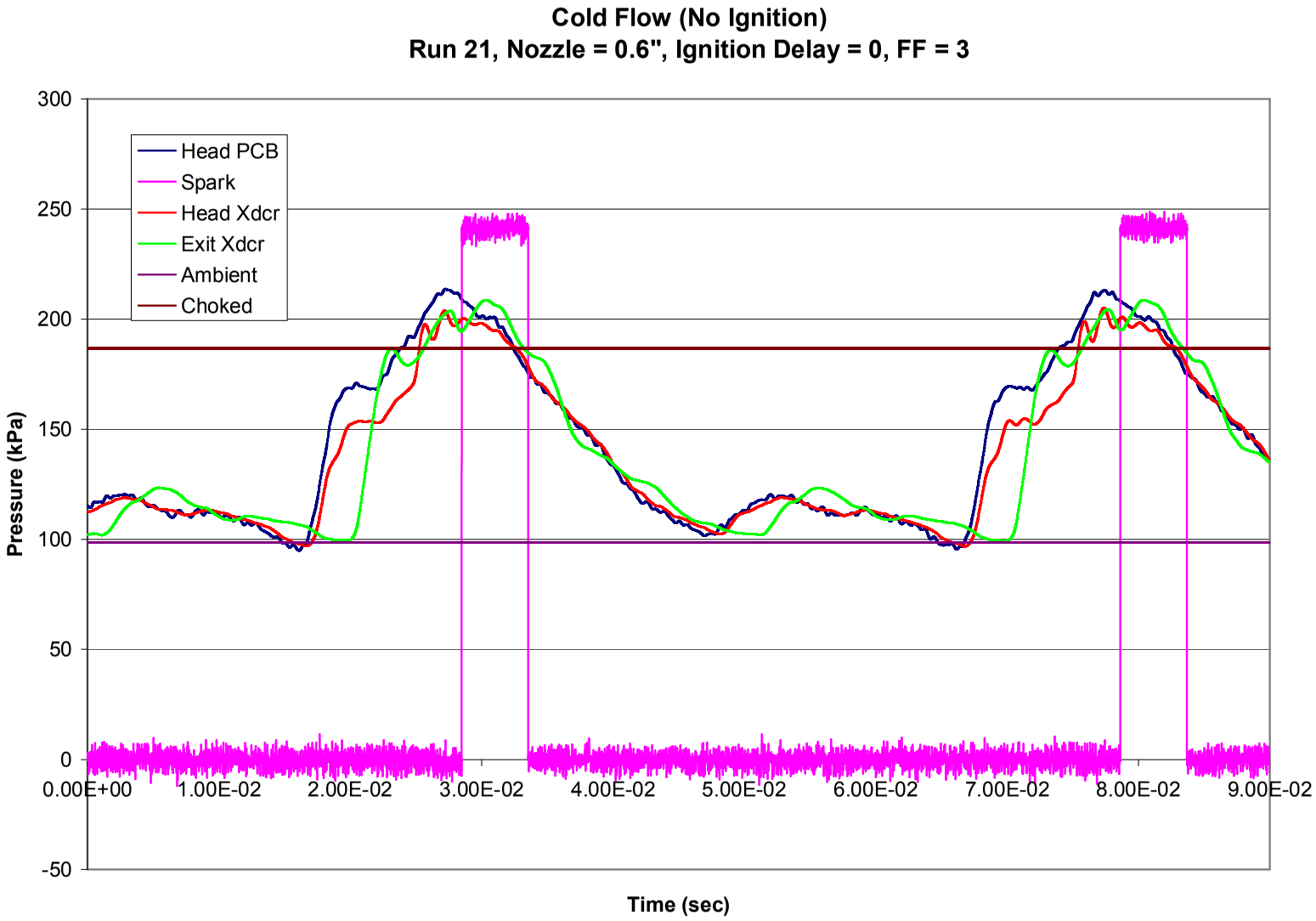
Cold Flow (No Ignition)
Run 21, Nozzle = 0.6", Ignition Delay = 0, FF = 3
Head PCB
Spark
Head Xdcr
Exit Xdcr
Ambient
Choked
Pressure (kPa)
300
250
200
150
100
50
0
-50
0.00E+00
1.00E-02
2.00E-02
3.00E-02
4.00E-02
5.00E-02
6.00E-02
7.00E-02
8.00E-02
9.00E-02
Time (sec)

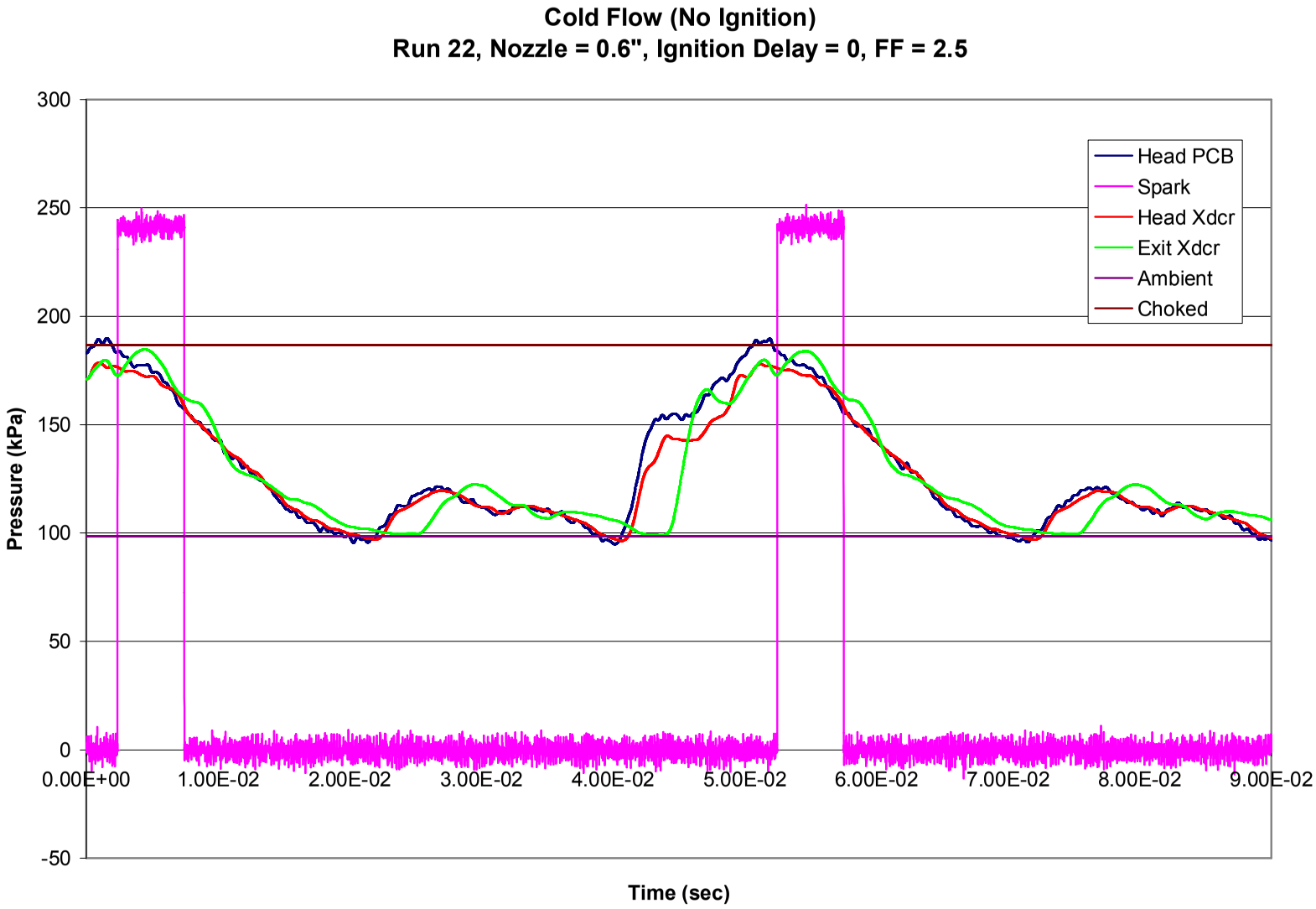
Cold Flow (No Ignition)
Run 22, Nozzle = 0.6", Ignition Delay = 0, FF = 2.5
Pressure (kPa)
300
250
200
150
100
50
0
-50
0.00E+00
1.00E-02
2.00E-02
3.00E-02
4.00E-02
5.00E-02
6.00E-02
7.00E-02
8.00E-02
9.00E-02
Time (sec)
Head PCB
Spark
Head Xdcr
Exit Xdcr
Ambient
Choked

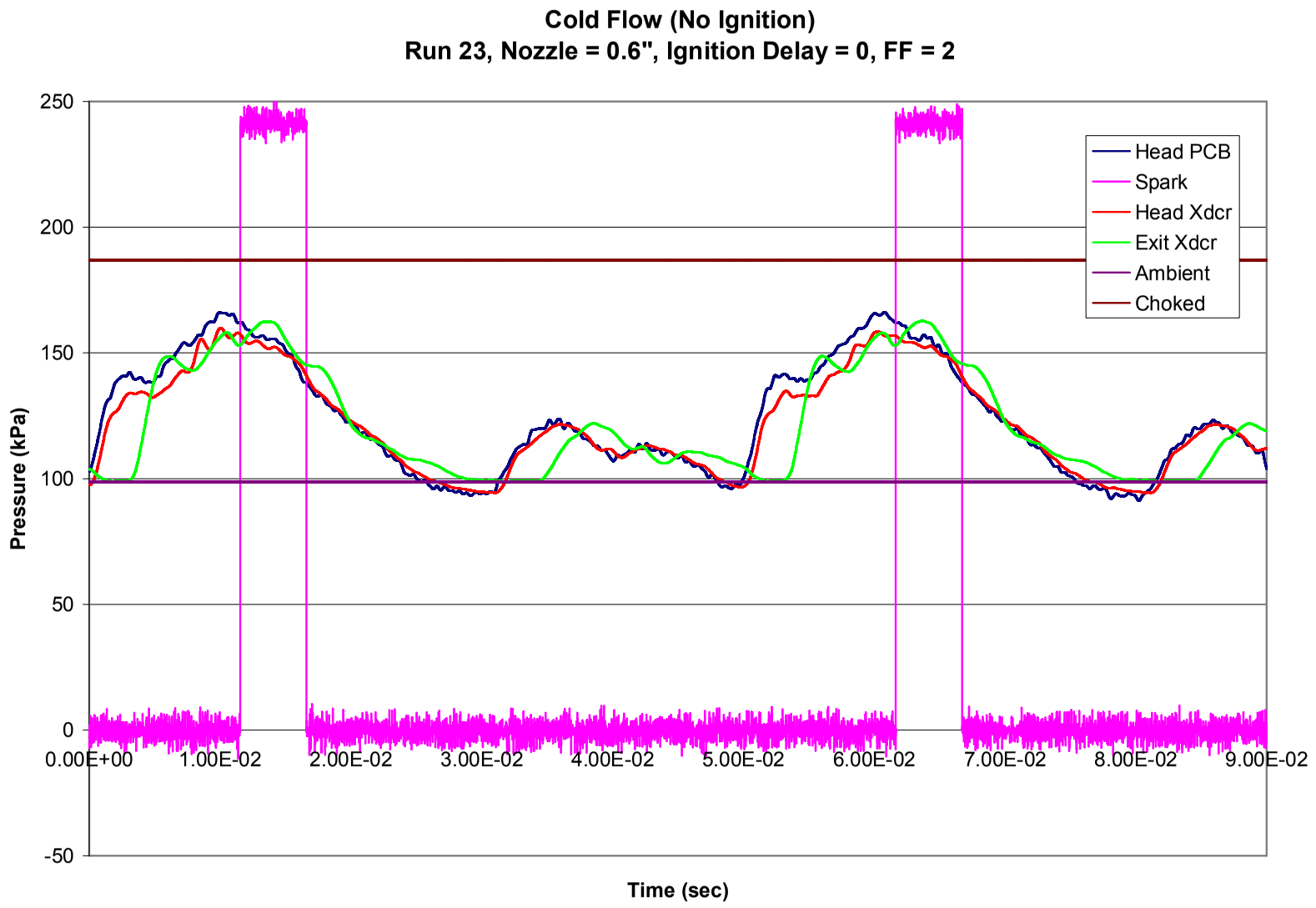
Cold Flow (No Ignition)
Run 23, Nozzle = 0.6", Ignition Delay = 0, FF = 2
Pressure (kPa)
250
200
150
100
50
0
-50
0.00E+00
1.00E-02
2.00E-02
3.00E-02
4.00E-02
5.00E-02
6.00E-02
7.00E-02
8.00E-02
9.00E-02
Time (sec)
Head PCB
Spark
Head Xdcr
Exit Xdcr
Ambient
Choked

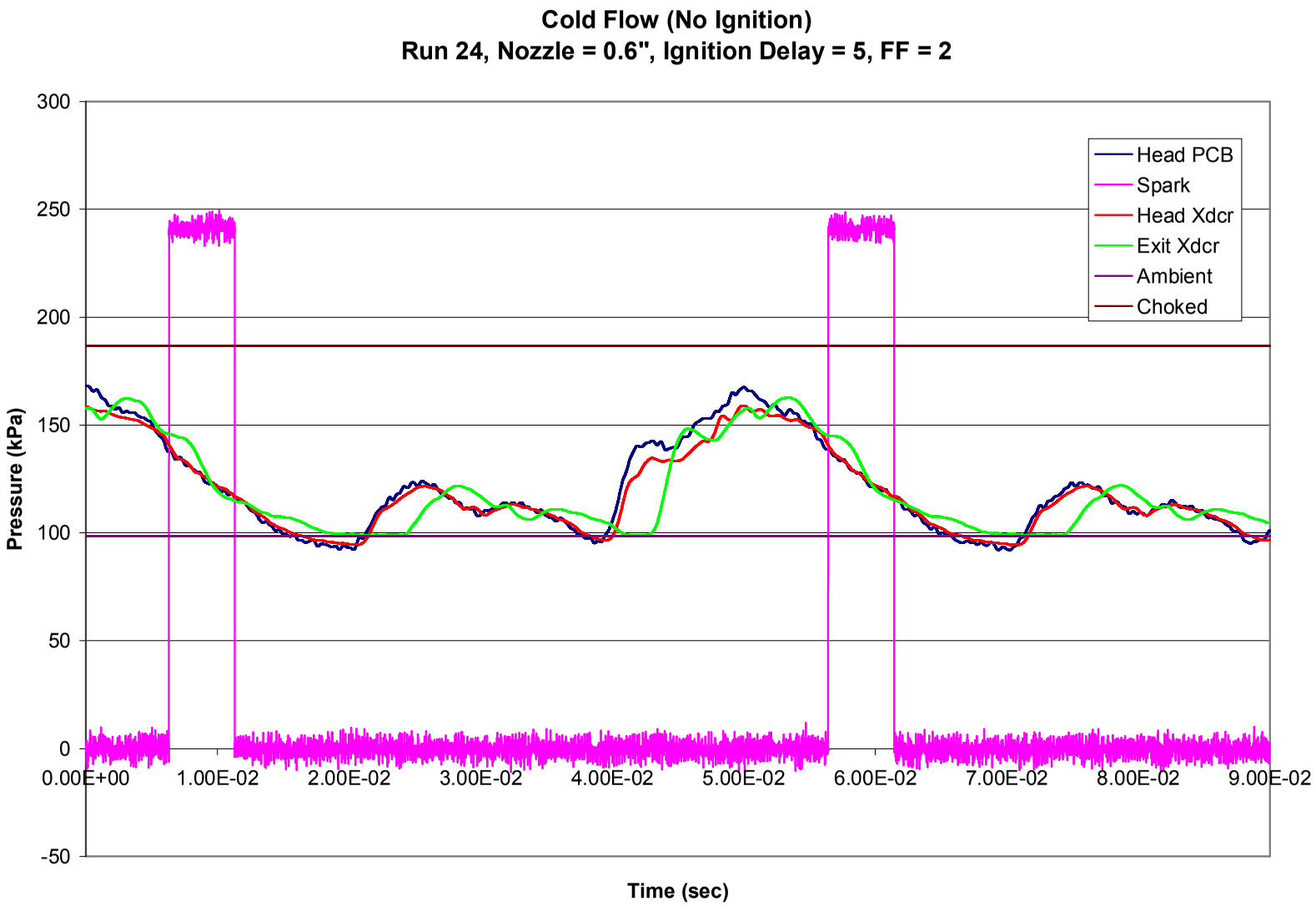
Cold Flow (No Ignition)
Run 24, Nozzle = 0.6", Ignition Delay = 5, FF = 2
Pressure (kPa)
300
250
200
150
100
50
0
-50
0.00E+00
1.00E-02
2.00E-02
3.00E-02
4.00E-02
5.00E-02
6.00E-02
7.00E-02
8.00E-02
9.00E-02
Time (sec)
Head PCB
Spark
Head Xdcr
Exit Xdcr
Ambient
Choked

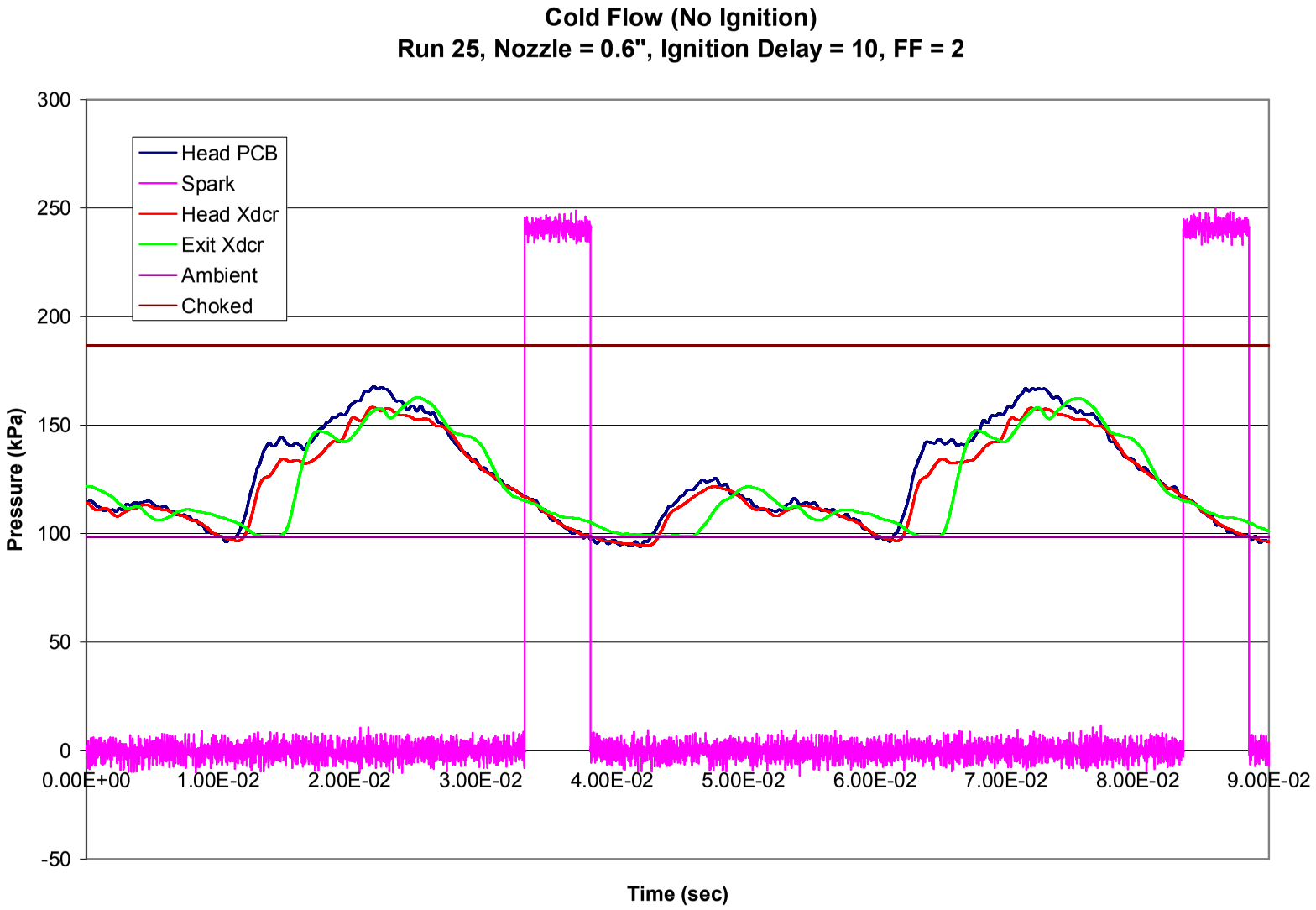
Cold Flow (No Ignition)
Run 25, Nozzle = 0.6", Ignition Delay = 10, FF = 2
Head PCB
Spark
Head Xdcr
Exit Xdcr
Ambient
Choked
Pressure (kPa)
300
250
200
150
100
50
0
-50
0.00E+00
1.00E-02
2.00E-02
3.00E-02
4.00E-02
5.00E-02
6.00E-02
7.00E-02
8.00E-02
9.00E-02
Time (sec)

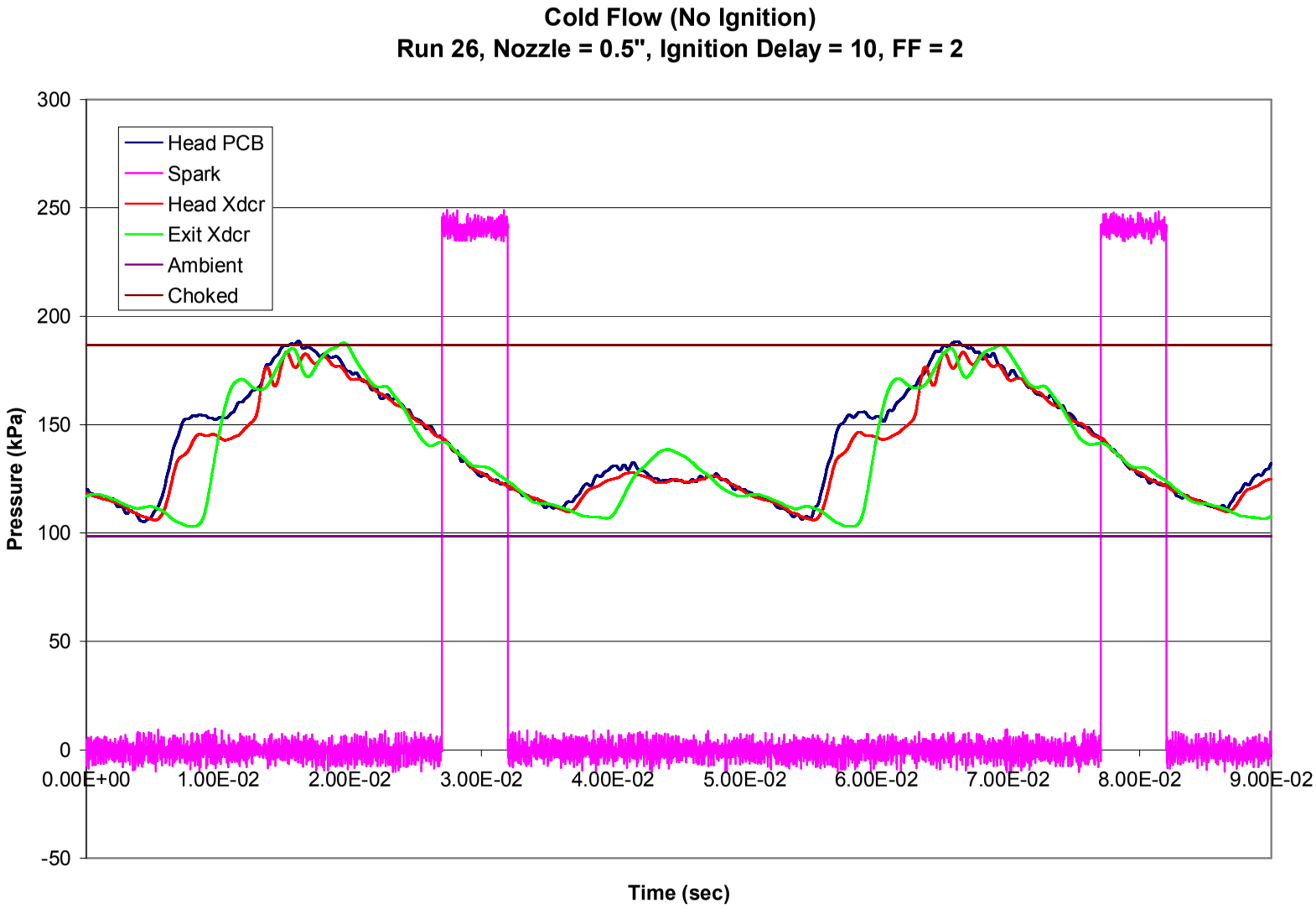
Cold Flow (No Ignition)
Run 26, Nozzle = 0.5", Ignition Delay = 10, FF = 2
Head PCB
Spark
Head Xdcr
Exit Xdcr
Ambient
Choked
Pressure (kPa)
300
250
200
150
100
50
0
-50
0.00E+00
1.00E-02
2.00E-02
3.00E-02
4.00E-02
5.00E-02
6.00E-02
7.00E-02
8.00E-02
9.00E-02
Time (sec)

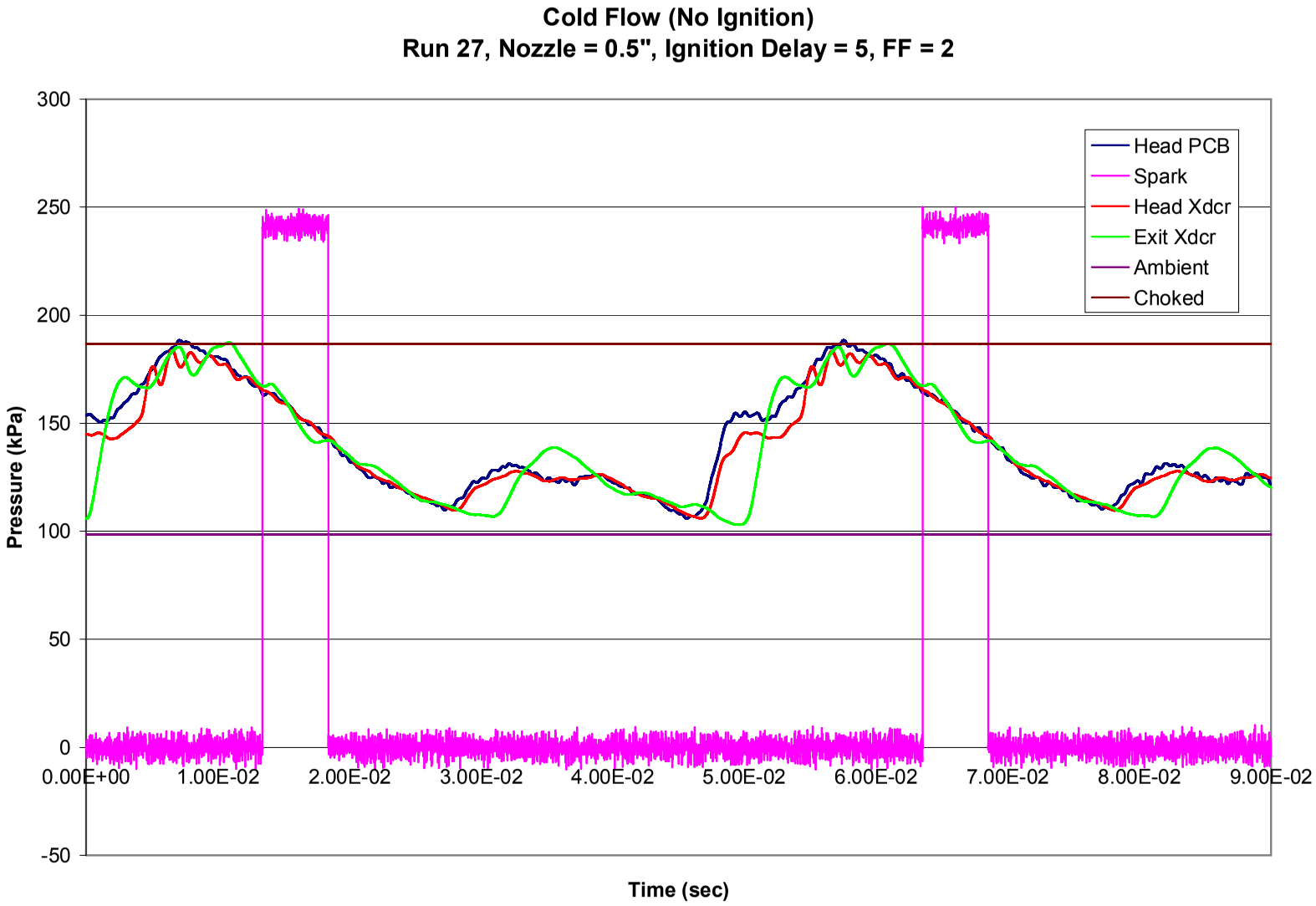
Cold Flow (No Ignition)
Run 27, Nozzle = 0.5", Ignition Delay = 5, FF = 2
Pressure (kPa)
300
250
200
150
100
50
0
-50
0.00E+00
1.00E-02
2.00E-02
3.00E-02
4.00E-02
5.00E-02
6.00E-02
7.00E-02
8.00E-02
9.00E-02
Time (sec)
Head PCB
Spark
Head Xdcr
Exit Xdcr
Ambient
Choked

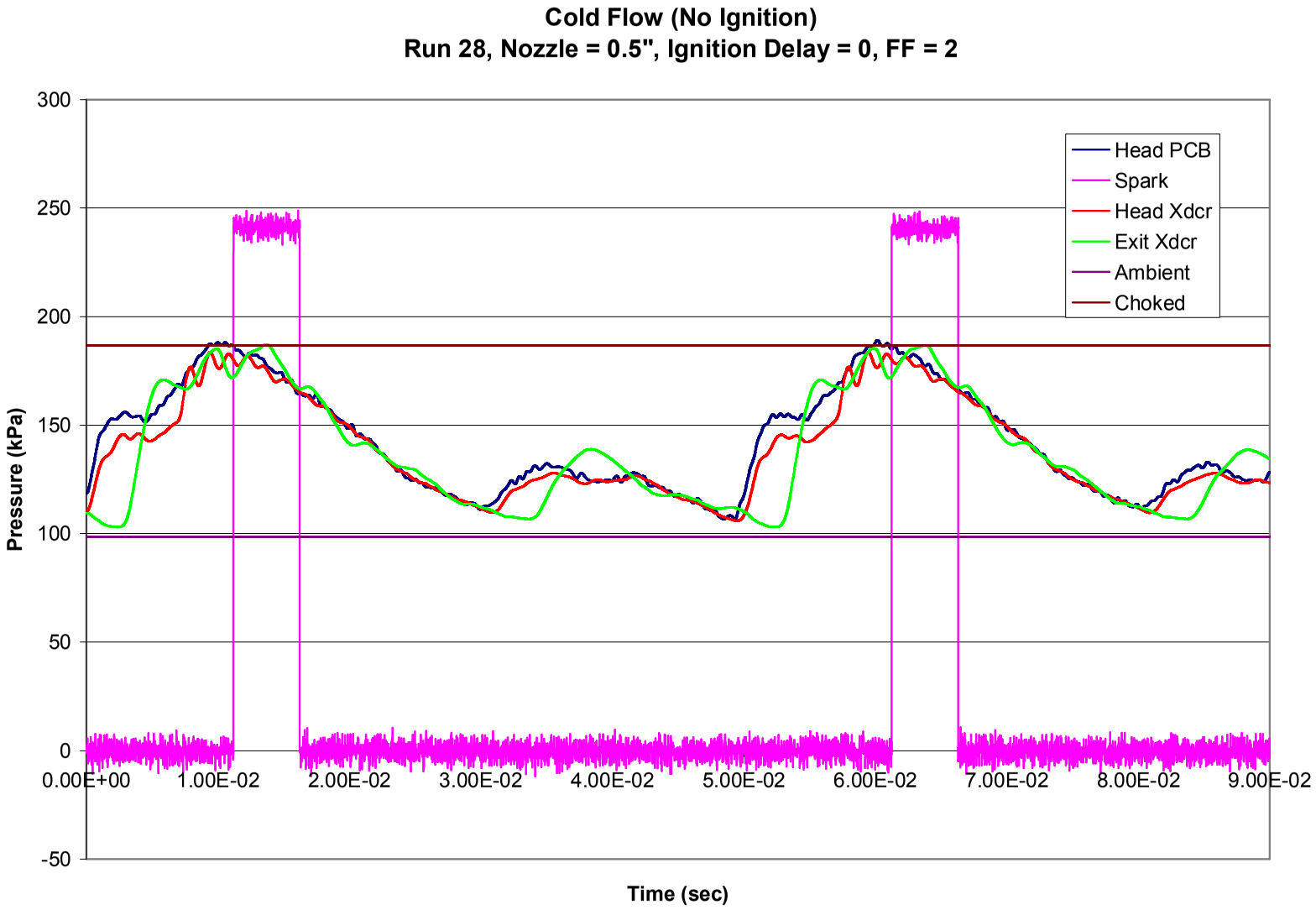
Cold Flow (No Ignition)
Run 28, Nozzle = 0.5", Ignition Delay = 0, FF = 2
Pressure (kPa)
300
250
200
150
100
50
0
-50
0.00E+00
1.00E-02
2.00E-02
3.00E-02
4.00E-02
5.00E-02
6.00E-02
7.00E-02
8.00E-02
9.00E-02
Time (sec)
Head PCB
Spark
Head Xdcr
Exit Xdcr
Ambient
Choked

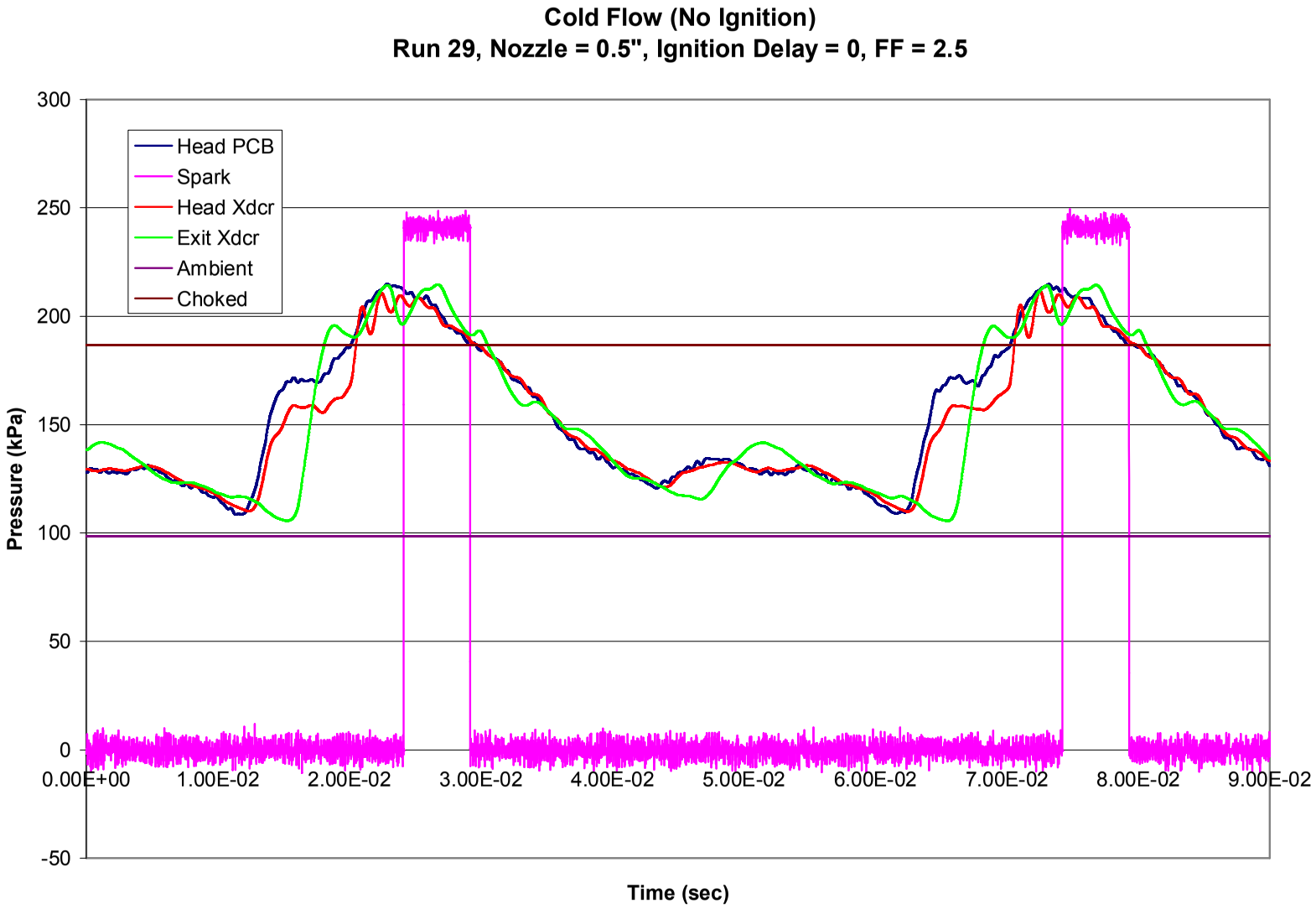
Cold Flow (No Ignition)
Run 29, Nozzle = 0.5", Ignition Delay = 0, FF = 2.5
Head PCB
Spark
Head Xdcr
Exit Xdcr
Ambient
Choked
Pressure (kPa)
300
250
200
150
100
50
0
-50
0.00E+00
1.00E-02
2.00E-02
3.00E-02
4.00E-02
5.00E-02
6.00E-02
7.00E-02
8.00E-02
9.00E-02
Time (sec)

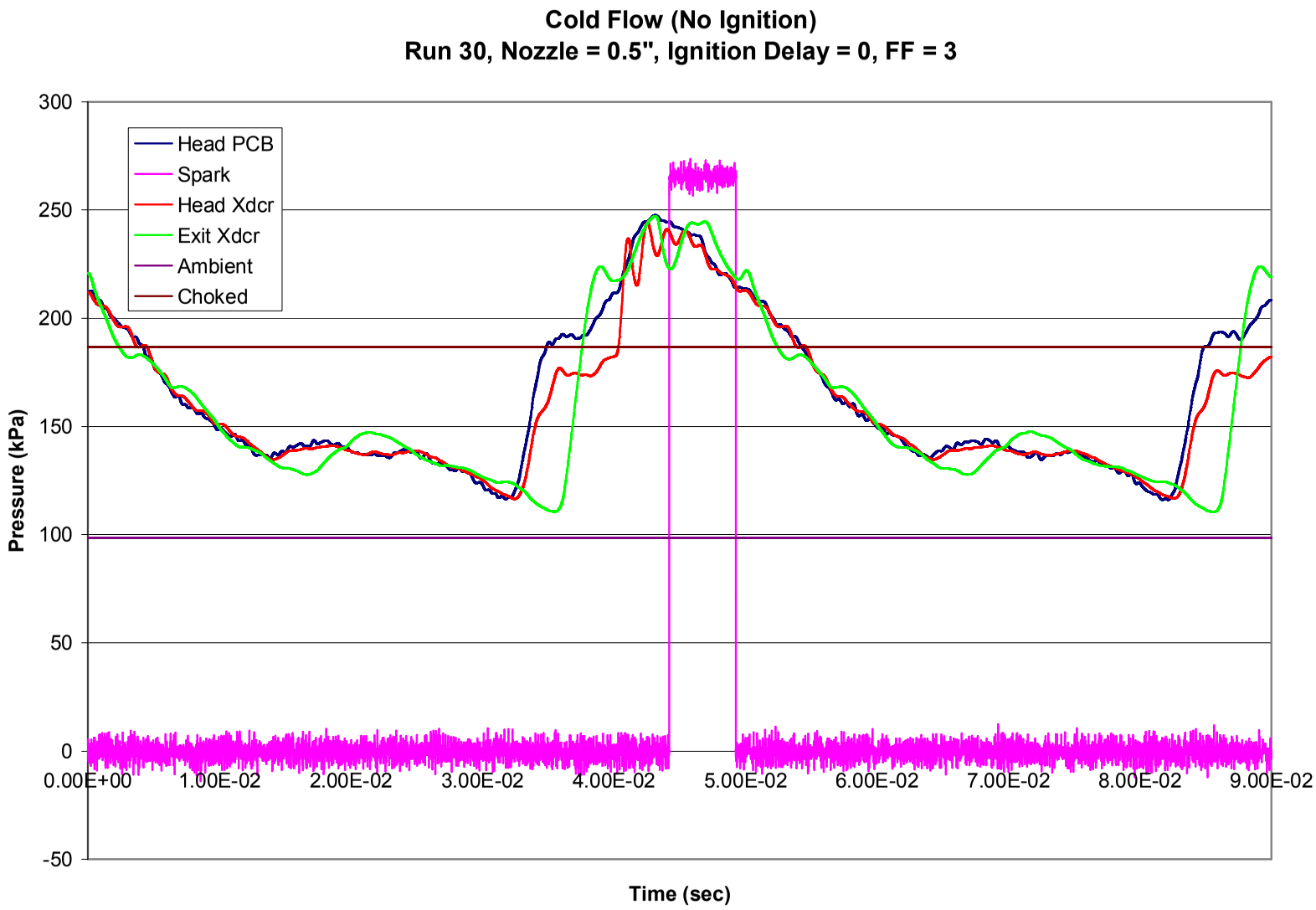
Cold Flow (No Ignition)
Run 30, Nozzle = 0.5", Ignition Delay = 0, FF = 3
Head PCB
Spark
Head Xdcr
Exit Xdcr
Ambient
Choked
Pressure (kPa)
300
250
200
150
100
50
0
-50
0.00E+00
1.00E-02
2.00E-02
3.00E-02
4.00E-02
5.00E-02
6.00E-02
7.00E-02
8.00E-02
9.00E-02
Time (sec)

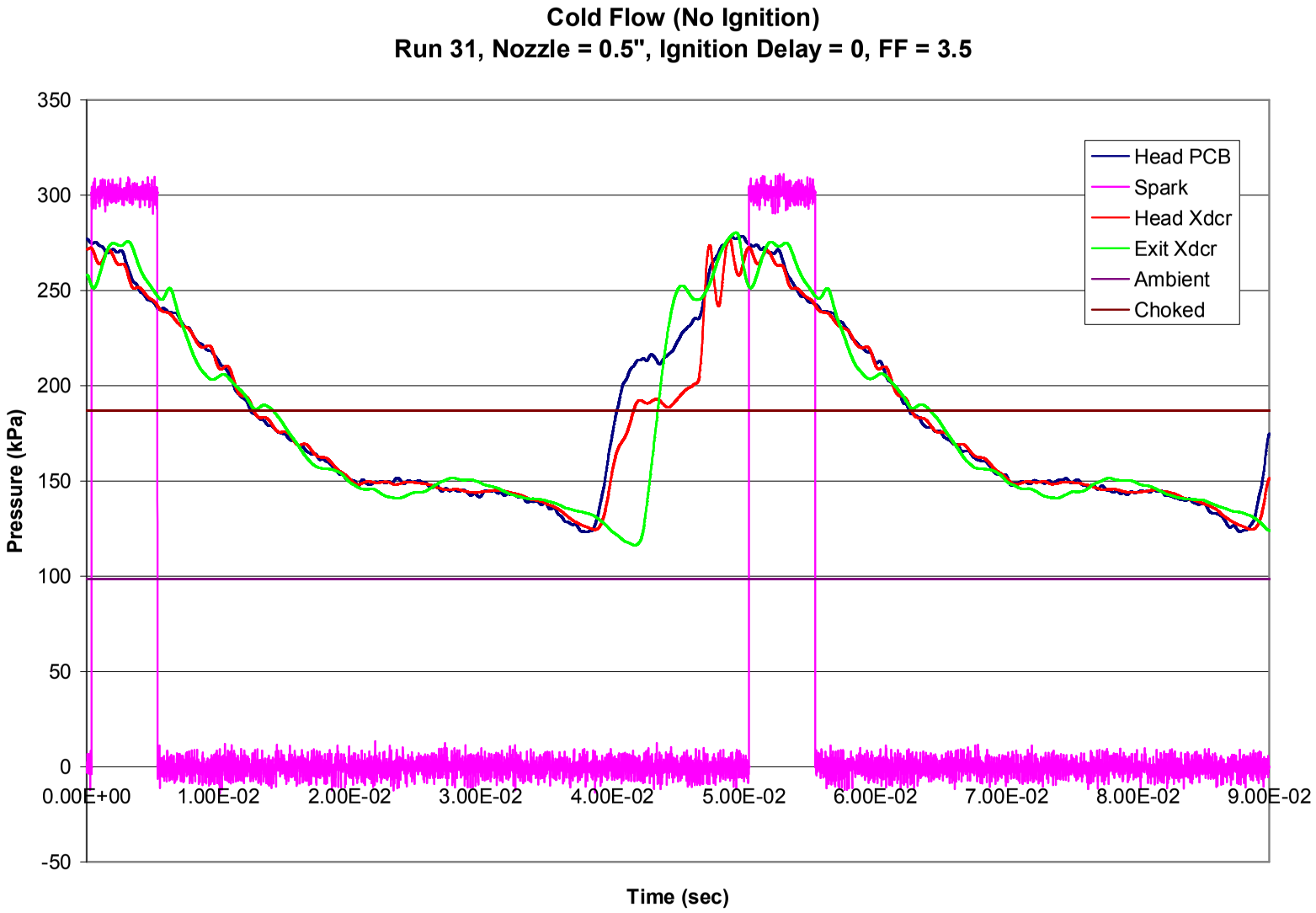
Cold Flow (No Ignition)
Run 31, Nozzle = 0.5", Ignition Delay = 0, FF = 3.5
Pressure (kPa)
350
300
250
200
150
100
50
0
-50
0.00E+00
1.00E-02
2.00E-02
3.00E-02
4.00E-02
5.00E-02
6.00E-02
7.00E-02
8.00E-02
9.00E-02
Time (sec)
Head PCB
Spark
Head Xdcr
Exit Xdcr
Ambient
Choked

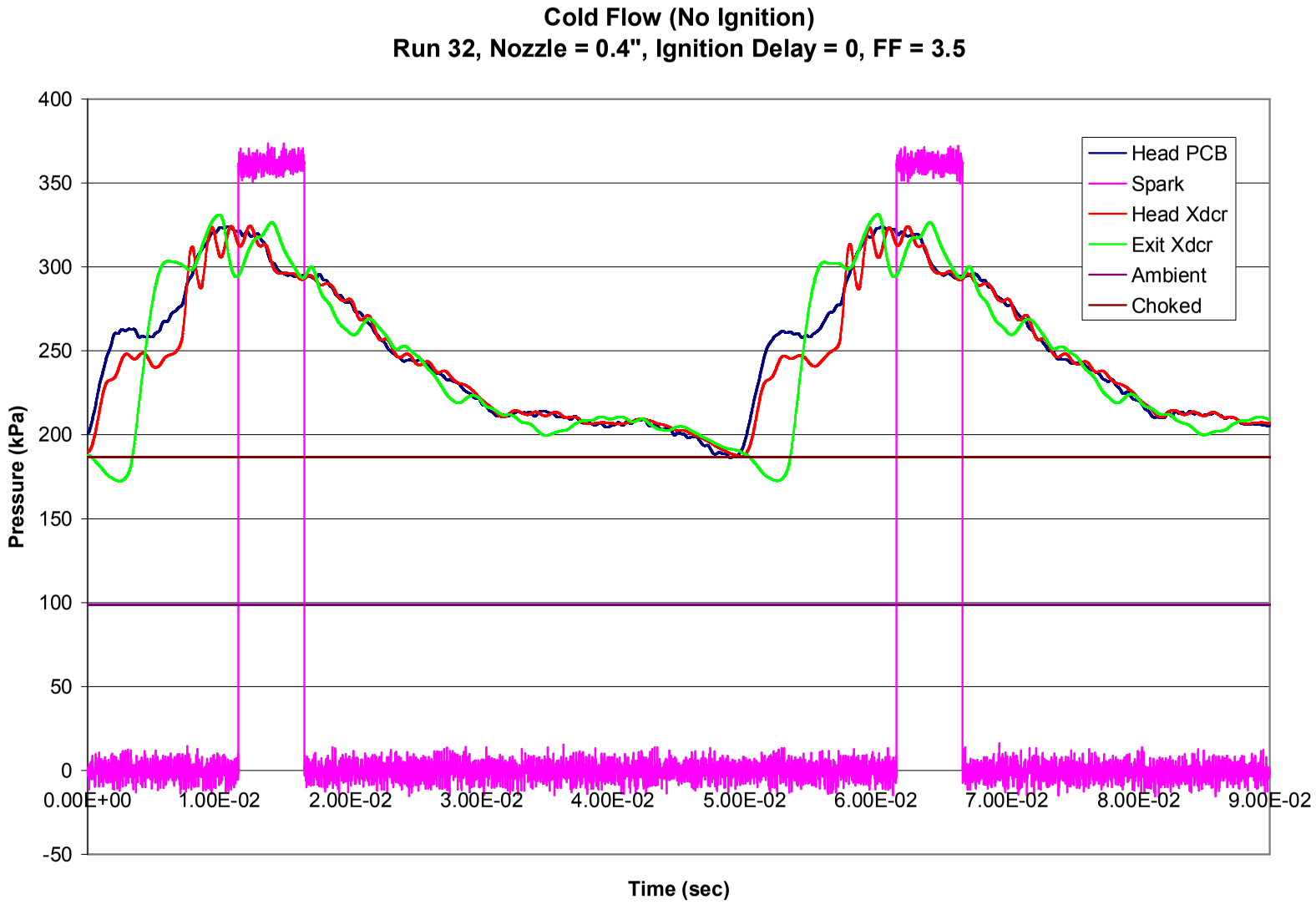
Cold Flow (No Ignition)
Run 32, Nozzle = 0.4", Ignition Delay = 0, FF = 3.5
Pressure (kPa)
400
350
300
250
200
150
100
50
0
-50
0.00E+00
1.00E-02
2.00E-02
3.00E-02
4.00E-02
5.00E-02
6.00E-02
7.00E-02
8.00E-02
9.00E-02
Time (sec)
Head PCB
Spark
Head Xdcr
Exit Xdcr
Ambient
Choked

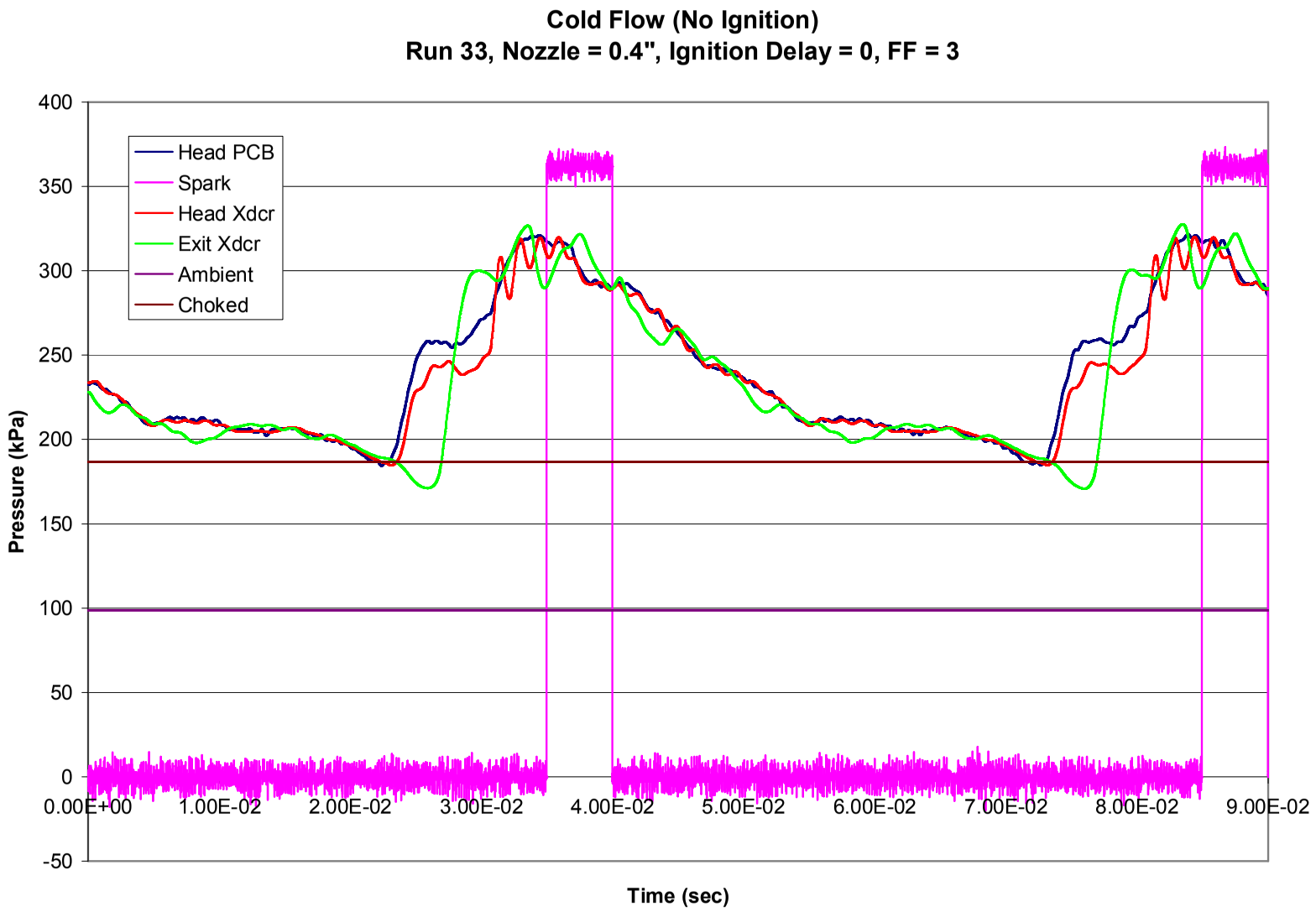
Cold Flow (No Ignition)
Run 33, Nozzle = 0.4", Ignition Delay = 0, FF = 3
Head PCB
Spark
Head Xdcr
Exit Xdcr
Ambient
Choked
Pressure (kPa)
400
350
300
250
200
150
100
50
0
-50
0.00E+00
1.00E-02
2.00E-02
3.00E-02
4.00E-02
5.00E-02
6.00E-02
7.00E-02
8.00E-02
9.00E-02
Time (sec)

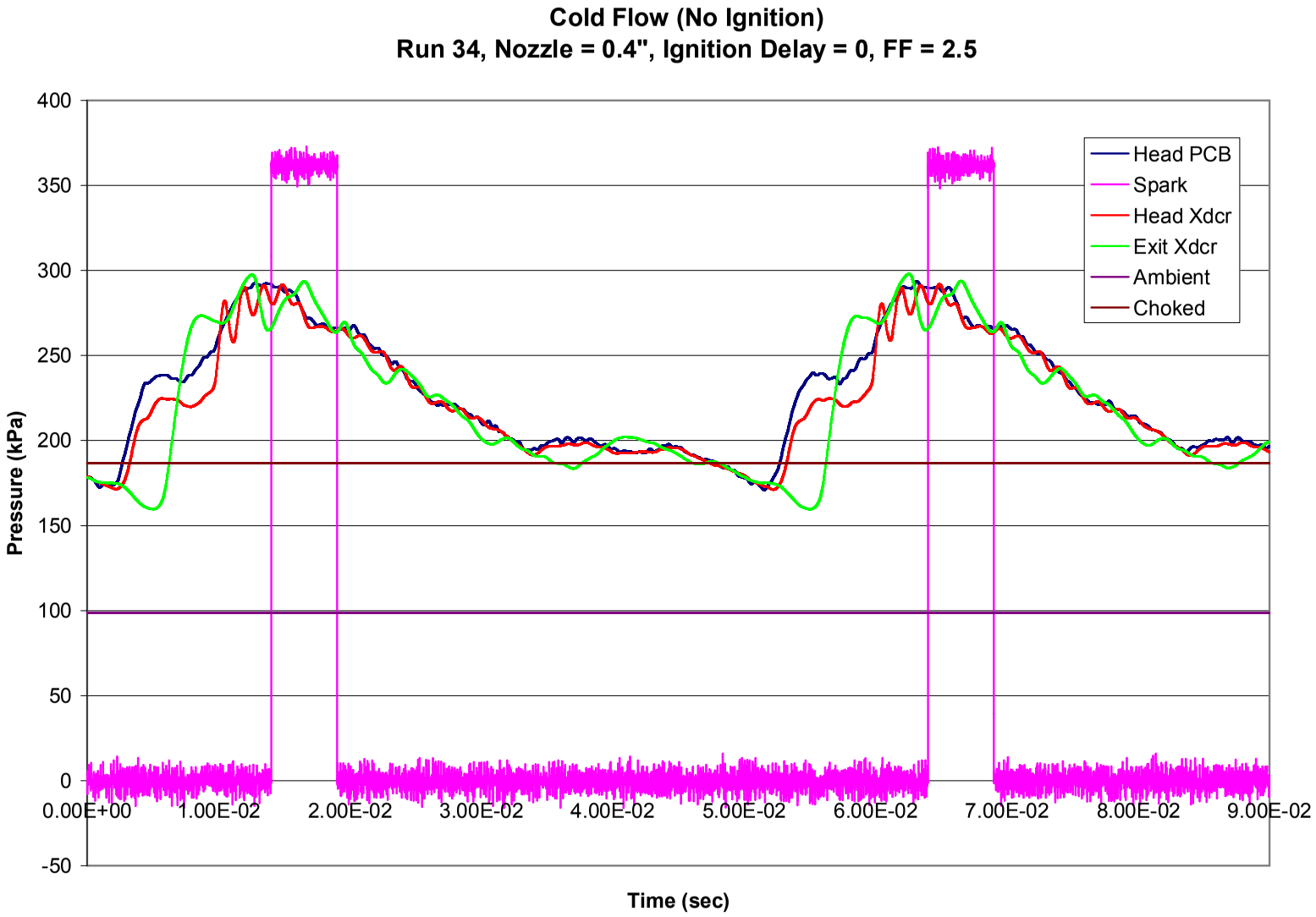
Cold Flow (No Ignition)
Run 34, Nozzle = 0.4", Ignition Delay = 0, FF = 2.5
Pressure (kPa)
400
350
300
250
200
150
100
50
0
-50
0.00E+00
1.00E-02
2.00E-02
3.00E-02
4.00E-02
5.00E-02
6.00E-02
7.00E-02
8.00E-02
9.00E-02
Time (sec)
Head PCB
Spark
Head Xdcr
Exit Xdcr
Ambient
Choked

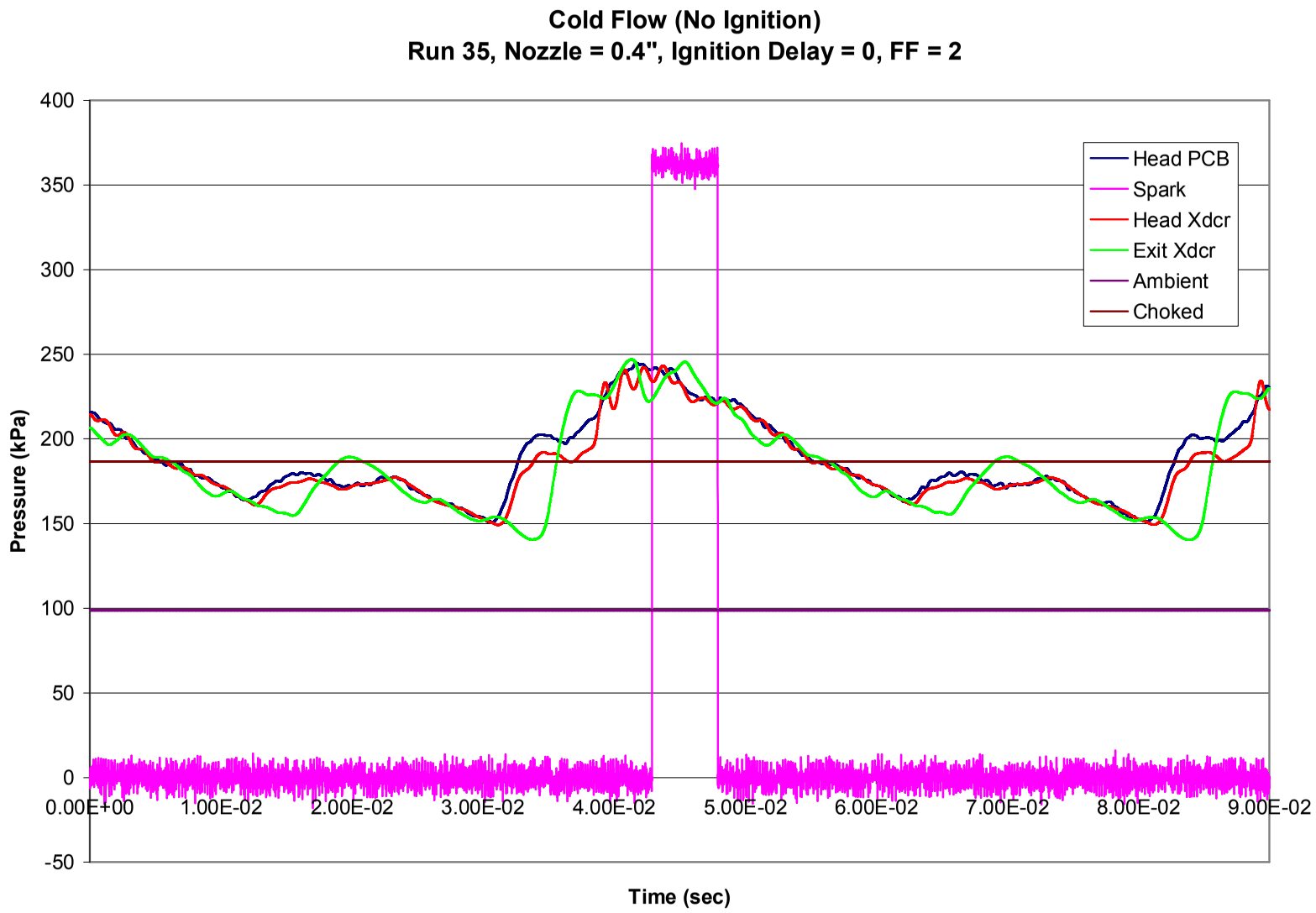
Cold Flow (No Ignition)
Run 35, Nozzle = 0.4", Ignition Delay = 0, FF = 2
Pressure (kPa)
400
350
300
250
200
150
100
50
0
-50
0.00E+00
1.00E-02
2.00E-02
3.00E-02
4.00E-02
5.00E-02
6.00E-02
7.00E-02
8.00E-02
9.00E-02
Time (sec)
Head PCB
Spark
Head Xdcr
Exit Xdcr
Ambient
Choked

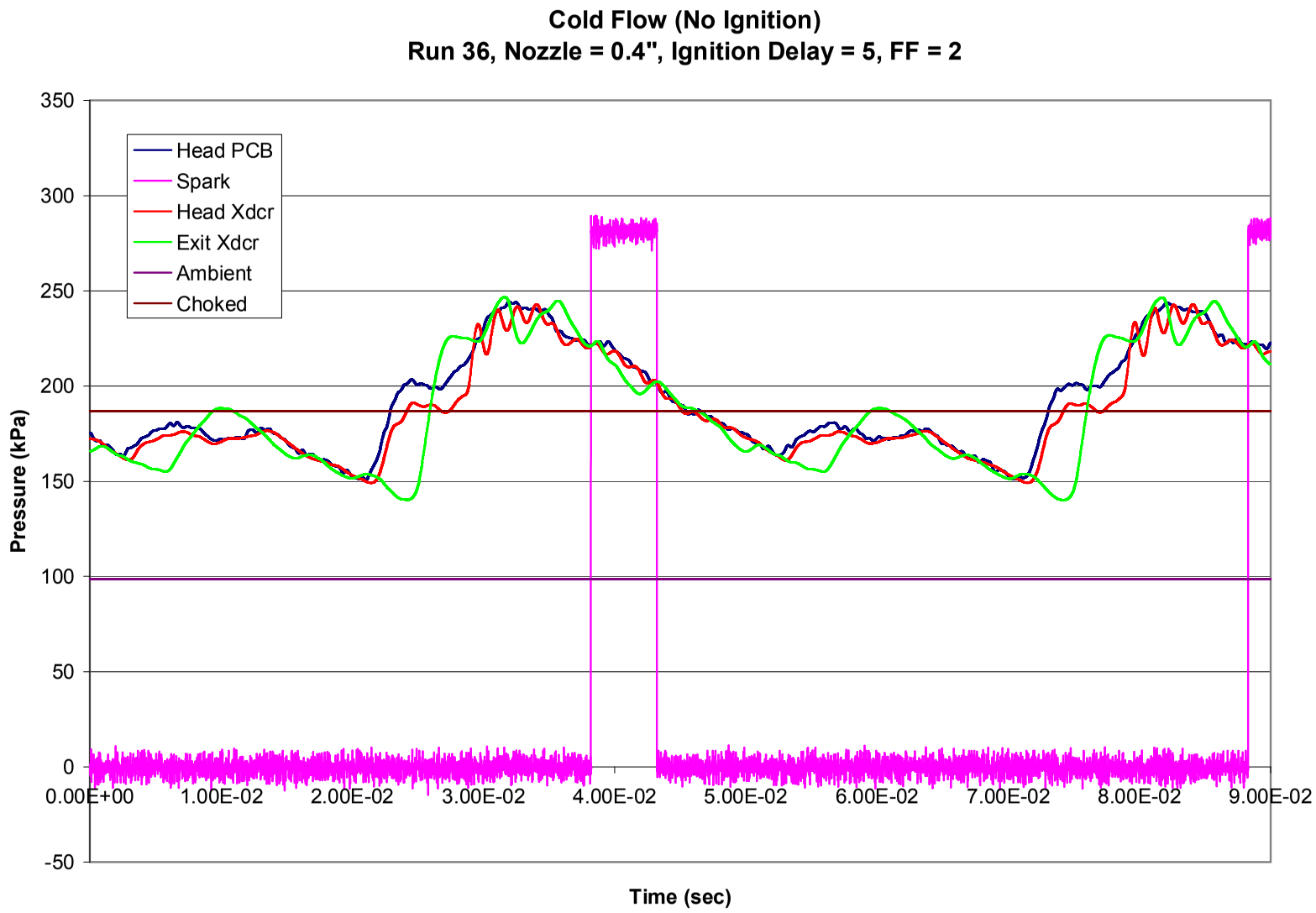
Cold Flow (No Ignition)
Run 36, Nozzle = 0.4", Ignition Delay = 5, FF = 2
Head PCB
Spark
Head Xdcr
Exit Xdcr
Ambient
Choked
Pressure (kPa)
350
300
250
200
150
100
50
0
-50
0.00E+00
1.00E-02
2.00E-02
3.00E-02
4.00E-02
5.00E-02
6.00E-02
7.00E-02
8.00E-02
9.00E-02
Time (sec)

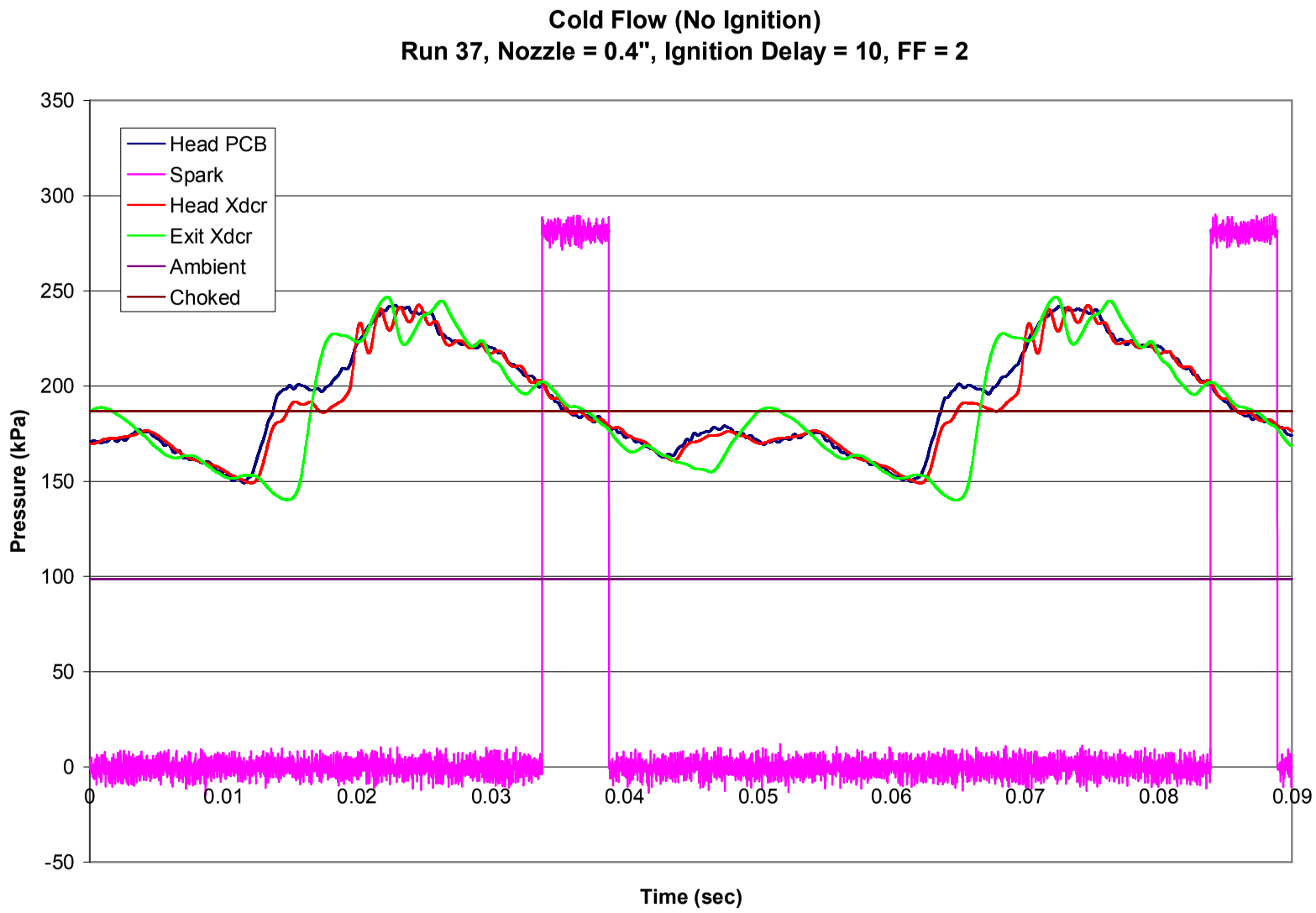
Cold Flow (No Ignition)
Run 37, Nozzle = 0.4", Ignition Delay = 10, FF = 2
Head PCB
Spark
Head Xdcr
Exit Xdcr
Ambient
Choked
Pressure (kPa)
350
300
250
200
150
100
50
0
-50
0
0.01
0.02
0.03
0.04
0.05
0.06
0.07
0.08
0.09
Time (sec)

Bibliography

Allgood, Daniel, Gutmark, Ephraim and Katta, Viswanath, "Effects of Exit Geometry on the Performance of a Pulse Detonation Engine," AIAA 2002-0613, 40th Aerospace Sciences Meetings and Exhibit, 14-17 January 2002, Reno, Nevada.

Anderson, John D., *Modern Compressible Flow with Historical Perspective, Third Edition*, New York, McGraw Hill, 2003.

Barbour, E. A. and Hanson, R. K., "A Pulse Detonation Tube with a Converging-Diverging Nozzle Operating at Different Pressure Ratios," AIAA 2005-1307, 43rd Aerospace Sciences Meeting and Exhibit, 10-13 January 2005, Reno, Nevada.

Barlow, Jewel B., Rae, William H. and Pope, Alan, *Low Speed Wind Tunnel Testing, Third Edition*, New York, John Wiley & Sons, 1999.

Cambier, J.L. and Tegner, J.K., "Strategies for Pulse Detonation Engine Optimization," *Journal of Propulsion and Power*, Vol. 14, No. 4, 1998.

Chuanjun, Y., Jun L., Wei, F., Liming, H., Hengren L., *Principle and Cycle Analysis of Pulse Detonation Engines*, National Air Intelligence Center, NAIC-ID(RS)T-0151-97, August 1997.

Colket, Meredith B. III and Spadaccini, Louis J., "Scramjet Fuels Autoignition Study," *Journal of Propulsion and Power*, Vol 17, No. 2, March-April 2001.

Cooper, M. and Shepherd, J. E., "The Effect of Transient Nozzle Flow on Detonation Tube Impulse," AIAA 2004-3914, 40th AIAA/ASME/SAE/ASEE Joint Propulsion Conference and Exhibit, 11-14 July 2004, Fort Lauderdale, FL.

Cooper, M. and Shepherd, J. E., "The Effect of Transient Nozzles and Extensions on Detonation Tube Performance," AIAA 2002-3628, 38th AIAA/ASME/SAE/ASEE Joint Propulsion Conference and Exhibit, 7-10 July 2002, Indianapolis, IN.

Cooper, M., Jackson and S., Sheperd, J. E., "Effect of Deflagration-to-Detonation Transition on Pulse Detonation Engine Impulse, GALCIT Report FM00-3, Explosion Dynamics Laboratory, GALCIT, May 2000.

Dorofeev, S.B., Sidorov, V.P., Kuznetsov, M.S., Matsukov, I.D., Alekseev, V.I., "Effect of Scale on the Onset of Detonations," *Shock Waves*, Vol. 10, Pages 137-149, 2000.

Dyer, R. S., Kaemming, T. A. and Baker, R. T., "Reaction Ratio and Nozzle Expansion Efffects on the PDE," AIAA 2003-4514, 39th AIAA/ASME/SAE/ASEE Joint Propulsion Conference and Exhibit, 20-23 July 2003, Huntsville, Alabama.

Dyer, R. S., Kaemming, T. A. and Baker, R. T., "The Thermodynamic and Fluid Dynamic Function of a Pulse Detonation Engine Nozzle," AIAA 2004-3916, 40th AIAA/ASME/SAE/ASEE Joint Propulsion Conference and Exhibit, 11-14 July 2004, Fort Lauderdale, FL.

Eidelman, S. and Yang, X., "Analysis of the Pulse Detonation Engine Efficiency," AIAA 98-3877, AIAA/ASME/SAE/ASEE Joint Propulsion Conference and Exhibit, 34th, Cleveland OH, 13-15 July, 1998.

Fox, Robert W., McDonald, Alan T. and Pritchard, Philip J., *Introduction to Fluid Mechanics*, John Wiley & Sons, 2003.

Glassman, Irvin, *Combustion*, San Diego, Academic Press, 1996.

Heywood, John B., *Internal Engine Combustion Engine Fundamentals,* New York, McGraw Hill, 1988.

Hinkey, J.B., Bussing T.R.A., "Shock Tube Experiments for the Development of a Hydrogen-Fueled Pulse Detonation Engine," 31st AIAA/ASME/SAE/ASEE Joint Propulsion Conference and Exhibit, 10-12 July 1995, San Diego CA.

Hoffman, H., *Reaction Propulsion by Intermittent Detonative Combustion*, German Ministry of Supply, AI152365, Volkenrode translation, 1940.

Holman, J. P., *Experimental Methods for Engineers*, *Seventh Edition*, New York, McGraw Hill, 2001.

Humble, R. W., Henry, G. N., Larsen, W. J., *Space Propulsion Analysis and Design* (Revised). New York: McGraw-Hill Publishing Company, 1995.

James, Helen, "Detonations", Discipline Information Note, DIN TD5 039, HSE Intranet, October 2001.

John, James E. A., *Gas Dynamics, Second Edition*, Boston, Allyn and Bacon, 1984.

Kailasanath, K., "A Review of Research on Pulse Detonation Engine Nozzles," AIAA 2001-3932, 37th AIAA/ASME/SAE/ASEE Joint Propulsion Conference & Exhibit, 8-11 July 2001, Salt Lake City, Utah.

Kailasanath, K., "A Review of Research on Pulse Detonation Engines," Proceedings of the 17th International Colloquium on the Dynamics of Explosions and Reactive Systems, Heidelberg, Germany, July 1999.

Kailasanath, K., "Recent Developments in the Research on Pulse Detonation Engines," AIAA 2002-0470, 40th AIAA Aerospace Sciences Meeting & Exhibit, 14-17 January 2002, Reno Nevada.

Kaneshige, Michael and Shepherd, Joseph E., *Detonation Database*, Explosion Dynamics Laboratory Report FM97-8, GALCIT, September, 1997.

Kanury, Marty A., *Introduction to Combustion Phenomena*, New York, Gordon and Breach, Science Publishers, 1975.

Kuo, Kenneth K., *Principles of Combustion*, New Jersey, John Wiley & Sons, 2005.

Kuo, Kenneth K., *Principles of Combustion*, New York, John Wiley & Sons, 1986.

Lee, J. H. S., Knystautas, R. and Guirao, C., "The Link Between Cell Size, Critical Tube Diameter, Initiation Energy and Detonability Limits," *Fuel-Air Explosions*, Montreal, Quebec, University of Waterloo Press, 1982.

Lefebvre, Arthur, Freeman, W. and Cowell, L., "Spontaneous Ignition Delay Characteristics of Hydrocarbon Fuel/Air Mixtures," NASA Contractor Report 175064 (NASA-CR-175064), Purdue University, West Lafayette IN, February 1986.

McMillan, R.J., *Shock Tube Investigation of Pressure and Ion Sensors used in Impulse Detonation Engine Research*, AFIT/GAE/ENY/04-J07, Air Force Institute of Technology (AU), Wright Patterson AFB OH, March 2004.

Miser Christen L., *Pulse Detonation Engine Thrust Tube Heat Exchanger for Flash Vaporization and Supercritical Heating of JP-8*, AFIT/GAE/ENY/05-M11, Air Force Institute of Technology (AU), Wright-Patterson AFB OH, March 2005.

Owens, Zachary C. Owens and Hanson, Ronald K., "Unsteady Nozzle Design for Pulse Detonation Engines," AIAA 2005-3649, 41st AIAA/ASME/SAE/ASEE Joint Propulsion Conference & Exhibit, 10-13 July 2005, Tucson, Arizona.

Panzenhagen, Kristin L., *Detonation Branching in a PDE with Liquid Hydrocarbon Fuel,* AFIT/GAE/ENY/04-M13, Air Force Institute of Technology (AU), Wright-Patterson AFB OH, March 2004.

Schauer, F.R., Miser, C.L., Tucker, K.C., Bradley, R.P. and Hoke, J.L., "Detonation Initiation of Hydrocarbon-Air Mixtures in a Pulse Detonation Engine," AIAA 2005-1343, 43rd AIAA Aerospace Sciences Meeting, January 10-13, 2005, Reno NV.

Schultz, E. and Shepherd J., *Validation of Detailed Reaction Mechanisms for Detonation Simulation*, Explosion Dynamics Laboratory Report FM99-5, GALCIT, February 2000.

Schultz, E., Wintenberger, E. and Shepherd J., "Investigation of Deflagration to Detonation Transition for Application to Pulse Detonation Engine Ignition Systems, California Institute of Technology," *Proceedings of the 16th JANNAF Propulsion Symposium*, Chemical Propulsion Information Agency, 1999.

Stuessy, W. S. and Wilson, D. R., "Influence of Nozzle Geometry on the Performance of a Pulse Detonation Wave Engine," AIAA 1997-2745, AIAA/ASME/SAE/ASEE Joint Propulsion Conference and Exhibit, 33rd, Seattle WA, 6-9 July, 1997.

Tucker, K. Colin, *A Flash Vaporization System for Detonation of HydrocarbonFuels in a Pulse Detonation Engine*, AFIT/DS/ENY/04-07, Air Force Institute of Technology (AU), Wright-Patterson AFB OH, September 2004.

Turns, Stephen R., *An Introduction to Combustion: Concepts and Applications*, New York, McGraw Hill, 2000.

Windergerden, Kees van, Bjerketvedt, Dag and Bakke, Jan Roar, "Detonations in Pipes and in the Open," Christian Michelsen Research, Bergen, Norway.

Yungster, S., "Analysis of Nozzle Effects on Pulse Detonation Engine Performance," AIAA 2003-1316, 41st Aerospace Sciences Meeting and Exhibit, 5-9 January 2003, Reno, Nevada.

Vita

Captain Wesley R. Knick graduated from Melbourne High School in Melbourne, Florida. A semi-native Floridian where he lived most of his life before entering service in the U.S. Air Force, he was born in Winston Salem, North Carolina. He entered undergraduate studies at the University of Florida in Gainesville, Florida to study mechanical engineering. After completing two successful years of undergraduate study he decided to enlist in the U. S. Air Force whereupon completing basic training and technical school at Chanute Air Force Base, Illinois he was assigned to Ellsworth Air Force Base South Dakota as an aerospace propulsion specialist. After being reassigned to Davis-Monthan Air Force Base, Arizona he again enrolled in school at the University of Arizona, Tucson where he graduated with a Bachelor of Science degree in mechanical engineering December, 1997. He was commissioned through the Air Force Reserve Officer Training Corps Detachment 020 at the University of Arizona where he was recognized as an Honor Graduate and nominated for a Reserve Commission in the United States Air Force. His first assignment upon being commissioned was to the Air Force Research Laboratory, Munitions Directorate, Eglin Air Force Base, Florida. Following his academics at AFIT he will be assigned to the Air Force Research Laboratory, Propulsion Directorate, Edwards AFB, CA. While on assignment at Eglin Air Force Base he met his wonderful and loving wife and now has a young daughter. His biggest joy in the world now is being a father.

REPORT DOCUMENTATION PAGE

Form Approved
OMB No. 074-0188

1. REPORT DATE *(DD-MM-YYYY)*	2. REPORT TYPE	3. DATES COVERED *(From – To)*
23 Mar 06	**Master's Thesis**	Sep 04 – Mar 06

4. TITLE AND SUBTITLE

Characterization of Pulse Detonation Engine Performance with Varying Free Stream Stagnation Pressure Levels

5a. CONTRACT NUMBER

5b. GRANT NUMBER

5c. PROGRAM ELEMENT NUMBER

6. AUTHOR(S)

Knick, Wesley R., Captain, USAF

5d. PROJECT NUMBER

5e. TASK NUMBER

5f. WORK UNIT NUMBER

7. PERFORMING ORGANIZATION NAMES(S) AND ADDRESS(S)

Air Force Institute of Technology
Graduate School of Engineering and Management (AFIT/ENY)
2950 Hobson Way
WPAFB OH 45433-7765

8. PERFORMING ORGANIZATION REPORT NUMBER

AFIT/GAE/ENY/06-M34

9. SPONSORING/MONITORING AGENCY NAME(S) AND ADDRESS(ES)

AFRL/PRTC
Attn: Dr. Frederick Schauer
1790 Loop Road DSN: 785-6462
WPAFB OH 45433-7765 e-mail: Frederick.schauer@wpafb.af.mil

10. SPONSOR/MONITOR'S ACRONYM(S)

11. SPONSOR/MONITOR'S REPORT NUMBER(S)

12. DISTRIBUTION/AVAILABILITY STATEMENT

APPROVED FOR PUBLIC RELEASE; DISTRIBUTION UNLIMITED.

13. SUPPLEMENTARY NOTES

14. ABSTRACT

A pulse detonation engine operates on the principle that a fuel-air mixture injected into a tube will ignite and undergo a transition from a deflagration to a detonation and exit the tube at supersonic velocities. Studies in the field of combustion have shown that both ignition time and deflagration to detonation transition time can vary as a function of pressure. It can be hypothesized that if ignition and deflagration to detonation transition times can be reduced by increasing the free stream stagnation pressure level of the tube, it would then be possible to shorten the detonation tube length and increase the cycle frequency resulting in a weight savings, and an increase in overall pulse detonation engine performance. By attaching varying sizes of nozzle orifices to the exhaust exit of the pulse detonation tube of the pulse detonation engine to choke, or increase the stagnation pressure levels of the detonation tube it was shown possible to vary the internal pressure of the pulse detonation tube and examine the effect on the performance parameters of ignition time, and detonation wave speed, distance, and time. By varying fill fraction, spark delay and equivalence ratio in addition to nozzle orifice size, a reduction in ignition and overall detonation time was achieved from a variation of nozzle orifice to detonation tube diameter ratios. The effects of pressure in this study produced a less beneficial effect on deflagration to detonation transition time and distance.

15. SUBJECT TERMS

jet propulsion, detonation, deflagration, ignition, pressure

16. SECURITY CLASSIFICATION OF:			17. LIMITATION OF ABSTRACT	18. NUMBER OF PAGES	19a. NAME OF RESPONSIBLE PERSON
REPORT	ABSTRACT	c. THIS PAGE			Dr. Paul I. King
U	**U**	**U**	**UU**	172	**19b. TELEPHONE NUMBER** *(Include area code)* (937) 255-6565, ext 4628; e-mail: paul.king@afit.edu

Standard Form 298 (Rev: 8-98)
Prescribed by ANSI Std. Z39-18